

THESIS

THE BACILLARY RESPONSE TO CHEMOTHERAPY IN PRECLINICAL ANIMAL
MODELS USED TO EVALUATE TB DRUGS

Submitted by

Donald R. Hoff

Department of Microbiology, Immunology,
and Pathology

In partial fulfillment of the requirements

For the Degree of Master of Science

Colorado State University

Fort Collins, Colorado

Spring 2010

COLORADO STATE UNIVERSITY

April 2, 2010

WE HEREBY RECOMMEND THAT THE THESIS PREPARED UNDER OUR SUPERVISION BY DONALD R. HOFF ENTITLED THE BACILLARY RESPONSE TO CHEMOTHERAPY IN PRECLINICAL ANIMAL MODELS USED TO EVALUATE TB DRUGS BE ACCEPTED AS FULFILLING IN PART REQUIREMENTS FOR THE DEGREE OF MASTER OF SCIENCE.

Committee on Graduate work

Francisco Olea-Popelka

Advisor: Anne J. Lenaerts

Co-Advisor: Randall J. Basaraba

Department Head: Edward Hoover

ABSTRACT OF THESIS

THE BACILLARY RESPONSE TO CHEMOTHERAPY IN PRECLINICAL ANIMAL MODELS USED TO EVALUATE TB DRUGS

Current drug treatment for tuberculosis (TB) consists of 6 to 9 months of daily multidrug therapy. The long duration of chemotherapy contributes to a high rate of treatment failure as patients fail to adhere to the prescribed regimen. The length of treatment is thought to be necessary to eradicate a small proportion of *Mycobacterium tuberculosis* bacilli that persist despite effective drug treatment. Developing drugs that target tubercle bacilli in this drug-refractory state must be found in order to shorten standard therapy. However, specific details on the nature of *M. tuberculosis* persistence are still lacking. Further hindering the drug discovery process is our incomplete knowledge of the how *M. tuberculosis* infects different animal models used to evaluate preclinical drug candidates. Pulmonary TB infection manifests and develops very differently between species routinely used to test these compounds and with respect to human infection. The main goal of this thesis is to facilitate the development of new, highly effective drugs for TB treatment by improving our understanding of *M.*

tuberculosis persistence and of the animal models used to test experimental compounds
in preclinical trials.

Donald R. Hoff
Microbiology, Immunology, and Pathology Department
Colorado State University
Fort Collins, Colorado 80523
Spring 2010

ACKNOWLEDGMENTS

I would like to thank the following people who have made this thesis possible:

Dr. Anne J. Lenaerts, my adviser, mentor, and boss, without whom none of this would be possible.

Dr. Randall Basaraba, my co-adviser whose work in tuberculosis research opened my eyes to the limitless applications of veterinary medicine.

Dr. Francisco Olea-Popelka, my outside adviser who has shown me that the impact of veterinary medicine can be just as (statistically) significant for humans as it is for animals.

Members of the Lenaerts laboratory: Emily Driver (my partner), Veronica Gruppo (my teacher), and Gavin J. Ryan (my comic relief)

TABLE OF CONTENTS

Signature page	ii
Thesis abstract	iii
Acknowledgments	v
Chapter 1: Background on <i>Mycobacterium tuberculosis</i>	1
1.1 What is Tuberculosis?	1
1.2 The Collapse of Consumption ... <i>Or So We Thought</i> ...	9
1.3 Pathology, Persistence, and Other Problems Complicating Chemotherapy	16
1.4 <i>Mycobacterium tuberculosis</i> Under Experimental Conditions	23
1.5 Facilitating the Development of Highly Effective Drugs for Tuberculosis Treatment	32
Chapter 2: Cross-species Comparison of the Location of <i>M. tuberculosis</i> in Pulmonary Granulomas of Mice and Guinea Pigs and Its Relationship to Drug Treatment	36
2.1 Introduction	36
2.2 Materials And Methods	41
2.3 Results	49
2.4 Conclusion	72
Chapter 3: Metronidazole Lacks Antibacterial Activity in Guinea Pigs Infected with <i>Mycobacterium tuberculosis</i>	81
3.1 Introduction	82
3.2 Materials And Methods	84
	vi

3.3 Results	87
3.4 Conclusion	95
Chapter 4: Investigating Anti-Tubercle Drug Killing Kinetics in a Murine Model of Bactericidal Activity	98
4.1 Introduction	98
4.2 Materials And Methods	103
4.3 Results	109
4.4 Conclusion	123
Chapter 5: Conclusion	130
References	140

CHAPTER ONE

BACKGROUND ON *MYCOBACTERIUM TUBERCULOSIS*

1.1 WHAT IS TUBERCULOSIS?

Introduction To Tuberculosis. From the isolated remains of an Egyptian mummy to a 1st class transcontinental flight in Andrew Speaker, *Mycobacterium tuberculosis*, the causative agent of tuberculosis (TB), has consistently reminded us of its presence today, its significance in the past, and most likely its continued persistence in the future. The past descriptive monikers given to TB (scrofula, consumption, ‘White Plague’, the King’s Evil to name a few) give one an idea of how successful this pathogen has been at co-evolving with its human host. Despite the development of effective chemotherapeutics nearly half a century ago, TB is the second leading cause of death worldwide by an infectious pathogen today behind those attributed to HIV/AIDS (101). There is clearly an urgent need for new, highly effective chemotherapeutic regimens to be developed, yet the standard frontline drugs prescribed to treat TB over 40 years ago are the same today. Reviewing the historical research contributing to our current understanding of TB and *Mycobacterium tuberculosis* (*M. tuberculosis*) provides insight into why this pathogen has been so difficult to eradicate.

Robert Koch. Little was known about the bacterium *M. tuberculosis* until March 24, in the year 1882, when Robert Koch put forth his now famous ‘Koch’s Postulates’

(24). These postulates outlined the experimental methodology that he followed to ultimately identify the etiologic agent of the ‘White Plague’. Using Ehrlich’s methylene blue and the brown dye *vesuvin*, Koch consistently found the rod-shaped bacterium in the tissues of infected humans and eventually cultured the organism after an extended incubation period on coagulated blood serum. The successful infection of guinea pigs using infected human tissue homogenates fulfilled his third postulate, and thus, Koch concluded his talk by identifying *M. tuberculosis* as the culprit of ‘consumption’.

Attributes Of Mycobacterium tuberculosis. Much has been learned since the work of Koch opened the door for TB research. This work has revealed that *M. tuberculosis* is a non-motile, bacillus-shaped, facultative anaerobe that is classified as an acid-fast organism. This latter characteristic indicates the bacterium can retain certain dyes after acid-alcohol de-colorization due to its unique cell wall structure. The cell wall of mycobacteria consists of arabinogalactan bound to a network of cross-linking peptidoglycan by mycolic acids (7). The cell wall of *M. tuberculosis* is the thickest known, and its integrity is required for viability. *M. tuberculosis* is also a slow-grower. *In vitro*, the doubling time of *M. tuberculosis* varies between 18 to 54 hours (55) while other bacteria, such as *Escherichia coli*, divide every 20 minutes. This slow-growing nature complicates drug treatment as most antibiotics target metabolic pathways required by bacteria to synthesize proteins and/or nucleic acids. As a consequence, the growth rate of bacteria directly influences the efficiency with which they are killed by drugs (79). TB treatment is also lengthy in part because this pathogen has the ability to persist in host

tissues in spite of a well-executed host immune response and prolonged, effective chemotherapy.

Pulmonary Route Of Infection. Tuberculosis is primarily acquired by inhalation of aerosol droplets containing approximately 1 to 3 *M. tuberculosis* bacilli that are inhaled deep into the lung (38). Tubercle bacilli become deposited into air spaces and are subsequently phagocytosed by alveolar macrophages (mΦ). Located within the phagosome, *M. tuberculosis* has evolved a number of strategies to avoid host immune detection and resist degradation. These mechanisms include preventing phago-lysosome fusion, blocking apoptosis, and interfering with major histocompatibility complex (MHC) class II antigen presentation. These strategies allow bacilli to replicate intracellularly sometimes resulting in lysis of the mΦ. Tissue mΦs and dendritic cells (DC) encountering the pathogen will then secrete interleukin-12 (IL-12) to alert other cells of the foreign invaders presence, which will initiate a cascade of pro-inflammatory cytokines and chemokines. In addition to mΦs, T cells will produce tumor necrosis factor-alpha (TNF-alpha) to recruit neutrophils to the site of infection. Natural killer (NK) cells respond to mycobacterial infection by secreting interferon-gamma (IFN-gamma). This type II interferon activates infected mΦs to kill their foreign cargo by producing reactive nitrogen intermediates. Engagement of Toll-like receptor-2 by microbial lipopeptides induces maturation of DCs as they migrate to draining lymph nodes to ultimately activate CD4+ and CD8+ T cells (40). Upon activation, CD4+ T cells differentiate into either T helper 1 (Th1) or Th2 cells that produce either Th1 pro-inflammatory (IFN-gamma, IL-2, and TNF-alpha) or Th2 immunosuppressive (IL-4, IL-

5, and IL-13) cytokines, respectively. In contrast, CD8⁺ T cells act predominantly as cytotoxic T lymphocytes (CTLs), lysing *M. tuberculosis*-infected cells via granulysin or by the activation of apoptotic pathways. However, the coordinated efforts of the innate and adaptive immune responses are not always effective in completely sterilizing the host of all *M. tuberculosis* bacilli. Under these circumstances, a TB infection is established in the host.

Tuberculosis Infection In Humans. Upon initial, primary infection of *M. tuberculosis*, there are generally three outcomes for an individual that may result. For some, a vigorous immune response to the infiltrating bacilli leads to rapid clearance of the pathogen from the host. However, the innate mechanisms that mediate this course of infection are poorly understood. Of all people who do not clear the pathogen, 10% are suspected to develop *active* disease, while the remaining 90% are generally thought to maintain a *latent* infection (105).

Active Infection. Individuals developing an active infection after the primary exposure to TB are unable to control the growth of *M. tuberculosis*. These patients may vary in their clinical symptoms, which can range from a mild flu-like illness to more severe symptoms characterized by a cough producing bloody discharge. As the infection progresses, some individuals may exhibit a progressive worsening of pulmonary pathology. An increase in inflammation and subsequent tissue degeneration leads to the production of a thick sputum that is the key diagnostic feature of active pulmonary TB disease (1). This sputum may contain infectious bacilli that can be transmitted

aerogenically to a susceptible host when coughed up into the air. Active TB may cause death due to extensive pulmonary inflammation ultimately leading to insufficient gas exchange if left untreated. Although the majority of people worldwide may not develop active TB, this is not the case in areas where the disease is endemic. There have been a number of factors attributed to predisposing the development of active TB including malnutrition, age, and immunosuppression. This type of disease outcome is having a significant impact in sub-Saharan Africa where the ongoing TB-HIV/AIDS epidemic is quickly spiraling out of control further impeding goals of global TB eradication.

Latent Infection. Patients with a latent TB infection (LTBI) orchestrate a robust immune response to *M. tuberculosis*. While unable to completely clear the pathogen, this host immune response is effective in containing the infection via inhibition of bacterial replication. These patients are not contagious and exhibit no clinical signs of disease as long as the balance between host immunity and pathogen is maintained. This latent-state may be maintained for the rest of the host's life. However, these patients also have the potential to reactivate, develop a progressive infection, and spread disease. Diagnosis of LTBI is difficult due to its variable presentations. Humans previously exposed to TB exhibit a delayed-type hypersensitivity (DTH) reaction to purified protein derivatives (PPD) of *M. tuberculosis*. The Center for Disease Control has defined a LTBI as a DTH reaction displaying as a localized inflammatory reaction at the site of injection greater than 5 mm in diameter. In conjunction with a positive PPD test, or as an alternative for patients previously vaccinated against TB, chest X-rays may be employed. However, the various radiographic manifestations of latent TB may also complicate an accurate

diagnosis. Upon radiographic examination, latently infected patients may reveal scarred remains of calcified lung lesions or may exhibit no pulmonary abnormalities whatsoever (105).

During a latent infection tubercle bacilli are refractory to drug treatment, a phenomenon that has led many to speculate on the metabolic state of *M. tuberculosis* under these conditions. This speculation has led to much confusion as latency has been used in the past to define both the clinical disease induced by *M. tuberculosis* (LTBI) and the metabolic state of bacilli during a latent infection ('latent' bacilli). When discussing *M. tuberculosis* and TB disease, it is important to clearly define these terms to fully understand the problems facing TB drug therapy.

'Dormancy' has often been substituted for latency implying that tubercle bacilli are metabolically inactive during a latent infection. Traditionally, dormancy has been associated with the ability of some bacterial species to produce endospores and/or cysts as a survival mechanism. These structures, formed in response to harsh environmental conditions, allow bacteria to survive for long periods of time until the appropriate conditions arise to support growth. The formation of spores/cysts coincides with a complete shutdown of metabolic activity by the organism. In the context of latent TB, however, both *in vitro* and *in vivo* studies have shown that this is not the case (32, 48). Inhibition of aerobic respiration by *M. tuberculosis* has been found to induce a set of 48 genes via the response regulator DosR (dormancy survival regulator) (135). The activation of the DosR regulon is associated with the transition of bacilli from a replicating to non-replicating state. Non-replicating bacilli are susceptible *in vitro* to rifampin, one of the most effective first-line drugs used to treat drug-susceptible TB,

albeit at a markedly reduced efficacy compared to actively growing bacilli (139). This implies that even under conditions of ‘dormancy’ some level of mRNA synthesis is likely maintained by the pathogen as this drug’s mechanism of action involves disrupting protein synthesis. However, the *in vitro* non-replicating state of *M. tuberculosis* may not accurately reflect the heterogeneous metabolic states of *M. tuberculosis* bacilli *in vivo*. Many of the factors contributing to the host-pathogen standoff during a latent TB infection are unclear. Whether *M. tuberculosis* is in a truly latent state or whether the rate of bacterial replication is being equaled by host cell-mediated killing is one such aspect that is currently being investigated by various researchers. Low-dose aerosol infection of C57BL/6 mice (one of the most common species used in *in vivo* TB research) with *M. tuberculosis* results in a chronic TB infection characterized by a long period in which the bacterial load in mice is maintained at a constant level. Recent evidence has shown that *M. tuberculosis* replicates throughout chronic infection in mice with bacterial replication balanced by host immune killing (55). Due to mounting experimental evidence suggesting TB bacilli are not completely metabolically inactive throughout infection, the term ‘dormancy’ will not be used in this thesis to describe the disease TB or the pathogen *M. tuberculosis*.

Reactivation. Finally, there is reactivation TB. This form of disease may arise from a previous active or LTBI or in patients who were treated but not fully cured. Latently infected patients may reactivate after years of harboring *M. tuberculosis* in a quiescent state as a result of exogenous secondary infection or due to some immunocompromising event. In either case, reactivation is associated with a rapidly

progressive form of disease that causes extensive inflammation and tissue necrosis. This form of TB disease usually occurs within 10 years of the initial infection of bacilli in the host (54). Reactivation is often associated with the development of cavitory disease (1), a manifestation of pulmonary TB that has significant consequences for global TB eradication and significant implications for TB drug development.

1.2 THE COLLAPSE OF CONSUMPTION ...OR SO WE THOUGHT...

The Bacille Calmette-Guérin Vaccine. Initial efforts to control the spread of TB came in the form of prevention. In 1908, Albert Calmette and Camille Guérin began working with a virulent bovine strain of *M. tuberculosis* isolated from a cow suffering from tuberculosis mastitis. Thirteen years, two hundred and thirty sub-cultures later, these two French investigators were eventually successful in obtaining an attenuated strain that had lost its virulence. Ultimately, this strain was developed into the first TB vaccine. The Bacille-Calmette Guérin (BCG) vaccine was introduced in the year 1921 and since has become the most widely used vaccine in the world with 85% of newborn infants with an estimated 100 million children vaccinated each year (2).

Despite its widespread use, BCG is far from ideal. Among other problems identified with this vaccine is a variable range in protective efficacy as well as duration of protection and implications for post-exposure diagnostic testing. BCG prevents the development of severe and fatal forms of TB disease in young children. However vaccination of adults, who represent the majority of TB cases worldwide, is often unsuccessful in reducing case incidence rates (121). A review assessing the protection rates conferred by BCG in clinical trials revealed a range in protective efficacy spanning from 0 to 80% (13). Variations in protection have been attributed to the biological diversity of BCG due to strain mutations, previous exposure to environmental mycobacteria, route of infection, and underlying genetic variability between different regional populations of people. Studies have indicated that protection afforded by this vaccine decreases in the years following immunization. In addition, individuals

vaccinated with BCG show cross-reactivity with most currently available diagnostic tests, and thus cannot be reliably tested for subsequent exposure. These limitations have led to recommendations of practicing BCG vaccination only where TB is endemic. It is not recommended for developing nations with the exception of individuals who meet certain criteria such as infants with high exposure risk or healthcare workers involved in the treatment of multidrug and extensively drug-resistant TB (MDR-/XDR-TB, respectively) patients (4).

Drug Development For Tuberculosis Treatment. TB chemoprophylaxis began in the early 1940's with the development of streptomycin (SM) and *para*-aminosalicylic acid (PAS) and virtually ended 14 years later with the introduction of rifamycins. The aminoglycoside SM was first shown to have a bactericidal effect against *M. tuberculosis* in 1944. This drug inhibits protein synthesis by binding to the conserved A site of 16S ribosomal RNA in the 30S ribosomal subunit thereby blocking amino acid attachment by transfer RNA (23). PAS is thought to competitively inhibit conversion of aminobenzoic acid to dihydrofolic acid and/or prevent iron uptake by mycobacteria (54). The frontline drugs isoniazid (INH), pyrazinamide (PZA), and ethambutol (EMB) were generated as nicotinamide analogues and introduced into therapy in 1952, 1954, and 1961, respectively. INH is one of the two most important anti-TB drugs used today for TB therapy. This prodrug is converted to its active intermediate in the bacterium by a catalase-peroxidase enzyme encoded for by KatG. Subsequently, this active intermediate has been reported to interact on multiple targets including NADPH-dependent enoyl reductase, encoded by InhA (133), and/or β -ketoacyl synthase, encoded by KasA (91).

Ultimately, INH inhibits cell wall synthesis by interfering with mycolic acid production. PZA is perhaps the most intriguing first-line drug used to treat drug-susceptible TB. Despite some unusual characteristics including an unusually high minimum inhibitory concentration for *M. tuberculosis* (6.25-50 µg/ml) and activity only under acidic conditions (i.e., pH 5.5), PZA is one of the most powerful sterilizing drugs we have available to treat TB. This prodrug is converted to its active form pyrazinoic acid (POA) by bacterial nicotinamidase/ pyrazinamidase which is effluxed out into the extracellular environment and protonated to HPOA (143). The specific mechanism of action by PZA from this point is somewhat of an unresolved issue. Microbial killing is thought to occur after HPOA re-enters the tubercle bacillus and either reduces the pH inside the bacterium, inhibits fatty acid synthesis, or disrupts the membrane transport capabilities of *M. tuberculosis* ultimately resulting in death of the pathogen (20, 58, 143). Like INH, EMB interferes with cell wall synthesis, but instead of mycolic acid formation this drug inhibits arabinosyl transferase. The action of EMB prevents *D*-arabinose from anchoring lipoarabinomannan to arabinogalactan resulting in an increase in mycobacterial cell wall permeability (123). The last truly novel drug to be implemented in anti-TB therapy was rifampin (RIF). RIF is one of the two most important drugs used to treat TB along with INH. This compound inhibits protein synthesis by disrupting mRNA transcription via binding of the β-subunit of DNA-dependent RNA polymerase (54).

Evolution Of The Standard Drug Regimen for TB Treatment. Early on in the TB chemotherapeutic era, the use of monotherapy was found to result in the emergence of drug resistance while administering multi-drug therapy abrogated this effect. The first

multidrug regimen prescribed to treat TB involved 18-24 months of SM, PAS and INH given daily. PAS was mainly used as a companion drug with INH to prevent emergence of drug resistance but development of the more effective EMB subsequently replaced PAS in standard therapy. RIF replaced SM in TB chemotherapy resulting in a significant reduction in treatment time from 18-24 months to 6-9 months of daily treatment. The contribution of PZA to TB therapy further reduced the duration of treatment and facilitated the use of 6 month drug regimens. The frontline drug regimen currently prescribed to treat drug-susceptible TB consists of a 2 month 'intensive phase' composed of INH+RIF+PZA+EMB followed by a 4 month 'continuation phase' in which only INH and RIF are administered. When prescribed and followed correctly, this regimen is very effective against drug-susceptible *M. tuberculosis* with low relapse rates (estimated 4-5%) and minimal occurrence of severe adverse reactions. The discovery and implementation of effective TB chemotherapy contributed to declining case rates around the world at first, and soon this disease was no longer perceived to be a threat. With the exception of a few rifamycin-based derivatives (i.e., rifabutin, rifapentine), no truly novel antibiotics have been introduced into routine TB treatment in almost 50 years. The lack of new antibiotics, coupled with the problems associated with current frontline therapy, however, has contributed to a reversal in these once-declining TB trends.

Tuberculosis Today. It is currently estimated that up to one-third of the world's population is latently infected with TB. In 2007 there was an estimated 9.27 million new cases of primary tuberculosis reported, which was slightly higher than the 9.24 million new incidences in 2006 (100). In addition to drug-susceptible TB, MDR- and XDR-TB

are also continued sources of concern. Of all new cases reported in 2007, 4.9% of the cases (or 511,000 patients) were positive for MDR-TB. MDR-TB is defined as disease caused by *M. tuberculosis* with resistance to at least the two frontline drugs INH and RIF. These patients are associated with poorer treatment outcomes as they must be treated with second-line drugs that are more toxic and less effective than current frontline therapy. In 2008, the highest rates of MDR-TB ever recorded by the World Health Organization (WHO) occurred in the former Soviet Union, where 1 in 10 of these patients had XDR-TB (99). XDR-TB has been defined as *M. tuberculosis* with resistance to at least INH and RIF, any drug from the fluoroquinolone class, and to at least one of the three second-line injectable drugs (amikacin, capreomycin, or kanamycin). It is estimated that 40,000 new cases of XDR-TB are diagnosed each year (62). These patients respond poorly to chemotherapy with approximately 60% considered treatable and therefore close to 40% considered not treatable. In addition to new cases of primary TB in 2007, 1.16 million cases occurred in patients who had already experienced at least one previous episode of TB in the past and had received at least one month of anti-TB treatment. Furthermore, 289,000 of the 511,000 reported incidences of MDR-TB in 2007 were documented in patients with this background (100). Issues concerning currently available TB chemotherapy have clearly contributed to the perpetuation of TB.

Tuberculosis And HIV/AIDS. Attributes of TB disease and *M. tuberculosis* are not the only things that must be contended with when searching for more effective TB chemotherapeutics. TB co-infection with HIV/AIDS is an ongoing epidemic that is wreaking havoc in sub-Saharan Africa. Of the 9.27 million estimated new cases of TB in

2007, roughly 15%, or 1.37 million, were HIV-positive (100). Immunosuppression is a key predisposing factor for the development of active TB disease, and the effects of HIV/AIDS on the host's immune system renders co-infected patients unable to control mycobacterial replication and dissemination. The potential negative interactions between anti-TB and antiretroviral (ARV) drugs are multi-fold (87). Co-administration of rifamycins with two of the most commonly used drugs prescribed for HIV (protease inhibitors and non-nucleoside reverse-transcriptase inhibitors) has been shown to decrease the drug plasma concentration levels of the latter drugs. Furthermore, toxicity issues stemming from simultaneous drug administration of anti-tubercle and ARV therapies has been implicated in the development of severe underlying diseases including hepatitis and/or immune reconstitution inflammatory syndrome. Any one of these factors may lead to a breakdown in effective TB treatment thereby increasing the likelihood of relapse, drug resistance, transmission, and ultimately contributing to the continued existence of *M. tuberculosis*.

Shortcomings Of Tuberculosis Therapy. The rate of treatment noncompliance by patients prescribed to the frontline TB drug regimen is unacceptably high. Although a variety of factors contribute to patient non-adherence, as reviewed by Munro *et al.* (94), a central underlying deficiency associated with the breakdown of patient therapy is the sheer length of time required to ensure clearance of *M. tuberculosis* bacilli without relapse. When TB patients do not successfully complete the 6-9 months of daily therapy, the risk of relapse is greatly increased and individuals may develop an active infection. In rare instances, the incomplete sterilization of tubercle bacilli from the host may result in

the rise of drug resistance, rendering previously effective treatments useless. The majority of TB infections involving drug-resistant strains of *M. tuberculosis* come about as a result of patient non-adherence or incorrectly prescribed treatments issued by doctors. The ability of *M. tuberculosis* to remain in a “drug-refractory” state is why currently available drug regimens take so long to be truly effective. We need more effective drugs designed to be bactericidal against persisting *M. tuberculosis* in order to shorten the length of TB treatment, however persistence and the underlying mechanisms/conditions that mediate it are still poorly understood.

...so why are persisting bacilli so complicated and tough to kill...?

1.3 PATHOLOGY, PERSISTENCE, AND OTHER PROBLEMS COMPLICATING CHEMOTHERAPY

Histopathologic Presentations of Tuberculosis. The primary site of infection for *M. tuberculosis* is the pulmonary cavity. The seeding of this location may result in the formation of distinct inflammatory lesions called granulomas. These granulomas are the distinguishing feature of pulmonary TB infection. *Granulomatous inflammation* is defined in Robbins and Cotran Pathologic Basis of Disease as a distinct mononuclear inflammation, usually in response to a persisting infectious agent, characterized by accumulations of activated macrophages called “epithelioid” cells (74). Humans infected with TB exhibit a myriad of pulmonary lesions: necrotic granulomas, inflammatory lesions and cavitary lesions to name a few. Each one of these ‘tuberculomas’ presents a distinct *in vivo* environment. Evidence suggests that environmental stimuli may affect certain metabolic pathways of *M. tuberculosis* by inducing the expression of certain genes required for survival (134). Thus, a better understanding of these micro-environments and the influence they have on *M. tuberculosis* bacilli must be elucidated in order to facilitate the development of more potent TB drugs.

Necrotic Granulomas. The classic, “hallmark” manifestation of pulmonary TB is the necrotic granuloma. Studies using animal models have suggested that necrotic granuloma formation is initiated early on after infection likely by the host innate immune response and later on by the subsequent adaptive immune response (127). The morphological structure of these granulomas consists of a central necrotic core

surrounded by a cellular layer composed of macrophages, lymphocytes, epithelioid cells, and Langhans giant cells. An acellular transition zone exists between the necrotic core and surrounding cell layer that may contain a few intact macrophages dispersed throughout its borders (48). Cells located at the periphery of the necrotic region are enmeshed in a fibrotic network forming the outer wall of the granuloma. One viewpoint on the purpose of these pathological structures from the standpoint of the host has been hypothesized to prevent bacterial dissemination and serve as a focused site to concentrate the immune response (129). During TB infection, necrotic granulomas may be partially or completely healed which is evidenced by fibrosis, mineralization, and even calcification. Although direct evidence is lacking, there is mounting evidence to suggest that these pulmonary lesions harbor decreased O₂ tensions. Several animal models exhibiting morphologically similar lesions to necrotic granulomas in humans have been shown by our laboratory (78) and others (132) to have depleted oxygen conditions in areas of caseous necrosis and dystrophic mineralization.

Non-Necrotic Granulomas. Although necrotic granulomas may serve to prevent bacterial dissemination, they are not always successful. *M. tuberculosis* bacilli may spread throughout the body using blood or lymph as means for transport after establishing a pulmonary infection. Circulating bacilli may re-infect the lung, at which time an inflammatory lesion, or non-necrotic granuloma, is formed (38). The main pathological feature that distinguishes necrotic from non-necrotic granulomas is the lack of necrosis in the latter. These inflammatory lesions may increase in size, but they maintain their cellular nature throughout infection. Another key difference setting non-

necrotic granulomas apart from necrotic ones is the presence of decreased O₂ conditions. Hypoxia is a condition generally not considered present in non-necrotic inflammatory lesions even though some level of decreased oxygen undoubtedly exists in these areas due to extensive immune cell infiltration interfering with efficient gas exchange.

Cavitary Lesions. Cavitary lesions are characterized by liquefactive necrosis that is surrounded by an outer wall of collagen. Cavitary lesions can occur in TB patients despite a robust cell-mediated immune response, however the process of liquefaction and subsequent cavitation are poorly understood. One speculative mechanism implicates a role for delayed-type hypersensitivity (DTH) in cavity formation (38). It has been proposed that DTH mediates a cytokine/chemokine response that increases the population of mΦs around solid caseum which become activated and produce large amounts of hydrolytic enzymes. High levels of β-galactosidase, a classical marker for mΦ activation, have been found in cells closest to liquefied caseum (72). The hydrolysis of proteins and macromolecules increases the osmolarity of the caseum drawing water in from surrounding tissues to contribute to the process of liquefaction. Cavitary lesions are of special concern because they can establish communication with surrounding airways and discharge the liquefied caseum into air spaces. At this time, an infected person may transmit *M. tuberculosis* to a new host by coughing and expelling this liquefied material into the air.

Implications Of Lesion Pathology. Each type of granuloma induced by *M. tuberculosis* presents a distinct micro-environment. The heterogeneity of the

environmental conditions present within each of these granulomas may be an underlying reason for the need of prolonged multi-drug therapy to successfully treat TB. Different environmental conditions can affect bacterial replication and metabolism which in turn changes the responsiveness of *M. tuberculosis* to drugs. The Wayne Model has shown that *M. tuberculosis* can enter two stages of non-replicating persistence (NRP) when grown under hypoxic conditions *in vitro* (140). The gradual shift-down of bacilli into this non-replicating state is associated with decreased susceptibility to first-line drugs that are effective against metabolically active bacilli. Detection of *M. tuberculosis* transcripts in lung tissue from human patients has also supported evidence that bacilli alter gene expression patterns in response to the different environmental conditions associated with the different types of granulomas induced by pulmonary TB infection (48). The significance of the results of all of these studies boils down to the fact that *M. tuberculosis* responds and adapts to its habitat. This means that new, highly effective therapy strategies must be found that are efficacious against all metabolic forms of *M. tuberculosis*. Therefore, the response of *M. tuberculosis* to the different *in vivo* environments it encounters must be elucidated so that novel drug regimens can target the microbial pathways that allow this pathogen to survive under each of these conditions.

Drug Tolerance. Drug tolerance (or phenotypic drug resistance) is a phenomenon whereby genetically homogenous population of bacteria can demonstrate a variable range of susceptibility to a known bactericidal antibiotic (79). This trend of decreasing antimicrobial efficacy over time is characteristic of almost all antibiotics and has been seen in many bacterial species (12). Most antibiotic killing curves exhibit an initial

exponential decrease followed by reduced bactericidal activity thereafter *in vitro*. The initial exponential decrease is associated with killing of the actively replicating microbial population which eventually leaves behind a small proportion of drug tolerant bacteria. This sub-population of 'tolerant' bacteria can grow to original titer in the absence of drug but will exhibit a similar pattern of drug susceptibility if re-exposed to the same drug. Thus, drug tolerance is not a result of genetically acquired resistance but must be the result of some other mechanism.

There are many theories attempting to explain the nature and mechanism of drug tolerance. One such theory has been attributed to preexisting physiological heterogeneities occurring within a minority population of genetically homogenous bacteria that can be observed prior to the administration of drug. Within a population of *Escherichia coli*, it has been observed that a small proportion of bacteria replicate at a slower rate compared to the majority prior to antibiotic exposure. This population of "slow-replicators" was found to be resistant to the effects of ampicillin while the majority of *E. coli* (the "normal-replicators") were susceptible (12). Thus, for some bacteria, drug tolerance may be the result of intrinsic differences in growth rates among genetically identical bacteria. This hypothesis is currently being studied in the context of *M. tuberculosis* by McKinney *et al.* using a microfluidics system that records cell division prior to the administration of antibiotics. Alternatively, drug tolerance is hypothesized by others to be a stochastic process. The random distribution of bacteria may present the "right" extrinsic and intrinsic signals to induce a phenotypic tolerant state for some bacteria but not for others under similar conditions (47). There is also evidence to suggest that DNA damage may serve as a signal for certain bacteria to switch to a phenotypically

tolerant state. This phenotypic switch is associated with the expression of a set of genes induced by DNA damage, termed the SOS response, that allow bacteria to arrest normal cell growth in order to focus on repairing nucleic acids (122). The protein LexA has been shown to mediate the SOS response in *E. coli* and similar genetic motifs for this protein have been found in other bacterial spp. including *M. tuberculosis* (41). Which one of these mechanisms, if any, contribute to *M. tuberculosis* drug tolerance remains a mystery. However, these hypotheses are currently being investigated in the context of tuberculosis which will undoubtedly aid the drug discovery and development process immensely.

In vivo Persistence Of Mycobacterium tuberculosis. Literally, to persist means to go on resolutely or stubbornly in spite of opposition (3). For TB infection *in vivo*, persistence refers to the ability of *M. tuberculosis* to remain viable in host tissues despite constant pressure from both the host immune response and bactericidal drug exposure. *M. tuberculosis* persistence can be demonstrated using the Cornell murine model (83-86). In this model drugs are administered to mice infected with *M. tuberculosis* until bacterial numbers are driven to undetectable levels and mice are apparently rendered sterilized. Antibiotic treatment is then stopped and mice are left untreated for a period of time before being euthanized for bacterial load determination. According to the model, a small proportion of these mice will have relapsed yielding cultures of drug susceptible *M. tuberculosis*. This ability of *M. tuberculosis* to persist in the face of drug treatment is the reason why standard chemotherapy takes 6-9 months of daily treatment to completely sterilize TB patients.

The Killing Kinetics Of Anti-Tuberculosis Drugs. Both drug tolerance and persistence are significant obstacles that must be overcome to develop more effective TB drugs. The need for prolonged chemotherapy for TB patients is believed to be required to kill drug tolerant/ persistent mycobacteria. TB drugs exhibit biphasic killing kinetics of *M. tuberculosis in vivo*, demonstrated by an initial period of rapid killing of actively replicating bacilli followed by an extended period of bacteriostatic activity despite the persistence of a small population of metabolically inactive mycobacteria. Drugs like INH (and the majority of anti-bacterial drugs in general) are most effective against metabolically active bacteria because they target pathways involved in aspects of cell division such as cell wall synthesis. These types of drugs are usually most effective early after the onset of treatment and are said to have ‘early bactericidal activity’ (EBA). Drugs like RIF, on the other hand, target processes like transcription, translation, or electron transport and are bactericidal against all metabolic populations of mycobacteria including NRP and persisting bacilli (139, 140). These types of drugs are said to have ‘sterilizing activity’ as their bactericidal activity either remains or begins at a time when drugs targeting actively dividing bacteria have lost efficacy. We need more effective sterilizing agents against *M. tuberculosis* in order to shorten standard chemotherapy. This underscores the importance of designing preclinical animal models to generate as much predictive information on an experimental drug as possible. Being able to distinguish a compound’s potential EBA or sterilizing activity early during the drug development process will greatly improve our ability to select only compounds with real potential of shortening TB treatment regimens for clinical trials.

1.4 MYCOBACTERIUM TUBERCULOSIS UNDER EXPERIMENTAL CONDITIONS

In vitro Models Of Mycobacterium tuberculosis. *In vitro* testing of drugs for TB activity is a necessary and relevant first step in the evaluation of an experimental compound. Experimental manipulation of *M. tuberculosis in vitro* has contributed much to our understanding of the genetics and growth kinetics required by the pathogen for survival. Much attention has been focused on studying the mycobacterial response to various nutrient depletions and how this response affects drug efficacy. A selection of *in vitro* studies that have greatly contributed to our knowledge survival mechanisms utilized by *M. tuberculosis* will now be briefly described below.

The Oxygen Depletion Model. Of the various environmental stimuli believed to be present during human TB infection, oxygen deprivation has likely been the most thoroughly investigated. Wayne *et al.* found that *M. tuberculosis* bacilli die when shifted abruptly from aerobic to anaerobic conditions but can enter a reversible, non-replicating state under conditions of gradual oxygen depletion (140). *M. tuberculosis* bacilli demonstrate three distinct phases of replication while suspended in a slowly stirred, limited head space ratio (0.5 HSR) culture tube. Initially, increased turbidity indicative of exponential growth is observed under aerobic conditions. As oxygen saturation approaches 1%, bacilli transition into non-replicating phase-I (NRP-I) and stop dividing. Bacilli shift from NRP-I to NRP-II when the oxygen tension drops to approximately 0.06% saturation at which time bacterial metabolism and protein synthesis ceases.

In addition to analyzing *M. tuberculosis* growth kinetics under various O₂ tensions, Wayne *et al.* also studied how these changes in growth rates affected the activities of different drugs with specific mechanisms of action (139, 140). The activities of the frontline drugs INH and RIF were compared to metronidazole (MET), a clinical drug currently used for a broad array of anaerobic infections (46). INH and RIF were highly effective against replicating bacilli in a continuously agitated, aerobic culture tube. However, the activity of INH especially declined concomitantly with diminishing O₂ levels. MET, on the other hand, had no effect against replicating bacilli under aerobic conditions and had only a marginal effect at high concentrations (64 µg/ml) against bacilli under microaerophilic conditions. Interestingly, MET was found to be most efficacious against older cultures of NRP-II bacilli under anaerobic conditions at 12 µg/ml (140). The results of these experiments suggest that drugs with distinct mechanisms of action can be used in combination to target multiple metabolic populations of bacilli in order to exert the maximal bactericidal effect against *M. tuberculosis*.

Genetic Characterization Of The In vitro Hypoxia Model. The work of Wayne *et al.* has sparked much *in vitro* research investigating the nature of oxygen-starved *M. tuberculosis*. Micro-array studies involving low oxygen culture conditions revealed a set of up to 48 genes under the control of the DosR regulon [reviewed in (134)]. The expression of these genes by *M. tuberculosis* is induced when aerobic respiration is inhibited by either oxygen deprivation (104) or the presence of nitric oxide (135). Recently, an isotope coded affinity tag-based (ICAT) proteomic analysis method was

utilized to examine differences in protein expression of log phase, NRP-I, and NRP-II bacilli (32). It was found that overall gene and protein expression was reduced in NRP-I bacilli (586 proteins) versus NRP-II bacilli (628 proteins). Furthermore, an increase in proteins involved in small molecule degradation was observed in NRP-I bacilli while an increase in proteins involved in energy metabolism was found to be increased in NRP-II bacilli. These studies suggest that a highly ordered down-regulation of transcription and translation by *M. tuberculosis* takes place while adapting to reduced O₂ concentrations. As bacilli sense decreasing O₂ conditions, energy stores are built up during NRP-I that are subsequently used during NRP-II to maintain viability (32). The underlying implications of the proteomic analysis on NRP-I and NRP-II bacilli are two-fold. First, the fact that gene and protein expression levels were somewhat increased in NRP-II compared to NRP-I bacilli further supports the misuse of the term “dormancy” to describe non-replicating bacilli. Secondly, this study provides insight into developing more effective chemotherapeutics against non-replicating bacilli as proteins expressed in NRP-II may represent potential drug targets.

In vivo Mycobacterium tuberculosis Models. To date, there have been a number of animal models used to study the different aspects of TB infection. These animal models have contributed greatly to our understanding of TB pathogenesis, pathology and immunology. Animal models have also proven invaluable for testing experimental drug compounds and vaccines in preclinical trials. However, there is not one animal model that shows all of the pathological features observed in human patients. The choice of animal model will depend on the scientific question to be addressed. Of all animals used

to model TB disease, four species (mouse, guinea pig, rabbit, and non-human primate), have been studied the most extensively for infection with *M. tuberculosis*.

The Murine Model. The most widely used animal model of TB used in research is the murine model. Considering the high cost of biosafety level-3 (BSL-3) animal work, mice are the most economical animal species due to their small size and ease of manipulation. The extensive collection of immunologic reagents and the availability of a wide array of gene knockout (GKO) mouse strains have been instrumental in elucidating key immune functions essential for host survival. Among the multitude of cytokines being induced following TB infection, IFN-gamma (52), TNF-alpha (53), and IL-12 (35) have been shown to be crucial for protection against *M. tuberculosis* infection in mice. In addition, both wild-type (WT) and GKO mice have proven very useful as preclinical models to test experimental compounds for anti-TB efficacy prior to entering clinical trials (70, 76). The limitations of the murine model with respect to human disease, however, must be taken into consideration when interpreting data. The most commonly used laboratory mouse strain is the C57BL/6 mouse. This resistant murine strain does not show all of the pathological characteristics or disease progression seen in human disease. Following a low-dose aerosol (LDA) infection with approximately 50-100 colony-forming units (CFU) of *M. tuberculosis*, the bacteria start to replicate. About 1 month post-aerosol infection, bacterial numbers stabilize between 10^5 and 10^6 bacilli in the lungs and a chronic infection is established. This chronic state is maintained for over a year in C57BL/6 mice before resumption in bacterial growth leads to death as mice age. The course of chronic infection in mice does not reflect the majority of human latent TB

infections worldwide. In human LTBI, the bacterial burdens are maintained at very low levels while the bacterial load in the lungs of C57BL/6 mice is far higher. WT mice form only one type of lesion that most closely resembles secondary lesions arising from hemolymphatic dissemination in humans (109). Furthermore, mice do not normally develop cavitory disease or caseous necrosis, the latter of which being seen rarely only during late stages of disease. Studies have gone on to show that hypoxic conditions are not generally encountered during TB infection in mice (8).

The Guinea Pig Model. Similar to mice, guinea pigs develop a chronic infection after LDA with approximately 30 CFU of *M. tuberculosis*. These animals are highly susceptible to TB and invariably die from the disease within a few months to a year. The guinea pig has had a profound impact on our understanding of granuloma formation (89), on bacterial virulence factors (19), and has been an important tool for the assessment of experimental drugs and vaccines (102, 117). Although not a complete representation of the full spectrum of human lung lesions, guinea pigs do form primary granulomas and secondary lesions that resemble necrotic granulomas and non-necrotic lesions in humans, respectively. Approximately 11 days after LDA infection with *M. tuberculosis*, guinea pigs show initial signs of granulomatous inflammation that progressively develop into primary granulomas about 1 month later. Primary granulomas in guinea pigs display a necrotic core that can become caseated, mineralized and develops hypoxia (78, 132) similar to necrotic lesions in humans. The onset of adaptive immunity coincides with the development of secondary lesions that maintain their cellular nature throughout the course of disease much like the non-necrotic granulomas seen in human pulmonary TB

infection. Guinea pigs are relatively inexpensive to house under BSL-3 conditions compared to larger animals such as the rabbit and non-human primate. The recent progress and availability of some basic immunologic reagents has allowed for the characterization of basic cellular immune responses in these animals (98) and has allowed for cytokine profile comparisons between primary granulomas and secondary lesions (81). However, the number of available immunologic reagents is still insufficient and needs further development. In the context of drug development, guinea pigs are often used as a secondary animal model to confirm anti-TB activity of lead compounds. The heterogeneity of pulmonary lesions in these animals means that drugs can be tested against bacilli inhabiting a variety of environments *in vivo* similar to the conditions encountered in human infection (78).

The Rabbit Model. Rabbits are considered the most resistant laboratory animal to infection with *M. tuberculosis*. In fact, it has been observed that some rabbits have completely cleared a TB infection after aerosol exposure (82) making this a useful animal to study the innate mechanisms mediating bacterial elimination early during human infections. These animals are uniquely susceptible though to the bovine specie of tuberculosis, *Mycobacterium bovis* (*M. bovis*). The work of Dannenberg *et al.* has shown that after infection with either *M. tuberculosis* or *M. bovis*, the Lurie rabbits can form primary granulomas with cores of caseous necrosis, secondary lesions, and cavitary disease (38). More recently, a rabbit model of TB meningitis has been developed and used to compare virulence between clinical and laboratory isolates of *M. tuberculosis* (125, 126) as well as differences in the immune responses modulating infection with each

of these strains (113). There are several features of the rabbit model, however, that limits their use including the high cost of BSL-3 containment and a lack of immunologic reagents available for use. These limitations have prevented the full characterization of immune regulators involved in TB infection of the rabbit and have thus restricted its widespread use in preclinical drug testing.

The Non-Human Primate Model. The non-human primate (NHP) is perhaps the only animal model that can accurately mimic the full range of human TB disease. Primates can develop both active and latent infection, exhibit the same heterogeneity in pulmonary pathology as humans, and have a wide array of immunologic and pathologic reagents available for analysis. The NHP model has been used to study HIV/AIDS-TB co-infection in humans since they are routinely used to study simian immunodeficiency virus (SIV). After LDA (approximately 15-25 CFU) with *M. tuberculosis*, about 40% of NHPs develop active TB while approximately 60% develop a latent TB infection (29). Primates (with both progressive disease or latently infected) display the full extent of pulmonary lesions seen in humans including necrotic granulomas, non-necrotic granulomas, and cavitory lesions (51). The similarities in disease progression and pathology of NHPs with humans make their use in the testing of experimental drugs and vaccines particularly relevant. Drugs in these animals are being evaluated against different populations of bacilli inhabiting a variety of micro-environments resembling conditions present in humans. However, there are a number of significant drawbacks that have limited the use of NHPs in TB research. The prohibitively high cost and large amount of space required to house these animals severely restricts the number of

specimens used for each experiment. In addition, other disadvantages associated with this model include the risk of TB outbreaks among primate colonies housed in research facilities, and the risk of exposure to personnel.

Significance Of Animal Models In Drug Development. Clearly, the strengths and weaknesses of each species preclude the designation of any one animal as the “best” model to study TB. Each animal model provides a unique perspective on the varied presentations of *M. tuberculosis* disease, but for the purposes of preclinical drug testing, the use of some species is simply not feasible. The high cost associated with the rabbit and NHP models will probably prevent their use from becoming commonplace in the evaluation of experimental chemotherapy. However, continued examination of the immunopathologic response to *M. tuberculosis* elicited by these animals will surely contribute to our understanding of the mechanisms that govern the outcome of infection in humans, and thus facilitate the development of new drugs. The most relevant (and feasible) animal models available to test anti-TB drugs with are most likely the mouse and guinea pig due mainly to their relatively low cost for BSL-3 containment. It is important to recognize, however, that differences in pulmonary TB infection between these two species and with humans means that experimental drugs are tested for different things in different animals. The mouse model is used to address long-term drug toxicity issues, multi-drug regimen efficacy studies, sterilizing activity in relapse of infection experiments, and assessing the effects of combination chemo-/immunotherapy. The guinea pig on the other hand has more relevant pathology than the mouse. The *in vivo* conditions present in the guinea pig allow for drugs to be tested under conditions similar

to those encountered in human pulmonary disease. When using animals to model TB in humans, it is clear that no one species serves as the gold standard with which to obtain information about *M. tuberculosis* or an experimental compounds efficacy in hopes of extrapolating it to human results. However, each animal can provide specific information on certain aspects of TB that has significant applications to human disease as long as care is taken when interpreting results.

The tools to study tuberculosis are there, so what needs to be done next...?

1.5 FACILITATING THE DEVELOPMENT OF HIGHLY EFFECTIVE DRUGS FOR TUBERCULOSIS TREATMENT

What We Need In New Drugs. The requirements of new, highly effective chemotherapeutics for TB therapy have been clearly laid out by institutions such as the Stop TB Partnership Working Group on New TB Drugs. We need drug regimens that: 1) achieve a cure in 1 to 2 months or less, 2) have novel mechanisms of action that are effective against MDR-/XDR-TB, 3) are able to be co-administered with ARV therapy, and, 4) are effective against latent TB (5). Finding a short-course cure for TB is vitally important. Current drug therapy effectively eliminates *M. tuberculosis* but is lengthy; therefore drug development should be concentrated on targeting persistent bacilli. In order to do this, we must fill the gaps in our knowledge of TB persistence including the location of this bacillary sub-population. Uncovering the location of persisting *M. tuberculosis* will undoubtedly provide much-needed insight into the mechanisms allowing this pathogen to survive. Developing drugs with novel mechanisms of action would potentially be applicable to treatment of not only drug-susceptible TB, but for the treatment of MDR-/XDR-TB as well. The highest priority for TB drug development is to shorten the length of chemotherapy while developing drugs to be effective against bacilli in a latent TB infection is secondary as active TB disease is responsible for the global TB mortality rate. Furthermore, when drug regimens highly active against *M. tuberculosis* are found, subsequent testing with ARV co-administration will be required to develop a new standard TB drug.

New Drugs In The Pipeline. Despite the overwhelming morbidity TB has caused since antiquity, there is reason to be optimistic for the future. There are a number of new drugs currently in the clinical trial pipeline for the first time in over 40 years. The compounds TMC207 by Johnson and Johnson, linezolid and derivatives by Pfizer, PA-824 by the TB Alliance for Drug Development and other nitroimidazoles by Novartis are all such compounds. The diarylquinolone TMC207 has a novel mechanism of action that targets adenosine tri-phosphate (ATP) synthase leading to ATP depletion and pH homeostasis, has excellent early bactericidal and sterilizing activity *in vitro* and in animal models, and is efficacious against drug-susceptible and drug-resistant *M. tuberculosis in vitro* (9). The oxazolidinone linezolid interferes with protein synthesis by inhibiting the formation of the 70S ribosomal initiation complex (21). This drug has been shown to be effective against MDR- and XDR-TB (108) and was successful in treating patients who had previously received TB therapy and were incompletely sterilized (23). The nitroimidazole PA-824 also has a novel mechanism of action that inhibits the oxidation of hydroxymycolates to ketomycolates thus interfering with cell wall synthesis in addition to other unknown activities (120). This compound has been shown to exhibit good early bactericidal and sterilizing activity in mice and to be active against non-replicating bacilli (77). Compounds like these have real potential for shortening TB therapy as drug regimens must exhibit bactericidal activity throughout treatment. This highlights the importance of developing animal models to test experimental compounds that will accurately indicate a compound's potential to have early bactericidal and/or sterilizing activity. Having reliable, predictive information about a compound in preclinical trials

will be invaluable for the design and implementation of subsequent human clinical trials which are both costly and difficult to undertake.

Thesis Objectives. The ultimate goal of this project is to facilitate the selection of experimental TB compounds that have real potential of shortening standard treatment for further clinical trial testing by improving our understanding of how TB manifests in different animals used in preclinical drug evaluations. To accomplish this objective, a multi-faceted approach was undertaken to characterize *M. tuberculosis* infection and the bacillary response to chemotherapy in animal models commonly used to test experimental drugs. The first aim was to determine the histological location of bacilli persisting over time after drug treatment in different animals used to evaluate TB drugs. The second approach was to evaluate the therapeutic value of metronidazole for treating TB in infected guinea pigs. Metronidazole is a compound previously shown to be effective against nonreplicating bacilli grown under anaerobic conditions. The final aim of this project was to determine if the killing kinetics of TB drugs obtained in human clinical trials can be predicted using a murine model of bactericidal activity and whether or not these killing kinetics indicate a compound's potential sterilizing activity during the initial days of treatment. The sum of the results obtained from these experiments should improve our understanding of how differences in TB disease between animals used in preclinical TB drug testing effect the bacillary response to chemotherapy. Fully dissecting the differences between these animals will significantly enhance our interpretation of drug efficacy data and will ultimately contribute to building a more detailed drug profile on an experimental compound in preclinical trials. New drugs and

drug regimens that target all metabolic forms of *M. tuberculosis* must be found in order to shorten current standard TB therapy. The search for these drugs and drug combinations will be aided by the selection of only the most promising compounds for clinical trial testing. Clinical drug trials require an immense amount of time and money to carry out so great care is taken in the selection of which experimental compounds to take part in such trials. Much of this decision is based on the performance of such compounds in *in vivo* preclinical trials underscoring the importance of understanding what drugs are being tested against in different animals. Efforts should therefore be focused on comparing *M. tuberculosis* infection in different animal models and how these differences translate to human research. It is important to understand the context with which to interpret results obtained from one species versus another. Therefore, we must first begin our search for novel drugs to shorten TB chemotherapy by developing a better understanding of the animal models used to test them.

CHAPTER TWO

CROSS-SPECIES COMPARISON OF THE LOCATION OF *M. TUBERCULOSIS* IN PULMONARY GRANULOMAS OF MICE AND GUINEA PIGS AND ITS RELATIONSHIP TO DRUG TREATMENT

2.1 INTRODUCTION

The dynamics of the host-pathogen interaction have important implications for the design of new antimicrobial agents to treat chronic or latent infections such as TB, which is notoriously refractory to conventional drug treatment. The development and subsequent implementation of the current standard chemotherapeutic regimen for TB brought years of declining incidences around the world. Although highly effective, one significant drawback with this regimen is the lengthy 6-9 months of daily multidrug therapy required to achieve sterilization without relapse. This lengthy treatment is thought to be necessary to eradicate a small sub-population of *M. tuberculosis* bacilli persisting in the face of drug pressure. The adaptations that allow this pathogen to persist in certain locations of the host despite a vigorous adaptive immune response likely contribute to the difficulty in curing TB with antimicrobial drugs.

Studies have shown that different environmental conditions can induce *M. tuberculosis* to alter its metabolic state and replication rate thereby rendering bacilli refractory to drug treatment (18, 93, 105). The most widely used *in vitro* models are based on the adaptation of *M. tuberculosis* from exponential growth to stationary phase

(60), or to microaerophilic conditions when grown under gradual oxygen depletion (138) among others. Under these conditions, tubercle bacilli show a change in transcript profiles such as the activation of the DosR regulon (95, 110, 134). In contrast to the controlled conditions of these specific *in vitro* culture environments, the bacillary environment *in vivo* is far more complicated and largely remains a mystery. Tubercle bacilli in TB patients are likely to be metabolically heterogeneous since different types of lesions with distinct pathological features may be adjacent to each other at any one time (28). Host tissue necrosis is arguably the most important pathologic characteristic of the human ‘classical’ granuloma. Non-progressive lesions of tuberculosis often have limited vascularisation causing limited oxygen supply and nutrient starvation, which might induce bacterial persistence in these lesions. The importance of these unique lesion morphologies is that they represent severe tissue destruction, which we have shown to harbor persistent bacilli that are difficult to treat with standard regimens (78). The adaptive ability of *M. tuberculosis* in response to its environment has important implications for the development of new chemotherapeutic strategies. New drugs must not only target metabolic processes required by tubercle bacilli under different conditions but must also be active under the same environmental conditions that induce *M. tuberculosis* to change its metabolic profile (i.e., hypoxia, acidic pH, etc.).

A better understanding of TB lesion pathogenesis is emerging from evaluating animal models that demonstrate a varied immunologic and pathologic response to experimental infections (10, 14, 132). The use of animal models is critical in preclinical vaccine and preclinical drug development. In the discovery and development stages of TB drugs, mouse models provide useful information regarding aspects such as

absorption, bioavailability, tissue distribution, and efficacy of novel therapeutics *in vivo* (39, 70, 75). A second animal model such as the guinea pig can provide additional information in advanced testing of drug leads to define their sterilizing properties against a heterogeneity of TB lesions (67). However, pulmonary TB develops quite differently in the mouse than in the guinea pig underscoring the importance of fully characterizing and understanding differences between these models. These differences then need to be taken into account when evaluating experimental compounds. Numerous studies on the relative tissue oxygen tension levels in wild-type C57BL/6 and Balb/c mice have been performed. The authors of these studies all found hypoxia to be completely absent in TB lesions of infected mice (8, 124, 132) as the progression of disease rarely reaches the stages of extensive necrosis and mineralization (109). Pulmonary lesions in these mice maintain a cellular morphology that is characterized as an exudative inflammatory lesion (109). Lung lesions in guinea pigs infected with *M. tuberculosis*, on the other hand, have greater similarities to natural infection in humans including mixed inflammatory lesions and hypoxic granulomas consisting of a central core of caseous necrosis that may become mineralized (127). Recently, more focus has been brought to the study of comparative pathology and pathogenesis in different animal models (14, 132). However, little information regarding the growth kinetics of *M. tuberculosis* in different animal models or the actual location of the bacilli within the heterogeneous pulmonary lesions from one animal to another is available. Furthermore, in animal models used for preclinical testing of experimental compounds, the efficacy of a drug is mostly measured as the overall reduction in bacillary burden in the organs (quantitative assessment) rather than visualizing the effect of drug treatment on the microbial population in certain lesion

locations (qualitative assessment). Having both a quantitative and qualitative assessment of antimicrobial action would undoubtedly build a more comprehensive drug profile for an experimental compound during preclinical trials.

The current histological detection method most commonly employed by investigators to identify *M. tuberculosis*, either in tissues or in sputum smears, is the Ziehl-Neelsen (ZN) acid-fast stain (6, 30, 57, 59, 73, 131, 137). Fluorescence is preferred over bright field microscopy when examining sputum smears because it provides greater specificity at a lower magnification yielding more consistent results with less user-fatigue (118). Among the various fluorochrome staining reagents used in TB detection, the most common are auramine (A) or the auramine-rhodamine (AR) combination of fluorescent acid-fast stains. A recent review of 30 articles directly compared the abilities of AR and ZN staining techniques to detect *M. tuberculosis* in sputum smears. The authors concluded that although both ZN and AR show similar specificity, the AR technique was more sensitive in detecting lower bacterial numbers and facilitated microscopic evaluations versus the ZN stain (119). Although used to a much lesser extent on tissues than sputum smears, AR has been used to identify genetic variations between different inbred mouse strains that confer resistance or increased susceptibility to TB infection (116, 141).

In this chapter, we studied the location of *M. tuberculosis* in lung samples from different mouse models as well as guinea pigs using a modified AR staining method for use on tissues. The modified AR staining method was chosen over the conventional ZN method in order to facilitate the evaluation of a large number of whole lung tissue sections from multiple animal models while minimizing user fatigue. In addition to

characterizing bacilli location, differences in TB pathogenesis between these animals were evaluated. Finally, we compared the efficacy of single drugs in these animal models that are routinely used in our drug discovery efforts, focusing on the clearance of bacilli across lung lesions.

2.2 MATERIALS AND METHODS

Bacterial isolates. The virulent *M. tuberculosis* strain Erdman (TMCC 107), the standard strain used for drug testing in mice in our laboratory, was prepared as previously described (70). Briefly, *M. tuberculosis* Erdman was grown from low passage seed lots to mid-log phase in Proskauer-Beck medium containing 0.01% Tween 80 (Sigma Chemical Co., St. Louis, MO) and stored in vials frozen at -70°C until use.

The H37Rv strain of *M. tuberculosis* (Trudeau Institute, Saranac Lake, NY) is used routinely in our laboratory for guinea pig infection studies (22). *M. tuberculosis* H37Rv was grown from low passage seed lots in Proskauer-Beck liquid medium containing 0.05% Tween 80 to early mid-log phase and frozen in aliquots at -70°C until needed. Cultures were diluted in sterile water prior to use.

Chemicals and drugs. Isoniazid (INH), rifampin (RIF) and ethambutol (EMB) were obtained from Sigma Chemical Co. (St. Louis, MO). Gatifloxacin (GTF) and moxifloxacin (MXF) were kindly provided by Southern Research Institute (SRI) (Birmingham, AL). All drugs, except for RIF, were dissolved in water. RIF was dissolved in 100% dimethyl sulfoxide (DMSO) prior to dilution in distilled water (5% final DMSO concentration). Drug formulations prepared in distilled water were prepared weekly and stored at 4°C. All drug doses for guinea pigs were prepared with final w/v 40% sucrose to increase palatability for the guinea pigs, as is our general procedure and were prepared weekly and stored at 4°C. For the guinea pig studies, INH was dissolved in 40% (wt/vol) sucrose and administered in 1 ml per guinea pig. TMC207 was provided by Johnson and

Johnson (Tibotec, Belgium) and was prepared monthly in a hydroxypropyl- β -cyclodextrin solution (CD) as described before (9). Briefly, compound was dissolved in 40% hydroxypropyl- β -cyclodextrin (Acros Organics, New jersey, USA) in half of the total volume of drug required to dose all guinea pigs receiving this treatment for the duration of the trial. The suspension was stirred for 24 h at RT and shielded from light. After mixing, 1N HCl was added to a final concentration of 1% to facilitate dissolution and filter sterilized using 0.2 μ M syringe filter. The drug solution was then added to an equal volume of 80% sucrose to increase palatability dosing and administered in 1 ml per guinea pig.

Immunocompromised mouse TB infection model. Several short and longer term experiments were performed, and the general steps of the methodology are described below. Eight- to ten-week-old female specific-pathogen- free, C57BL/6-Ifngtm1ts gamma interferon gene-knockout (GKO) mice were purchased (Jackson Laboratories, Bar Harbor, Maine), and the experiment was performed largely as previously described (76), except for drug treatment being extended to day 49. Briefly, mice were exposed to a low-dose aerosol infection (LDA) with *M. tuberculosis* strain Erdman (TMCC 107) in a Glas-Col inhalation exposure system (Glas-Col Inc., Terre Haute, IN) (70). One day post LDA, three mice were sacrificed to verify bacterial uptake of 50 to 100 CFU per mouse. Each treatment group consisted of 5 mice for every subsequent time point. Treatment was initiated 18 days after LDA and lasted up to 49 days post LDA. Untreated mice cannot control the bacillary load and succumb to disease 28-30 days after LDA. INH was administered at 25 mg/kg, GTF and MXF at 100 mg/kg,

and all drugs were administered via oral gavage for 7 days/week. One control group of infected mice was sacrificed at the start of treatment, and a second group of infected untreated mice was sacrificed at different time points. Mice were sacrificed after 2, 5, 7, 10, 17, and 31 days after the start of treatment.

An additional experiment was undertaken to determine if the onset and progression of necrosis in the lungs of untreated IFN-gamma GKO mice coincided with the development of hypoxia. This experiment was performed largely as just described previously for the immunocompromised murine trials with the following exceptions: i) no mice were administered drug treatment, and ii) groups of 4 mice were sacrificed 15, 17, 20, 22, 25, and 29 days post-LDA and tissues were taken for histology.

Immunocompetent mouse TB infection model. Several short and long term experiments were performed, and the different protocols are described below. Six- to eight-week-old female specific-pathogen-free, immunocompetent C57BL/6 mice (Charles River, Wilmington, MA) were infected via a LDA exposure to *M. tuberculosis* Erdman as described before (70). Three mice from both aerosol runs were sacrificed one day post LDA to verify bacterial uptake of 100 CFU/mouse.

In short term experiment, drug treatment started 3 weeks after LDA and lasted for 7 days. INH was administered at 25 mg/kg, EMB at 150 mg/kg, MXF at 100 mg/kg, and RIF at 10 mg/kg, and all drugs were administered via oral gavage for 7 days. Groups of 5 mice each were sacrificed at the start of treatment and after 2, 5, and 7 days of drug therapy.

In a long term experiment, two successive aerosol runs with 90 mice each were completed, and the long-term mouse model was largely carried out as previously described (77). Briefly, treatment was started 3 weeks post-LDA and continued for 12 weeks. Five infected mice were sacrificed at the start of treatment to establish a baseline CFU. INH was administered at 25 mg/kg and RIF at 20 mg/kg, 5 days/week via oral gavage. Bacterial loads in lungs and spleens of treated and untreated groups were determined at 2, 6, and 12 weeks after the start of treatment.

Guinea pig TB infection model. Four to five month-old, female Hartley guinea pigs (Charles River, Wilmington, MA) weighing approximately 500 g each were exposed to a LDA of *M. tuberculosis* in a Madison aerosol chamber device as previously described (67). Briefly, guinea pigs were infected with a LDA resulting in approximately 20 lesions in the lungs. At 30 days post-LDA, 5 guinea pigs were sacrificed in order to determine bacterial load at the start of treatment. Guinea pigs were divided in groups consisting of 5 guinea pigs per group and each was treated by administering 1ml in the back of the mouth. Control groups received daily oral administration of 1 ml of 40% (wt/vol) sucrose. Drug treated groups were administered INH at 30 mg/kg, the bioequivalent dose achieving similar plasma levels in humans established previously in our lab (61), and TMC207 at 15 mg/kg for 5 days/week. Guinea pigs were sacrificed at 2, 4, and 6 weeks after the start of drug treatment.

Bacterial load determination in mice and guinea pigs by culturing. Mice were sacrificed by CO₂ inhalation, and spleens and left lung lobes were aseptically removed

and disrupted in a tissue homogenizer as previously described (77). The number of viable organisms was determined by plating serial dilutions of the homogenates on nutrient Middlebrook 7H11 agar plates (GIBCO BRL, Gaithersburg, MD). The plates were incubated at 37°C in ambient air for 4 weeks prior to the counting of viable CFU.

Guinea pigs were first anesthetized with ketamine and then euthanized by sodium barbital injection (Sleepaway; Fort Dodge Laboratories). Organs were aseptically removed and plated out as previously described (78). Briefly, right cranial lung lobes were excised and homogenized in 4.5 ml of 0.85% sterile saline with a tissue homogenizer (Kinematic Polytron; Brinkman Instruments Services, Westbury, NY). The number of viable organisms was determined by plating serial dilutions of the homogenates on nutrient Middlebrook 7H11 agar plates (GIBCO BRL, Gaithersburg, MD). The plates were incubated at 37°C in ambient air for 3 to 4 weeks prior to the counting of viable CFU.

Histology and acid fast staining. The lower right lung lobe was infused *in situ* with 10% neutral-buffered formalin and preserved until processed for histopathological assessment. At the time of processing, all tissues were embedded in paraffin and stained with hematoxylin and eosin (H&E).

Four µm thick sections were prepared from paraffin-embedded, formalin-fixed tissue. Staining with auramine and rhodamine was performed using the protocol from Becton, Dickinson and Company (Sparks, MD), modified for optimal staining of bacilli in animal tissues and by using counterstains to visualize the surrounding lung cells and tissue. Staining was performed with a combination of auramine O and rhodamine B

(Becton, Dickinson), hematoxylin QS (Vector Laboratories, Inc., Burlingame, CA) and 4'6-diamidino-2-phenylindole (DAPI from Sigma Chemical Co.). Tissue sections were dewaxed in xylene and rehydrated through a graded alcohol series, then stained with TB Auramine-Rhodamine T for 30 minutes. After washing excess stain with ddH₂O, slides were decolorized with TB Decolorizer TM (BD) until the excess stain was visibly dissolved. Counterstaining was performed with hematoxylin QS for approximately 5 seconds. After washing with ddH₂O to remove excess hematoxylin, slides were stained for 15 minutes with DAPI (diluted 1:5000) and then washed in ddH₂O.

Entire lung sections were then examined and scored using a set of criteria that gives an estimate of the total number of auramine-rhodamine positive (AR+) bacilli per tissue section. For murine lung tissue, at least 5 lung sections from each animal per group were evaluated and scored for each sacrifice time point. Untreated tissue sections were scored using the following criteria. Each lesion, airway, and blood vessel encountered in a tissue section was scored 0-8 where 0 equals no AR+ bacilli found and 8 equals >50 AR+ bacilli found. AR+ bacilli found in normal lung parenchyma were also scored on a scale of 0-8 where 0 equals no AR+ bacilli found in normal tissue and 8 equals >50 AR+ bacilli found in normal lung parenchyma throughout the tissue section being evaluated. In addition, whether or not AR+ bacilli were found intracellular or extracellular and relative proportions of each population were estimated. For drug-treated murine tissue sections, the same criteria described for the untreated tissue sections was used. Furthermore, the effect of drug treatment on AR+ bacilli clearance and lung pathology was evaluated by comparing tissue sections from early and late treatment time points with untreated control tissues.

For guinea pig tissues, 5 lung sections from 3 representative animals per group at each sacrifice time point were examined. With the exception of distinguishing between AR+ bacilli found in primary granulomas from those in secondary lesions, the same scoring criteria described for murine tissues was utilized for guinea pigs. It must be emphasized that the results of AR staining animal lung tissues are only valid under the experimental conditions observed.

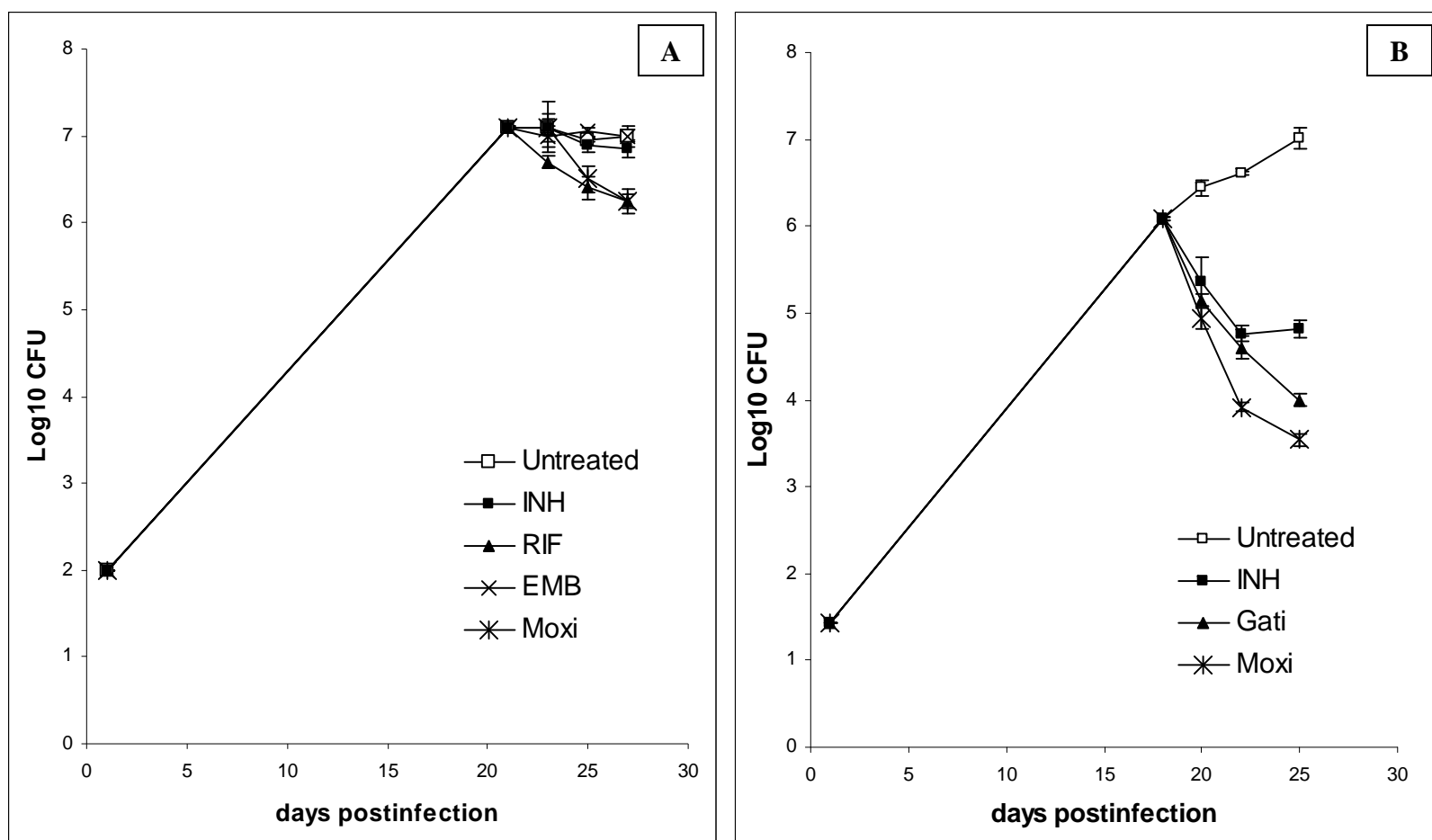
Pimonidazole staining of GKO lung tissues. H&E stained tissue sections from the lungs of untreated IFN-gamma GKO mice were examined 15, 17, 20, 22, 25, and 29 days post-LDA to characterize the onset and progression of necrosis. In addition, pimonidazole was used as described before (78) to detect hypoxia in the lungs of INF-gamma GKO mice at each of these time points. Pimonidazole is a 2-nitroimidazole that is able to identify regions of hypoxia ($<4 \mu\text{M O}_2$ saturation or O_2 tensions of 10 mm Hg) in animal organs after injection. Pimonidazole forms protein adducts with thiols groups in cells adjacent to hypoxic regions which stain distinctly with a monoclonal antibody (11). *M. tuberculosis*-infected mice were injected intraperitoneally (i.p.) with pimonidazole hydrochloride (Chemicon, Hampshire, United Kingdom) at a dose of 60 mg/kg mouse body weight dissolved in 1x PBS at 1.5 h prior to sacrifice at days 15, 17, 20, 22, 25, and 29 post-LDA. Five micron sections of paraformaldehyde-fixed, paraffin-embedded tissue sections were cut and mounted on slides for processing. Tissue sections were deparaffinized with xylene before performing antigen retrieval with pronase (Fisher Scientific, Schwerte, Germany) for 40 min. at 40°C. Endogenous peroxidase activity was reduced with 1% hydrogen peroxide in TBS for 20 min. at RT in the dark. The blocking

reagents avidin D and biotin were then added to each slide for 15 min. each. Sections were blocked with a mouse Ig blocking reagent (Vector) for 1 h at RT. Biotinylated anti-mouse IgG was pre-labeled with the anti-pimonidazole antibody for 10 min. and was applied to slides overnight at 4°C. DAB (Sigma) was applied to slides for 5-10 min. in the dark to visualize the reaction. Finally, slides were counterstained with Gill's Hematoxylin (Sigma) for 10 min. and cover-slipped.

2.3 RESULTS

Drug efficacy in immunocompetent vs. immunocompromised mice. The efficacy of drug panels was evaluated in the IFN-gamma GKO mouse (INH, gatifloxacin [Gati], moxifloxacin [Moxi]) versus the WT C57BL/6 mouse (INH, RIF, ethambutol [EMB], and Moxi) infected via LDA with *M. tuberculosis*. Results are presented in Figure 2.1. At the start of treatment, the bacterial load in the lungs reached $6.2 \log_{10}$ CFU in the GKO mice and approximately $7.0 \log_{10}$ CFU in the WT C57BL/6 mice (at 18 days post-LDA for both). At the completion of the study, the bacterial load in the untreated control group remained largely similar for the WT mice whereas the bacillary burden in the GKO increased by more than $1 \log_{10}$ CFU (Fig. 2.1). The activities of the tested drugs were evaluated over 7 days with sacrifice points after 2, 5 and 7 days of treatment. INH reduced the bacterial load only slightly over time in the lungs in the WT mice ($0.25 \log_{10}$ CFU reduction), whereas in the immunocompromised GKO mice INH showed significant activity over the first 5 days of treatment ($0.85 \log_{10}$ CFU reduction) (Fig. 2.1). The difference in drug activity between the two mouse strains was even more pronounced for MXF at 100 mg/kg, which reduced the bacterial load in the WT mice with $0.85 \log_{10}$ CFU and more than $3.5 \log_{10}$ CFU in GKO mice after 7 days of treatment when compared to untreated mice at the start of treatment.

Figure 2.1. Viable *M. tuberculosis* in the lungs of **A**, WT C57BL/6 and **B**, IFN-gamma GKO mice infected *M. tuberculosis* (\log_{10} CFU \pm SEM) and treated or not for 7 days starting 18 days post-LDA. **A**, WT mice received monotherapy with isoniazid (INH), rifampin (RIF), ethambutol (EMB) or moxifloxacin (Moxi). **B**, IFN-gamma GKO mice received monotherapy with INH, gatifloxacin (Gati), or Moxi. (5 animals per group).



Lung histopathology and location of *M. tuberculosis* in WT C57BL/6 mice.

lung sections from C57BL/6 mice 5 weeks post-LDA, pulmonary inflammatory lesions consisted of large lymphocyte (LC) aggregates surrounding multiple, smaller accumulations of macrophages (mΦ). This observation agrees with previously published data (109, 128). The majority of AR+ bacilli (about 90%) were found intracellular in the multiple mΦ aggregates surrounded by LCs (Figure 2.2 A and B). A small proportion of AR+ bacilli (about 10%) was observed in foamy mΦs (FM) located outside of the LC cuff. Nine weeks after LDA, most of the inflammatory lesions displayed a well-defined, highly organized lesion structure consisting primarily of a central core of mΦs and polymorphonuclear cells (PMN) surrounded by a distinct, sometimes incomplete LC rim. These advanced lesions sometimes exhibited a mild degree of tissue necrosis. A distinct increase in AR+ bacilli number was observed at this time, of which the majority (about 80%) was found intracellular within mΦs distributed throughout the central portions of inflammatory lesions within LC cuffs (Fig. 2.2 C). A small proportion of AR+ bacilli (about 20%) were found within FMs located outside of LC cuffs in the surrounding alveolar air spaces (Fig. 2.2. D). AR+ bacilli were not found in areas of necrosis.

After 2 weeks of chemotherapy with INH, RIF, or MXF, the inflammatory lesion pathology and location of bacilli in the lungs of mice were similar to those observed in the infected, untreated animals. Although pulmonary inflammation was reduced after 6 weeks of therapy compared to 2 weeks, lung pathology from drug-treated mice exhibited the same cell morphology and spatial distribution versus the untreated controls. A moderate decrease in the number of AR+ bacilli across the lungs of mice was evident after 6 weeks of chemotherapy. AR+ bacilli remaining after treatment were

predominantly intracellular within mΦs. The majority of AR+ bacilli (about 70%) was located inside of the LC cuffs of pulmonary lesions within mΦs composing the cores while the minority (about 30%) was found outside of the LC cuffs within FMs situated at the peripheral edges of inflammatory lesions (Fig. 2.2 E and F).

Figure 2.2. Modified AR stained lung tissues from untreated (**A-D**) and MXF-treated (**E** & **F**) lungs of WT C57BL/6 mice infected with *M. tuberculosis*. Scale bars = 100 μ M

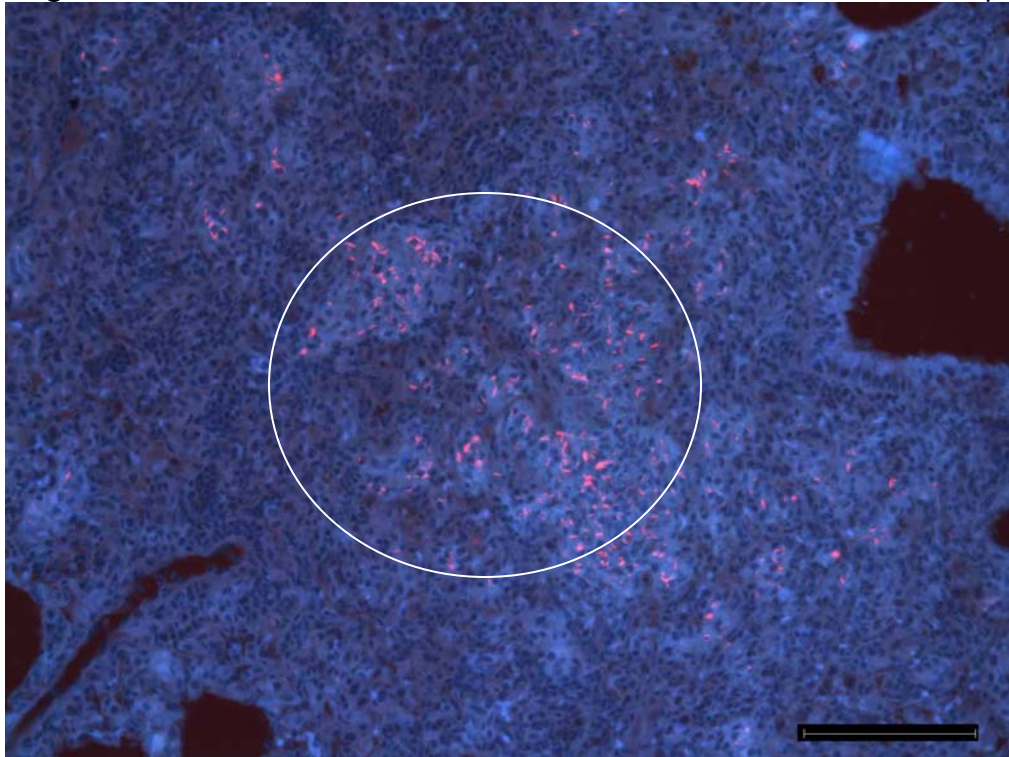


Fig. 2.2A Inflammatory lesion 5 weeks (wks) post-LDA (200x)

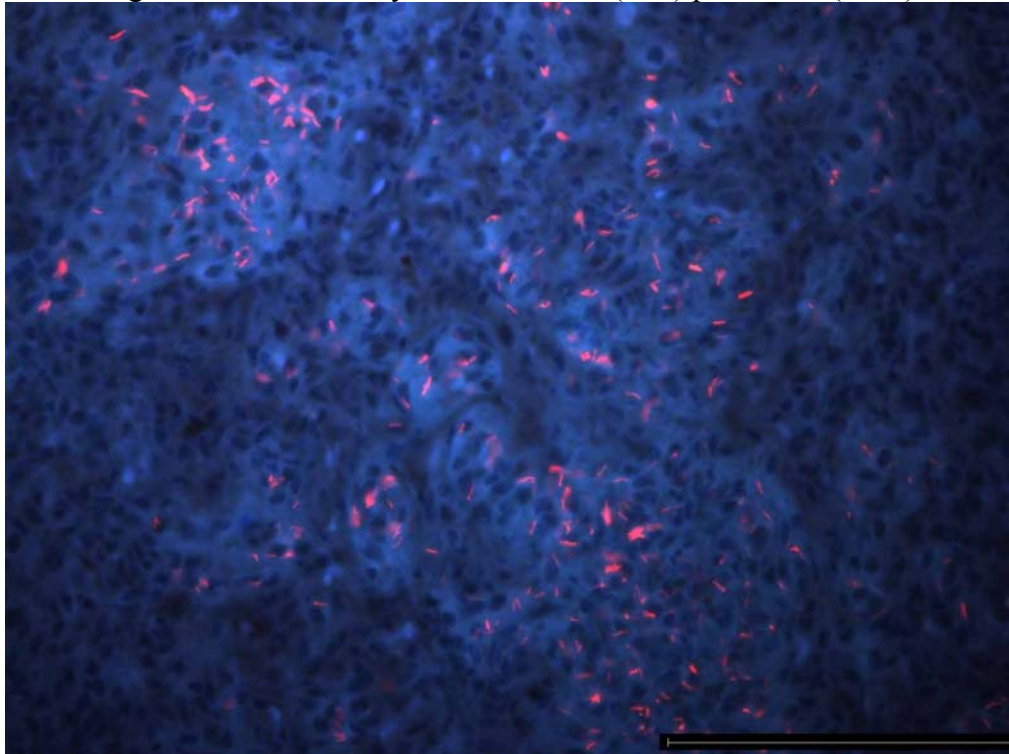


Fig. 2.2B Close-up of Fig. 2.3A (400x)

Fig. 2.2C Lesion 9 wks post-LDA (200x)

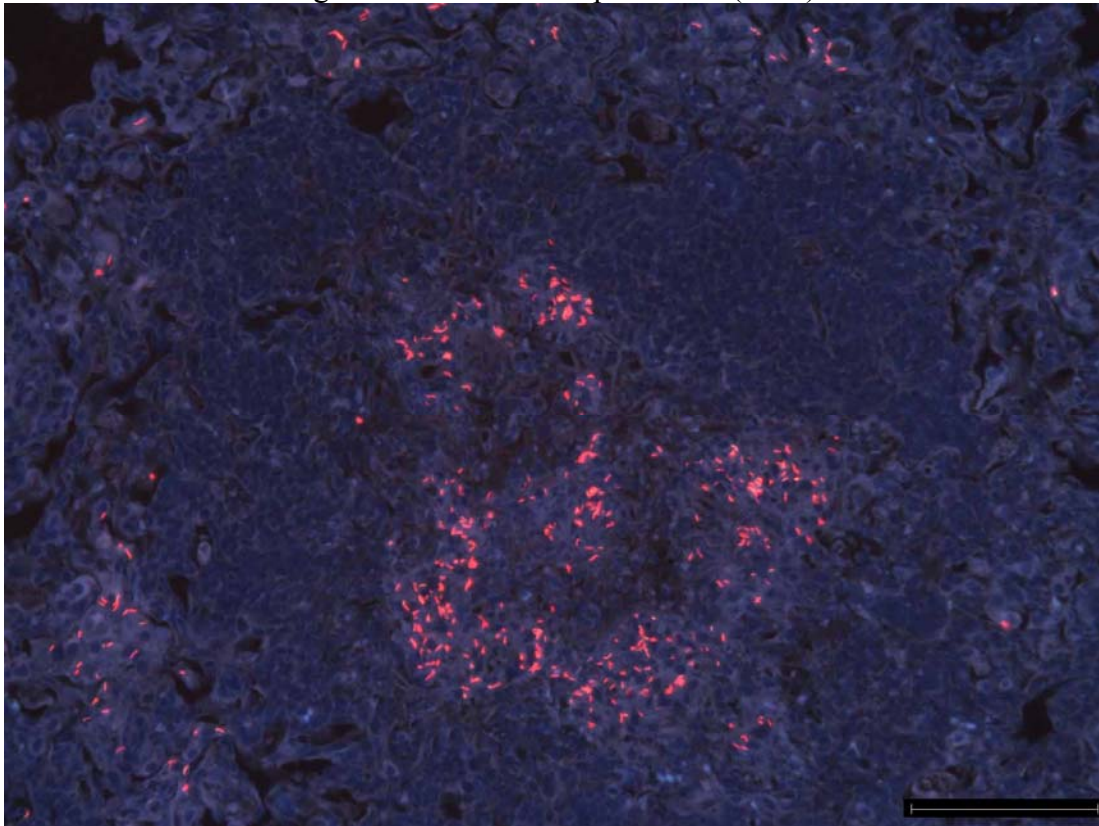


Fig. 2.2D Bacilli in FMs 9 wks post-LDA (200X)

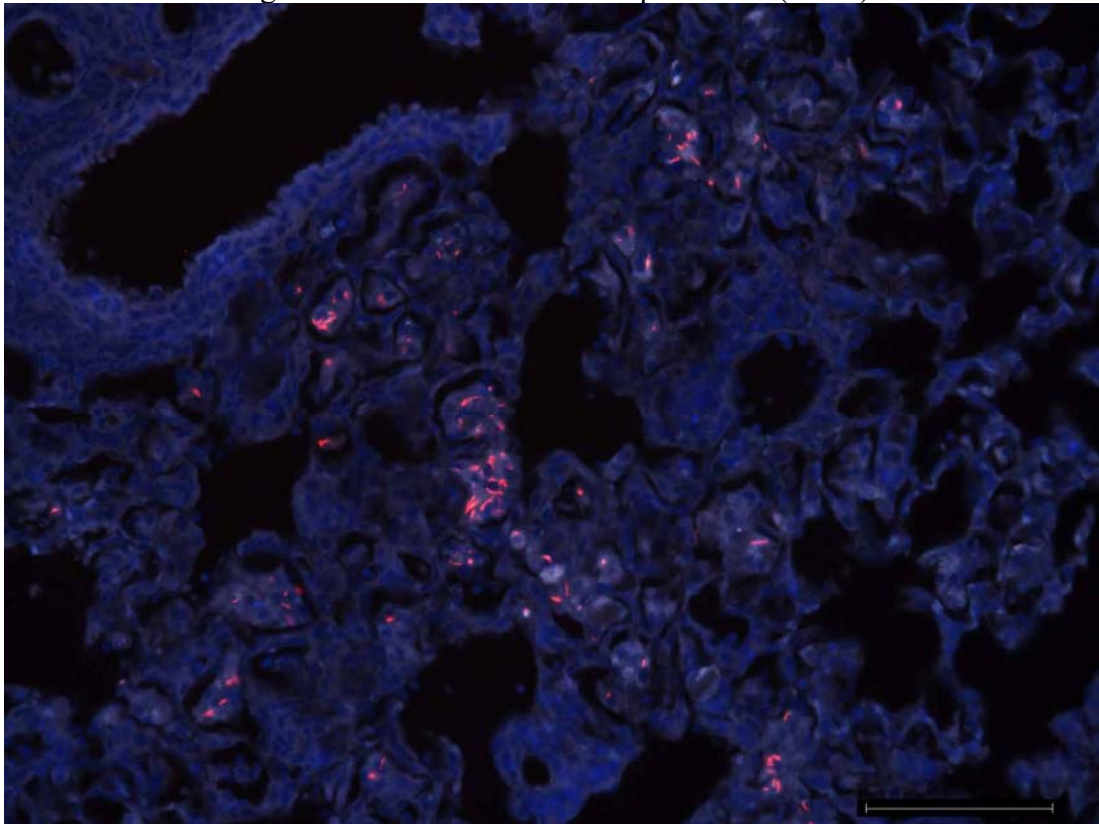


Fig. 2.2E Lesion after 6 wks of MXF therapy (200x)

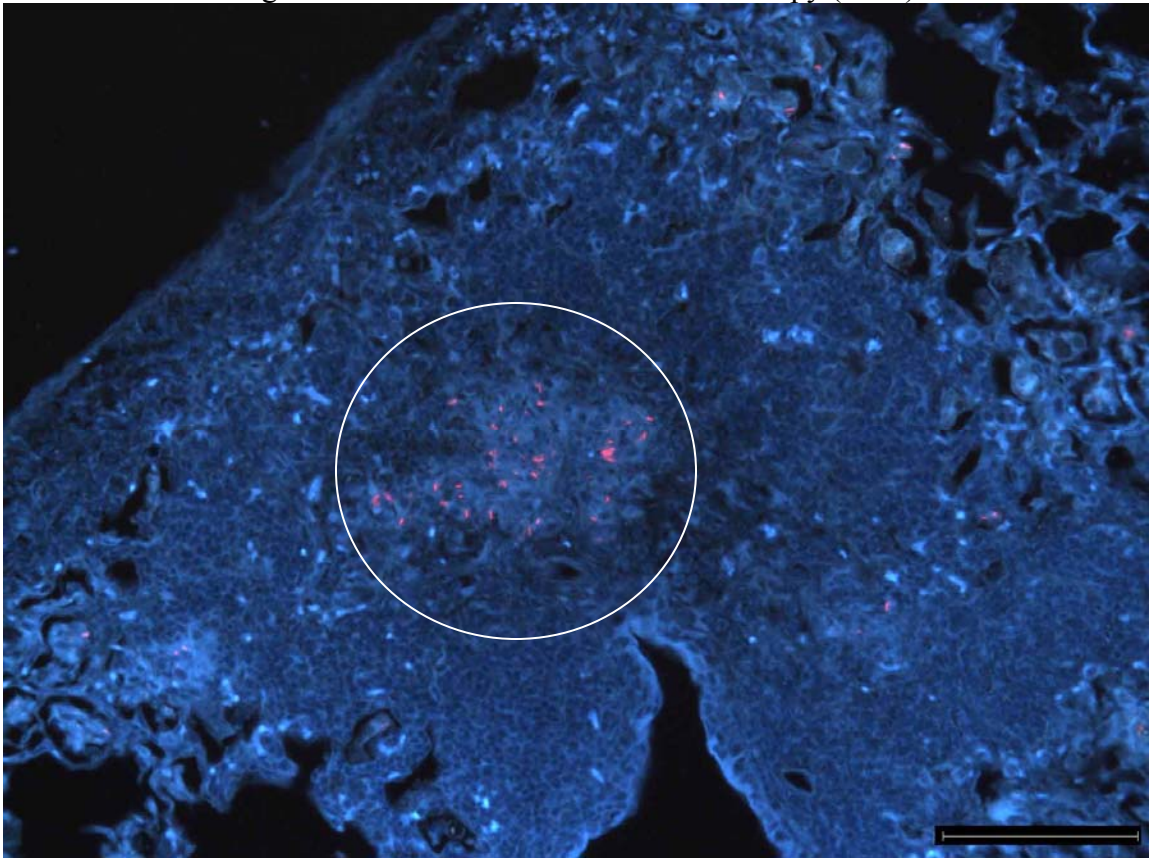
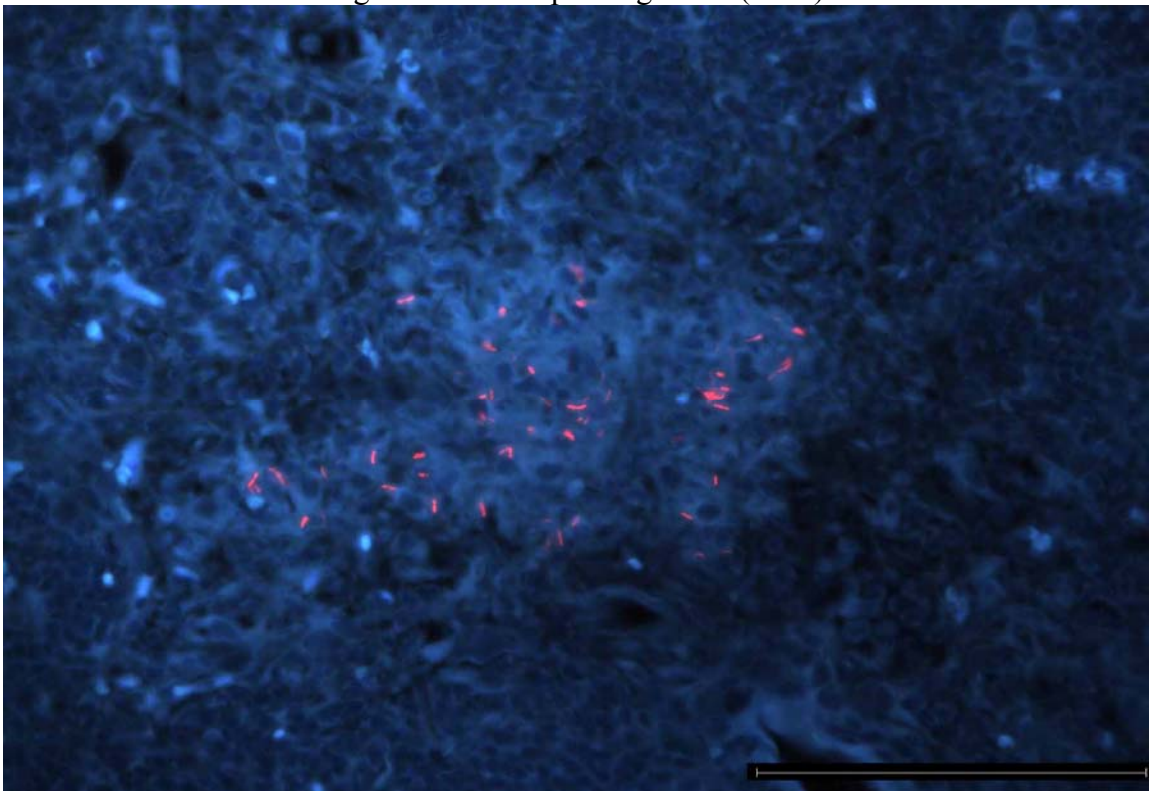


Fig. 2.2F Close-up of Fig. 2.3D (400x)



Lung histopathology and location of *M. tuberculosis* in GKO mice. Lung sections from IFN-gamma GKO mice studied at the start of treatment (18 days post-LDA) contained well-defined inflammatory lesions consisting primarily of LC, m Φ , and PMN cell accumulations arranged in an unorganized manner as earlier described (34, 106). The majority of AR⁺ bacilli (about 85-90%) were found uniformly distributed across these lesions, whereas a minority was found in and around airways, blood vessels and randomly dispersed throughout non-inflamed lung parenchyma (Figure 2.3 A and B). AR⁺ bacilli were predominantly intracellular early on during infection within m Φ cells. At a later stage of infection (20 to 22 days post LDA), alveolar septa within inflamed tissue began to erode resulting in multiple necrotic foci within pulmonary lesions while many adjacent alveoli become filled with cellular debris. At this stage the AR⁺ bacillary population transitions from being exclusively intracellular to becoming increasingly extracellular within areas of necrosis. By 28 days post-LDA, which is about 1 week before untreated mice succumb to disease, multiple lesions had coalescing necrotic foci forming massive areas of inflammation with extensive necrosis. These lesions contained exceptionally large numbers of both intracellular bacilli found within m Φ s and multinucleated giant cells (MNGC) (about 50%) and extracellular AR⁺ bacilli found residing in necrotic tissue and alveolar spaces filled with cellular debris (about 50%) (Fig. 2.3 C and D). A small proportion of AR⁺ bacilli were found in and around blood vessels and in non-granulomatous lung parenchyma (Fig. 2.3 E).

Little effect on lesion pathology as well as the distribution of the exclusively intracellular bacilli across pulmonary lesions was observed in lung tissues examined over the first 4 days of either INH or RIF treatment. Inflammatory lesions began to show the

initial signs of resolution after 7 days of therapy, and a reduction in both pulmonary inflammation and AR+ bacilli number becomes clearly evident. After 10 days of treatment, much of the pulmonary parenchyma was free of inflammation. The few remaining inflammatory lesions had diminished in size compared to earlier time points and were composed predominantly of mΦs and LCs. At this time, a significant reduction in the number of AR+ bacilli was clearly evident. Most of the AR+ bacilli (about 90%) were located within the few remaining lesions, or were situated peripherally within adjacent alveoli (Figure 2.3 F). A minority of AR+ bacilli (about 10%) was found dispersed in non-inflamed lung tissue. All bacilli remaining after drug therapy were exclusively intracellular within mΦs and MNGCs as no necrosis developed during treatment.

Figure 2.3. Modified AR stained lung tissues from untreated (*A-E*) and INH-treated (*F*) GKO mice (200X mag. unless otherwise noted). Scale bars = 100 μ M

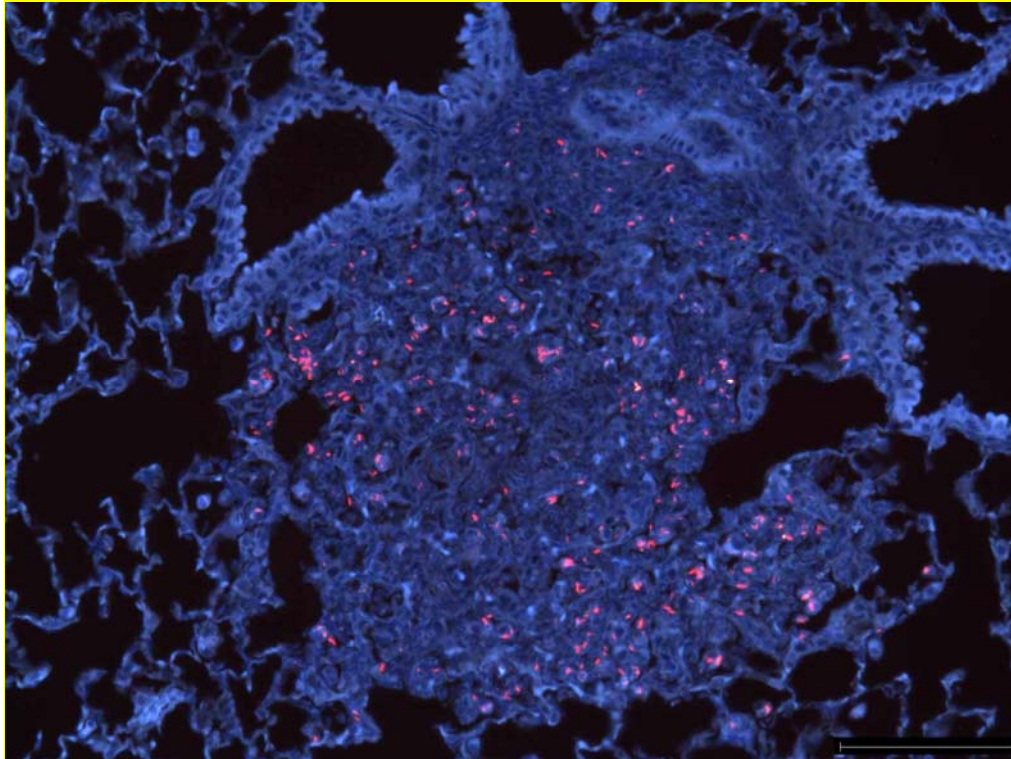


Fig.2.3A Lung lesion 18 days (d) post-LDA

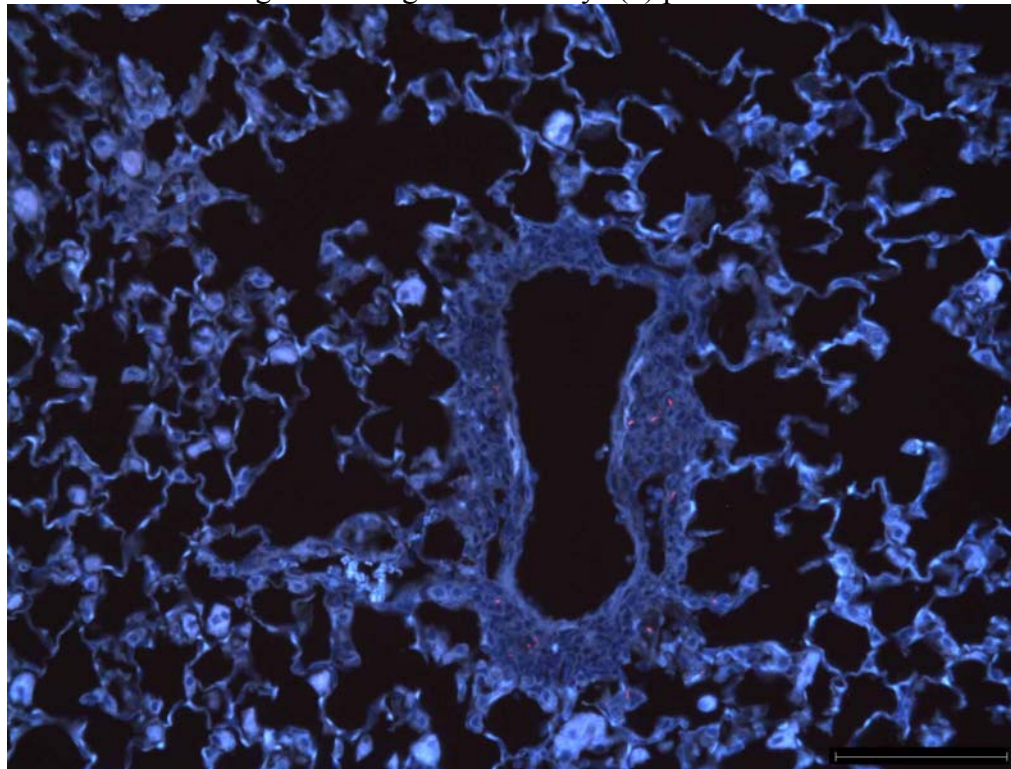


Fig.2.3B Blood vessel 18d post-LDA

Fig. 2.3C Inflammatory lesion 28d post-LDA (100X)

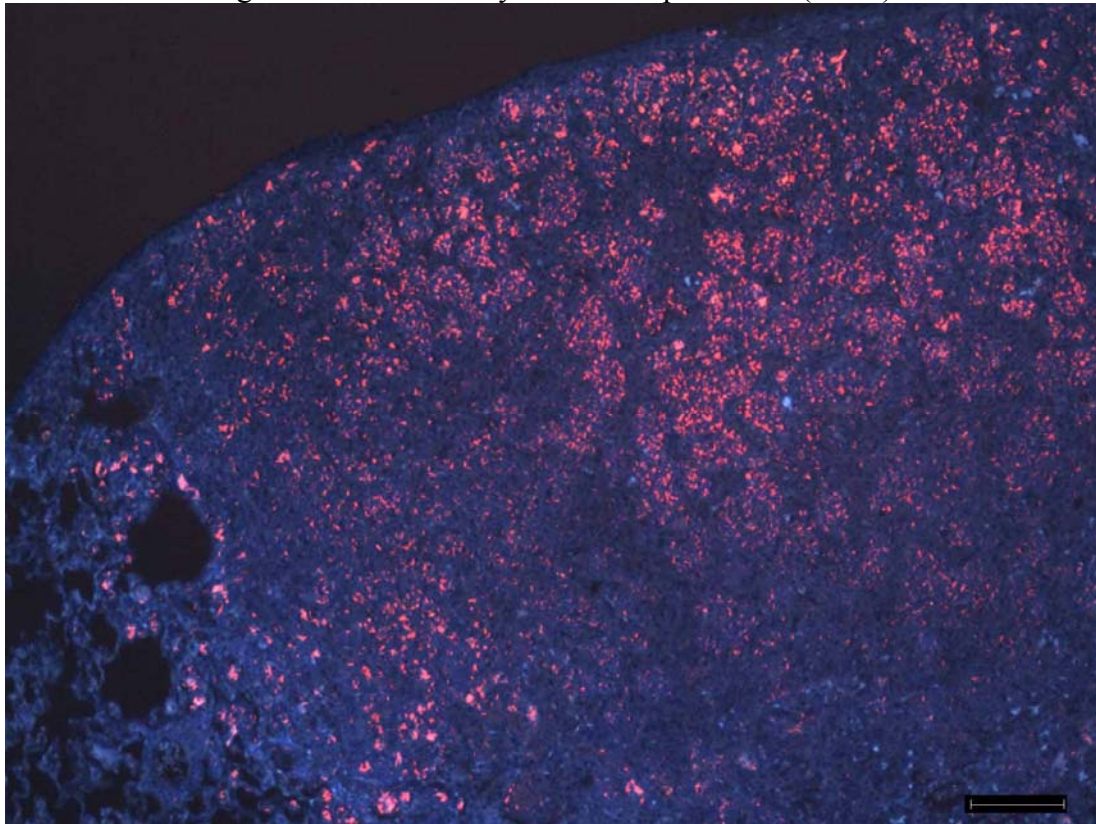


Fig. 2.3D Airway 28d post-LDA

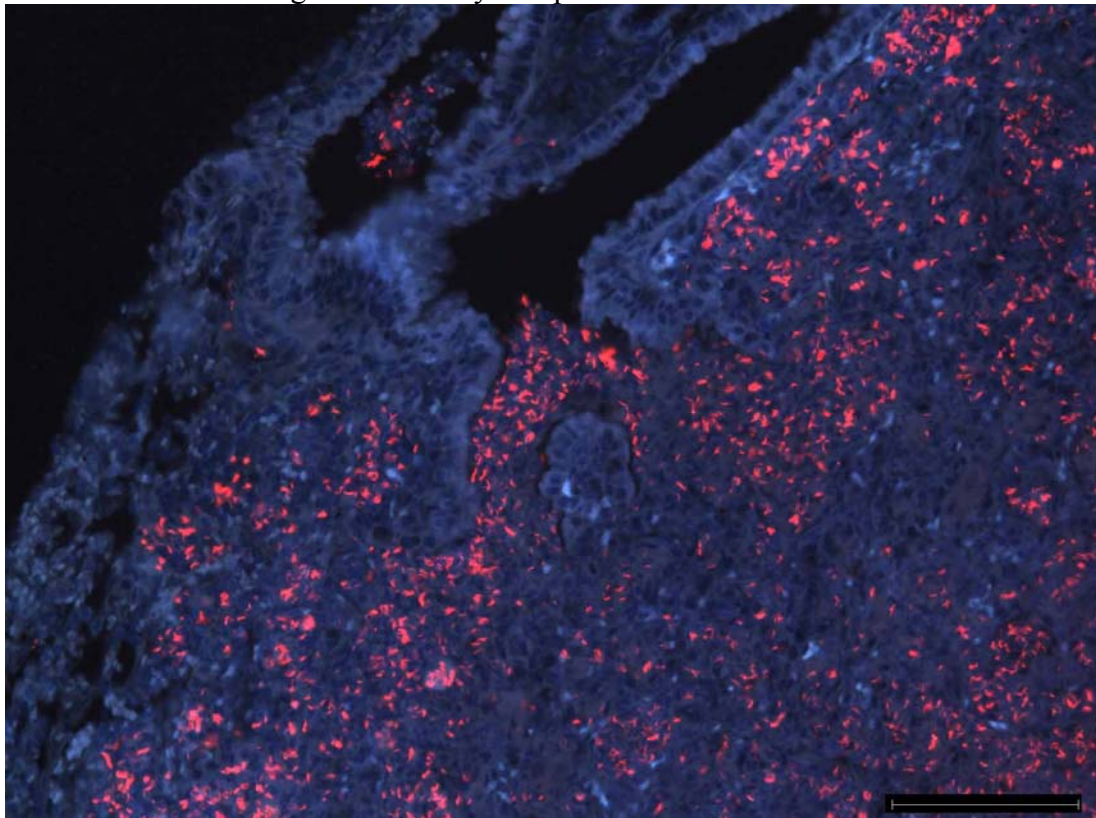


Fig. 2.3E Non-granulomatous tissue 28d post-LDA

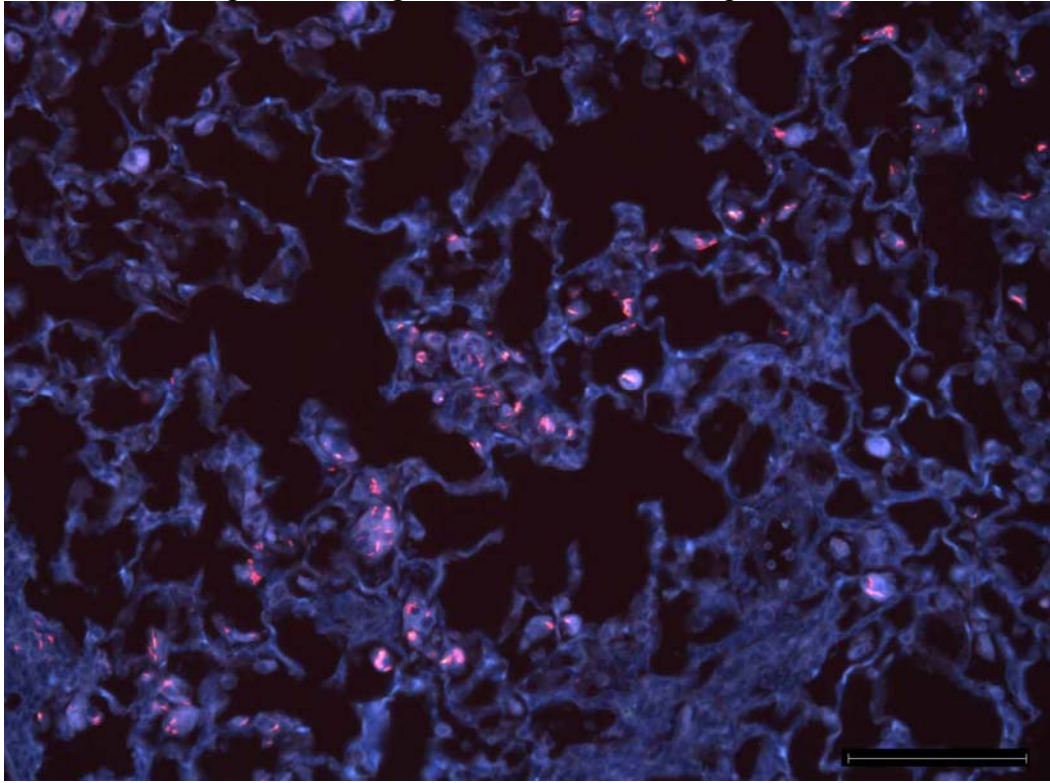
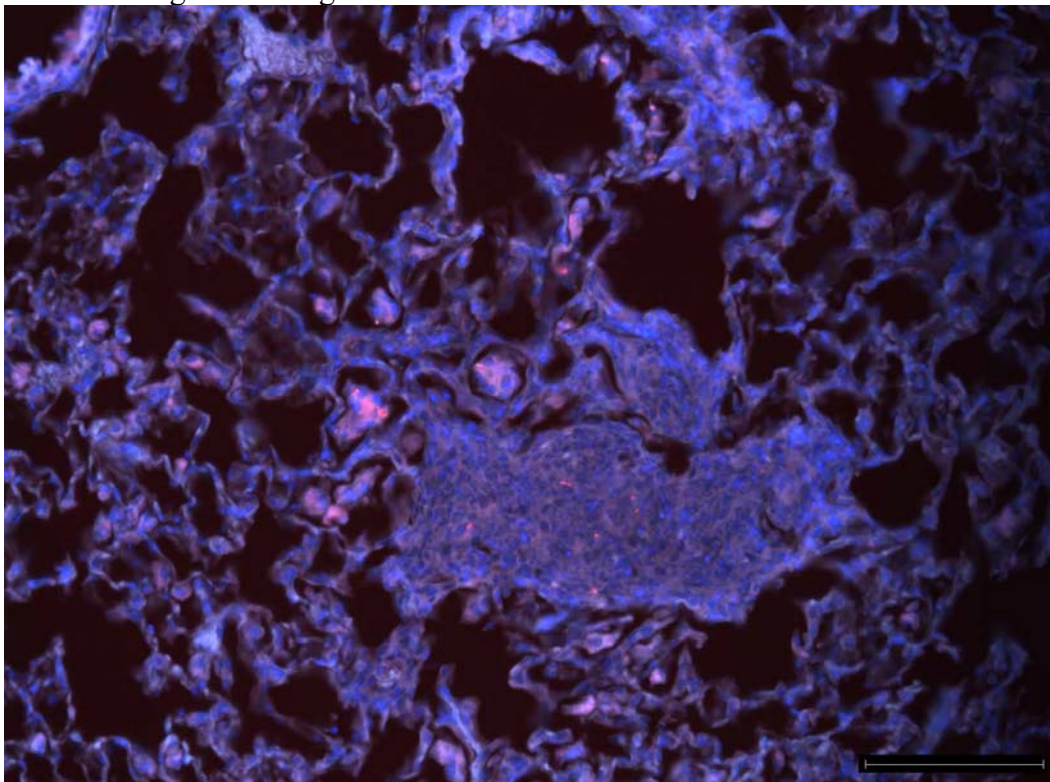


Fig. 2.3F Lung lesion after 10d of INH treatment



Necrosis formation and development of hypoxia in lungs of IFN-gamma GKO mice. In Figure 2.4, the progression of necrosis as revealed by H&E staining is chronicled. Fifteen to seventeen days post-LDA, lesions in the lungs of GKO mice were composed of well-defined cellular accumulations consisting of mΦs, LCs, and other inflammatory cells (Fig. 2.4 A). Closer examination of these lesions revealed distinct accumulations of PMN cells prior to the onset of necrosis (Fig. 2.4 B). Necrosis begins to develop within lesions and alveolar spaces of the lung approximately 20 to 22 days post-LDA and is composed of the cellular remains of the previously mentioned PMN infiltrates (Fig. 2.4 C). Lung sections 29 days post-LDA revealed large inflammatory lesions with coalescing necrotic foci resulting from the erosion of multiple adjacent alveolar septa. Some pulmonary lesions examined in tissue sections from untreated mice exhibited very similar morphology to primary granulomas that develop in guinea pigs. The similarities of lesions in GKO mice to primary granulomas include: 1) a central core of necrosis, 2) a surrounding capsule of fibrosis, and 3) an outer cell layer (Fig. 2.4 D).

Interestingly, the areas of necrosis within the pulmonary lesions of GKO mice appeared to be very similar to the necrosis seen in the cores of guinea pig primary granulomas that we have previously shown to be hypoxic (78). To determine if and when lung lesions in the lungs of IFN-gamma GKO mice infected with *M. tuberculosis* become hypoxic, mice were injected i.p. with the hypoxia marker pimonidazole 1.5 h prior to euthanasia on days 15, 17, 20, 22, 25, and 29 post-LDA. The results of pimonidazole staining are shown in Figure 2.5. Although hypoxia was detected in the lungs of GKO mice starting approximately 25 days post-LDA, pimonidazole staining was most distinct 29 days post-LDA. Strong hypoxic signals were detected within and around areas of

necrosis in pulmonary lesions of GKO mice (Figure. 2.5 A and B). Furthermore, hypoxic conditions were detected in FMs found outside areas of granulomatous tissue (Fig. 2.5 C and D). These results indicate that the decreased O₂ conditions associated with pulmonary TB lesions formed during human pulmonary infections is a pathological feature present in the lungs of IFN-gamma GKO mice during TB infection as well.

Figure 2.4. TB lesion progression in GKO mice *A* & *B*, 17d, *C*, 22d, *D*, 29d post-LDA.

Fig. 2.4A Early cellular lesion (100X mag.)

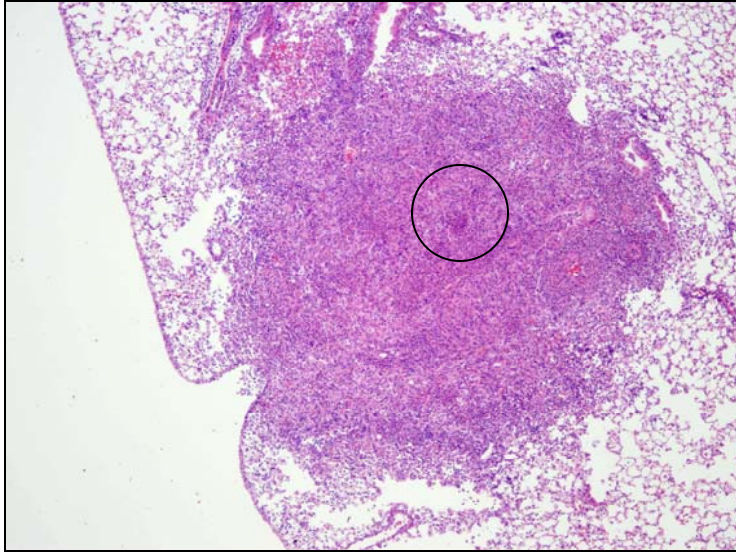


Fig. 2.4B Close-up 2.4A showing granulocyte influx (40X)

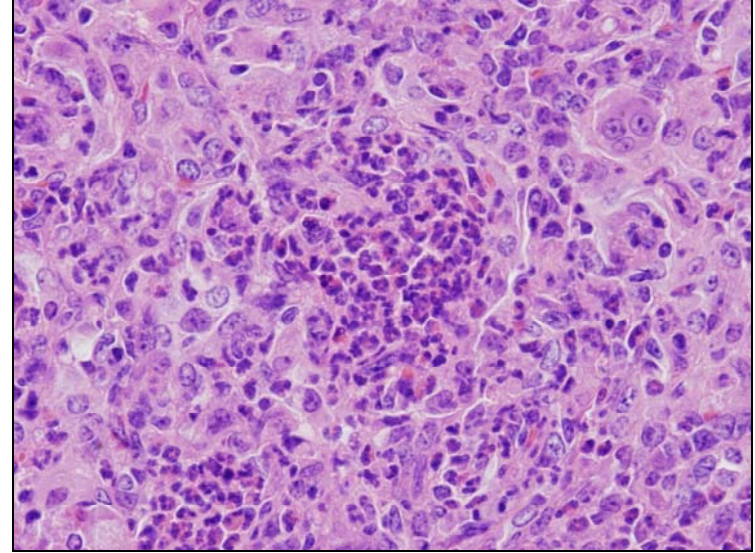


Fig. 2.4C Onset of necrosis (N) (100X)

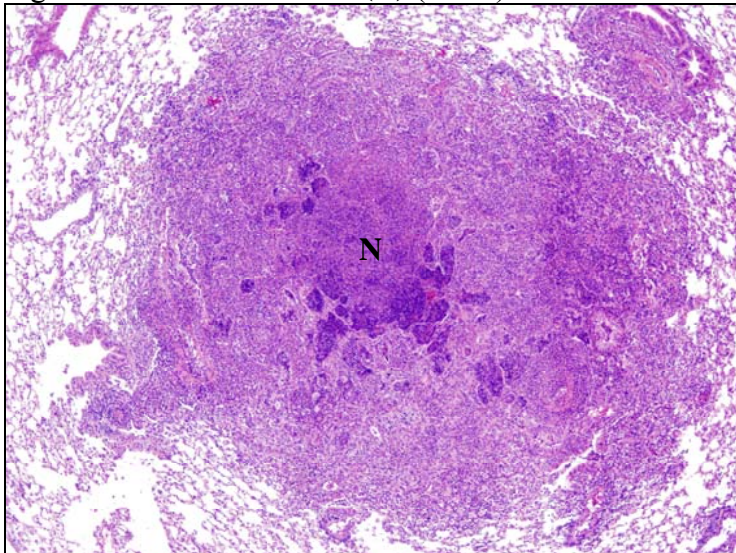


Fig. 2.4D Necrotic lesion with fibrous capsule (F) (100X)

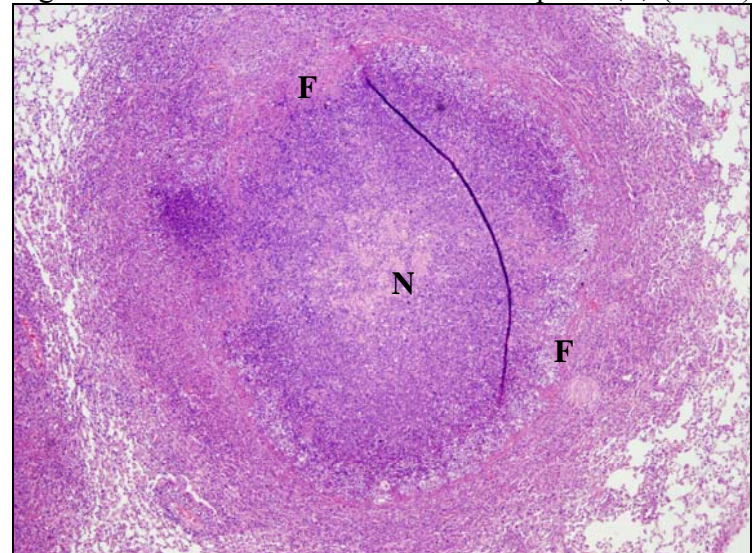
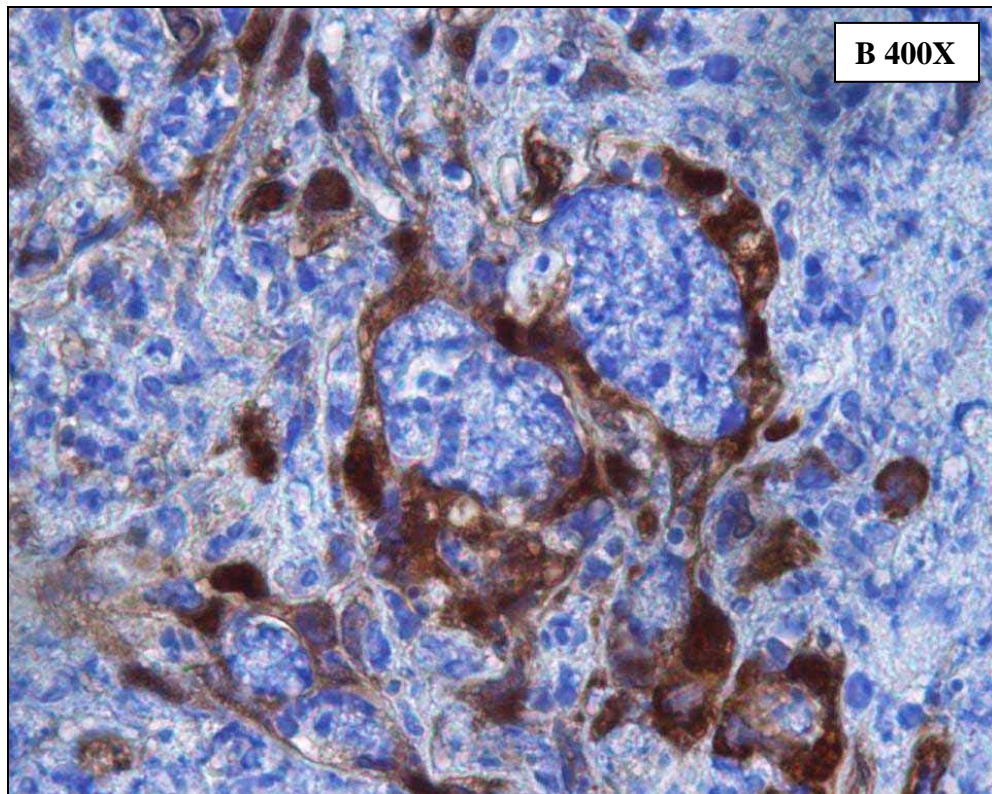
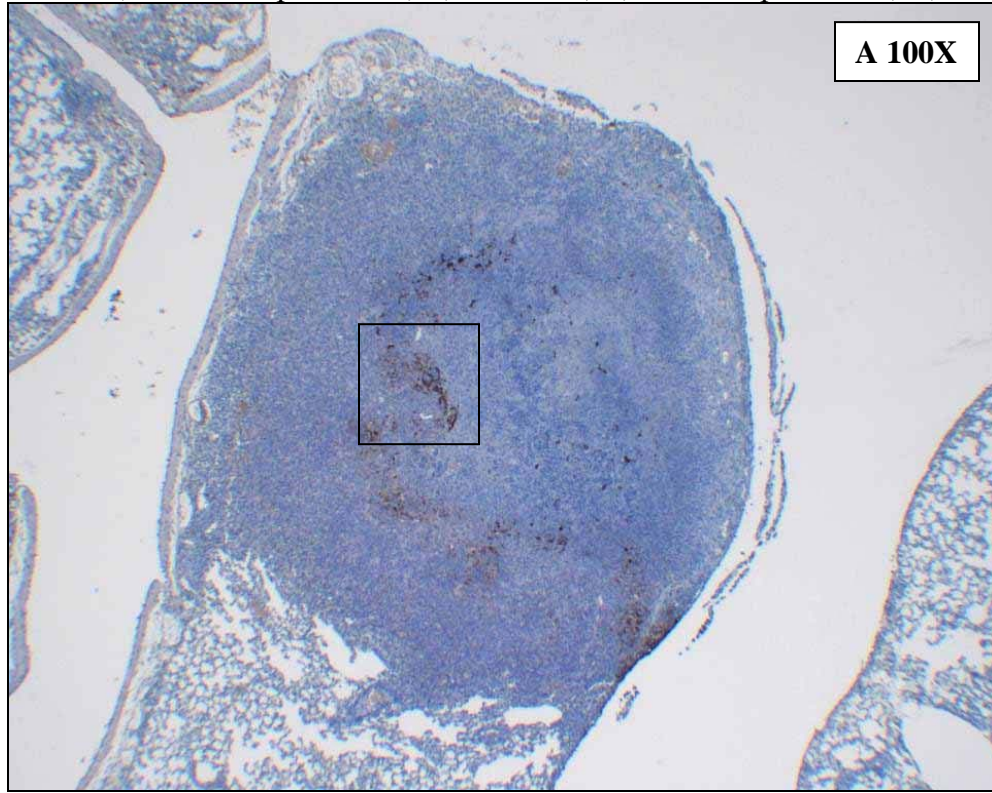
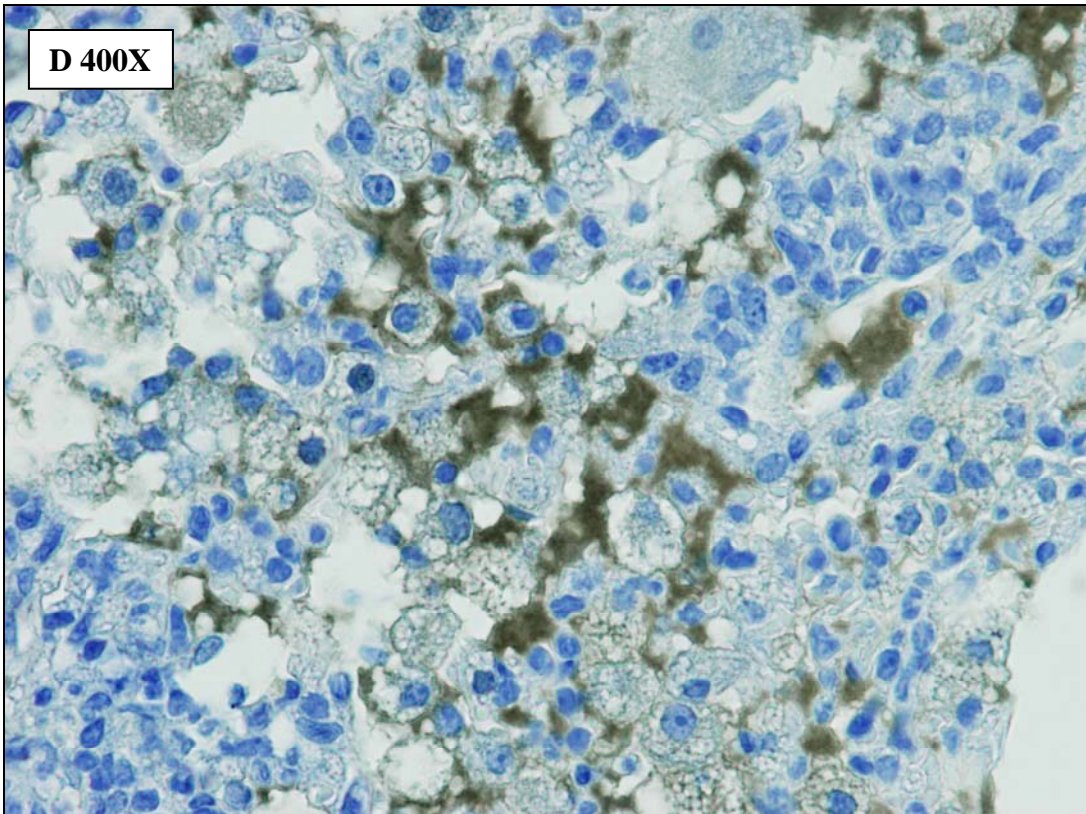
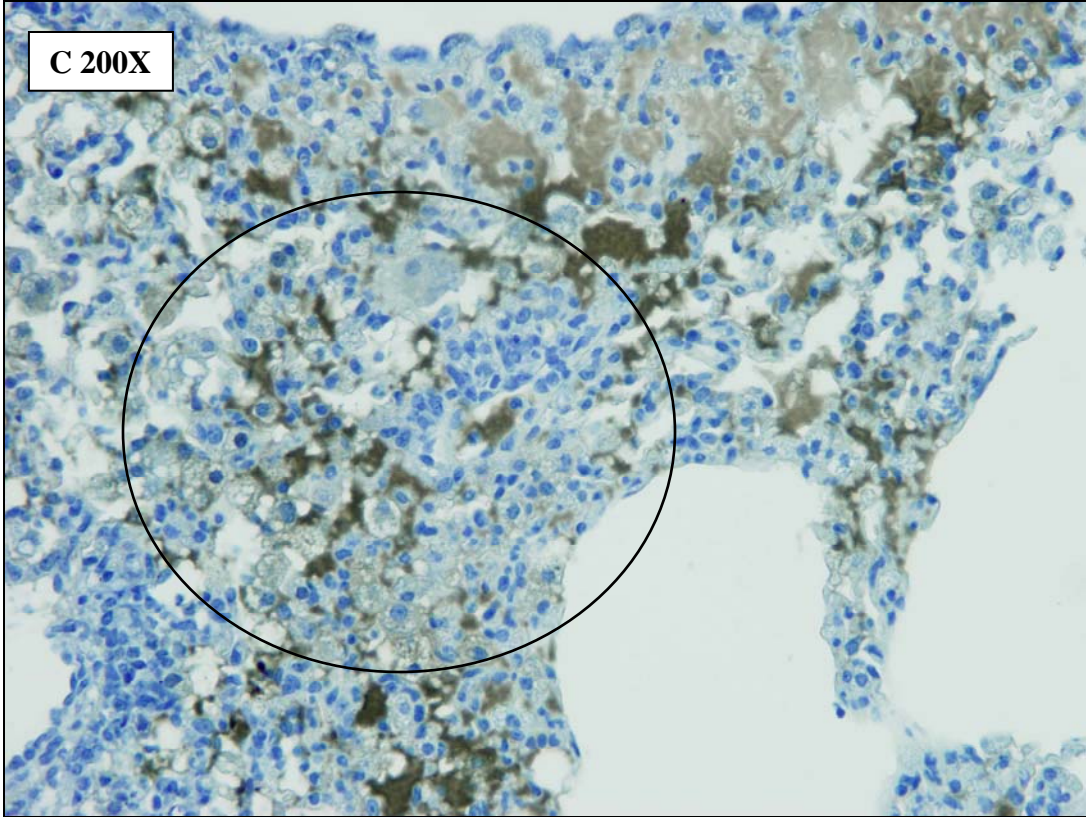


Figure 2.5. Hypoxia (brown staining) in the lungs of GKO mice infected with *M. tuberculosis*. **A**, lesion 29d post-LDA, **B**, inset of **A**, **C**, FMs 29d post-LDA, **D**, inset of **C**.





Lung histopathology and location of *M. tuberculosis* in guinea pigs. Lung sections from guinea pigs 4 weeks post-LDA infection contained multiple granulomatous lesions with differing morphologies. Primary granulomas could be differentiated from secondary lesions based on the presence of a necrotic core surrounded by LCs, as has been previously described (89, 127). Approximately 30 days post-LDA, primary granulomas were composed of a distinct necrotic core surrounded by an acellular rim separating the inner necrotic core from the outer cell layer. The majority of AR+ bacilli (about 70%) was found extracellular dispersed predominantly throughout the necrotic areas of primary granulomas (Figure 2.6 A and B). Another sub-population of AR+ bacilli (about 20%) was found intracellular within mΦs that were in close proximity to the necrotic cores of primary granulomas. A small number of AR+ bacilli (about 10%) were found within mΦ cells composing secondary lesions (Fig. 2.6 C). By 10 weeks post LDA, necrotic cores of primary granulomas had progressed to a state of complete dystrophic mineralization. A modest decrease in AR+ bacilli number was observed at this time. However, AR+ bacilli were now almost exclusively extracellular (about 95%) within necrotic cores and the surrounding, acellular rims in contrast to earlier time points (Fig. 2.6 D). Most secondary lesions contained few detectable bacilli if any (data not shown).

A differential drug effect of INH was observed in guinea pigs for primary granulomas compared to secondary lesions. INH chemotherapy clearly targeted and eliminated secondary lesions first, and after 6 weeks of therapy these lesions were largely resolved. On the other hand, primary granulomas required prolonged therapy for their resolution. In contrast to the secondary lesions, the pathologic progression and cell

composition of primary granulomas after drug treatment was very similar to those of the untreated controls throughout the course of treatment. The AR+ bacilli population steadily declined across the lungs of the infected, drug-treated guinea pigs. After 6 weeks of INH treatment, bacilli were present in the same locations as for the infected, untreated controls but in moderately reduced numbers versus those without drug exposure. The majority (about 95%) of drug-treated AR+ bacilli were located in primary granulomas dispersed extracellularly within the necrotic cores and surrounding acellular rims with fewer bacilli found intracellularly in the surrounding m Φ and LC cell layer (Fig. 2.6 E). An AR+ bacterial population (about 5%) was found within m Φ cells composing the few remaining secondary lesions, however the majority of these lesions contained no detectable bacilli (data not shown).

In addition to those treated with INH, lung tissue sections from guinea pigs treated with the compound TMC207 were also evaluated. TMC207 is a compound that exhibits very potent *in vitro* and *in vivo* activity against *M. tuberculosis*. After 6 weeks of INH treatment the log₁₀ CFU in the lungs of guinea pigs was reduced by approximately 2 logs when compared to pre-treatment controls whereas TMC207 treatment for 6 weeks yielded an approximate reduction of 3.5 logs in lung CFU (data not shown). Lungs of infected guinea pigs treated with TMC207 showed largely distinct, preferential clearance of secondary lesions as seen in groups receiving INH therapy for 6 weeks. However, treatment with the TMC207 compound also effectively reduced the number of primary granulomas. The numbers of AR+ bacilli were clearly reduced in the lungs of guinea pigs by the end of TMC207 therapy compared to both the pre-treatment controls and guinea pigs treated with INH. The AR+ bacilli remaining after 6 weeks of TMC207 treatment

were still present in the same locations and in similar proportions as observed for the other treatment groups with the majority in the necrotic core and a small population in the surrounding acellular rim of remaining primary granulomas (Fig. 2.6 F).

Figure 2.6. Modified AR stained lung tissues from untreated (**A-D**) and INH- (**E**) or TMC207- (**F**) treated guinea pigs infected with *M. tuberculosis*. Scale bars = 100 μ M

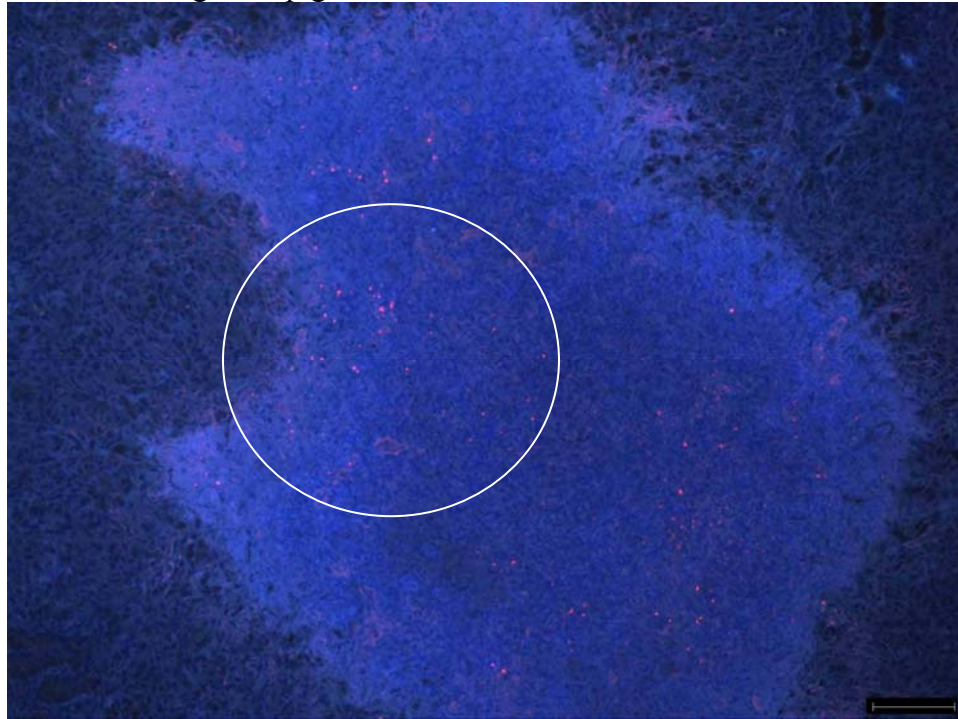


Fig. 2.6A Primary granuloma 4 wks post-LDA (100X mag.)

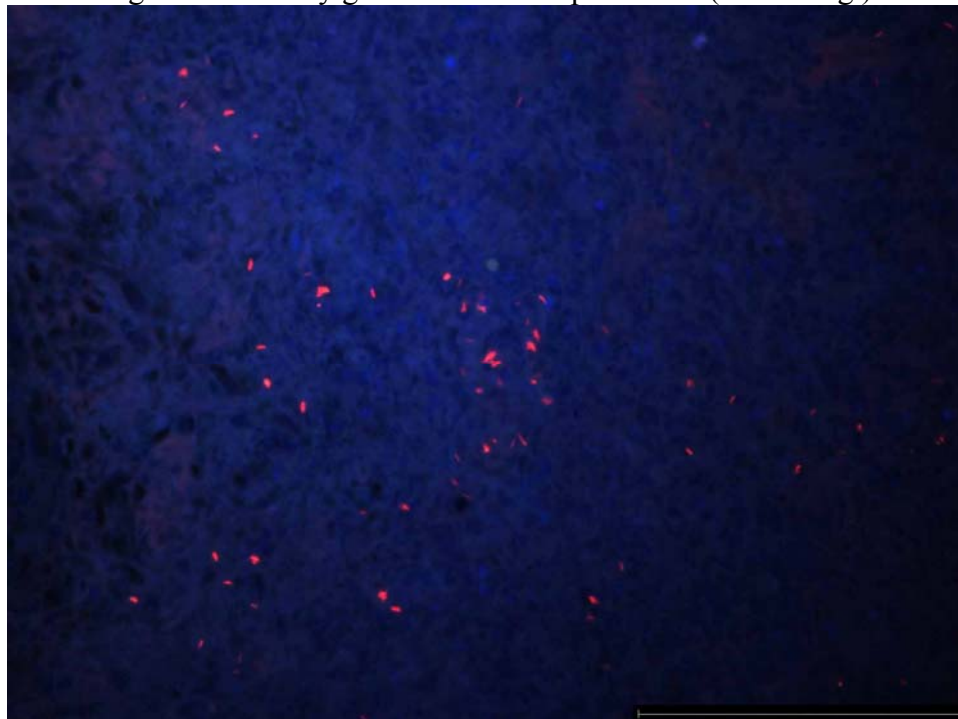


Fig. 2.6B Close-up of Fig. 2.6A (400X)

Fig. 2.6C Secondary lesion 4 wks post-LDA (200X)

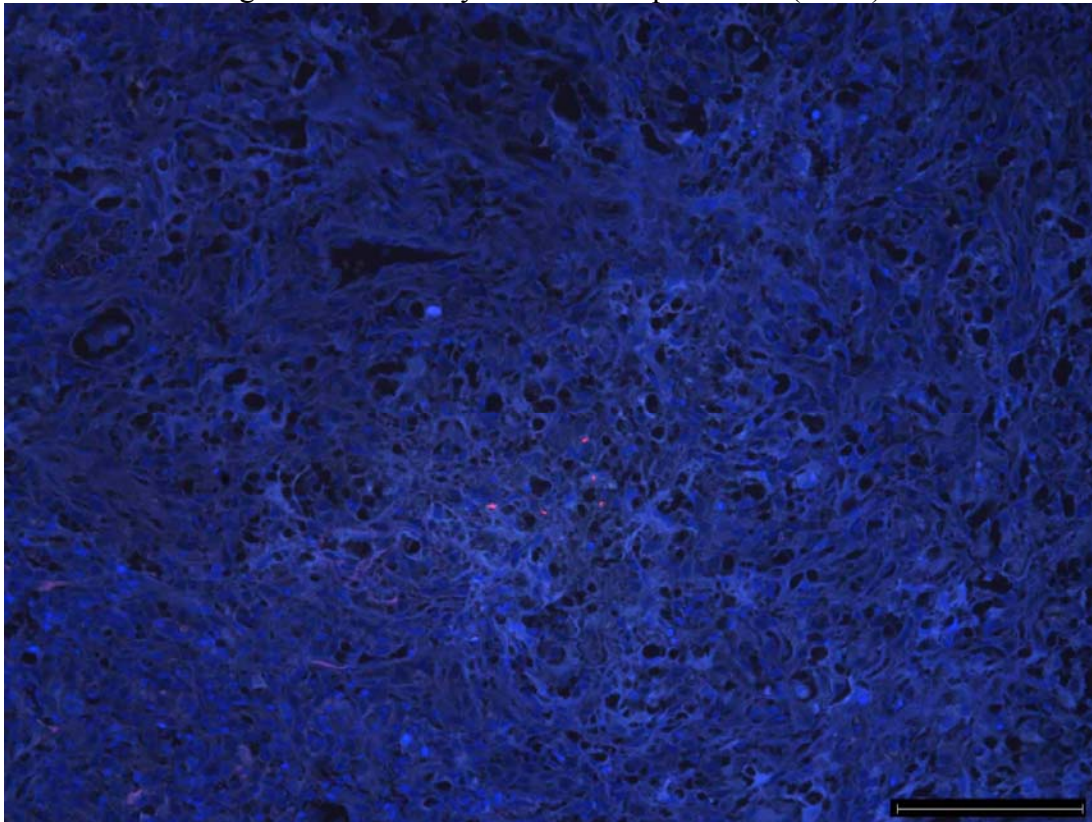


Fig. 2.6D Primary lesion 10 wks post-LDA (200X)

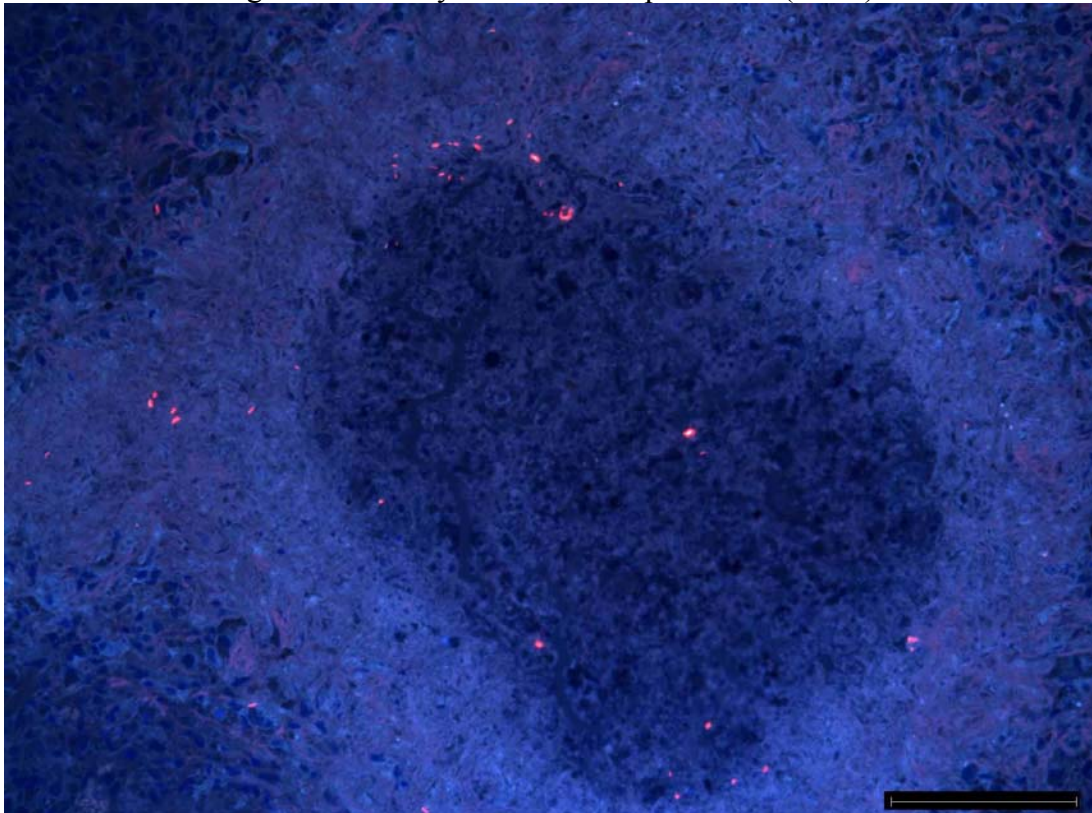


Fig. 2.6E Primary lesion 6 wks after INH therapy (200X)

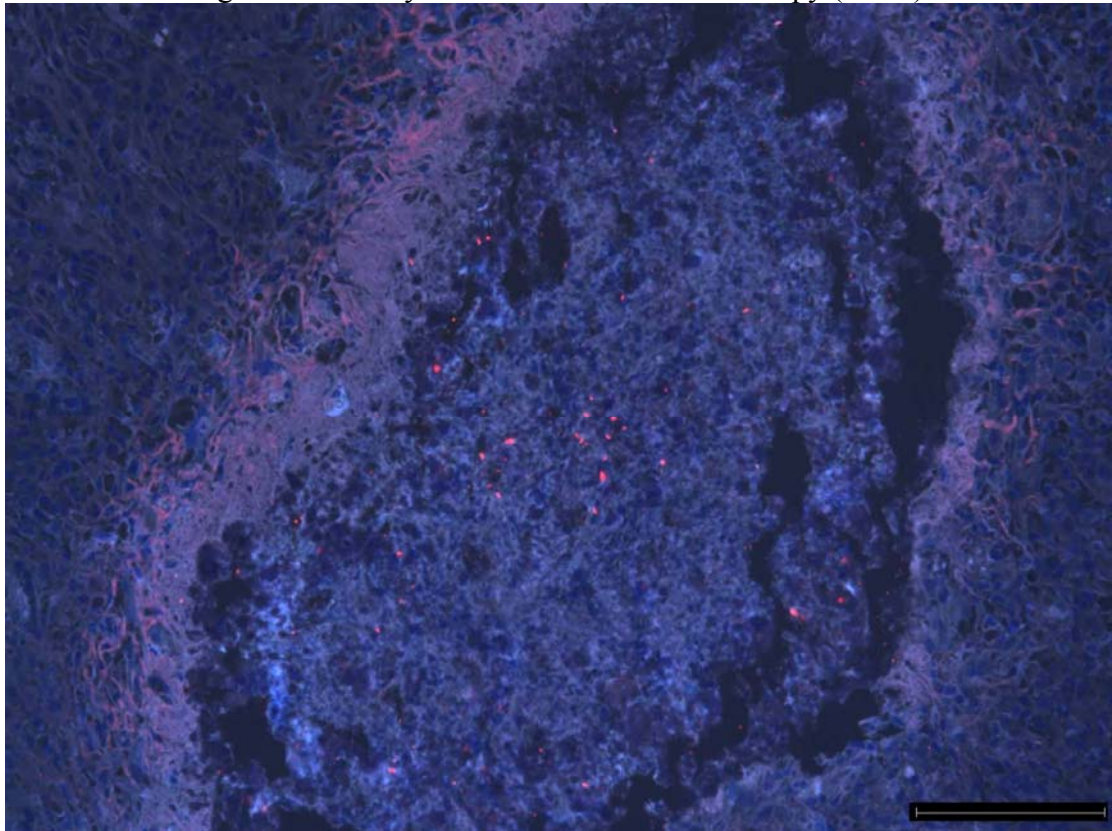
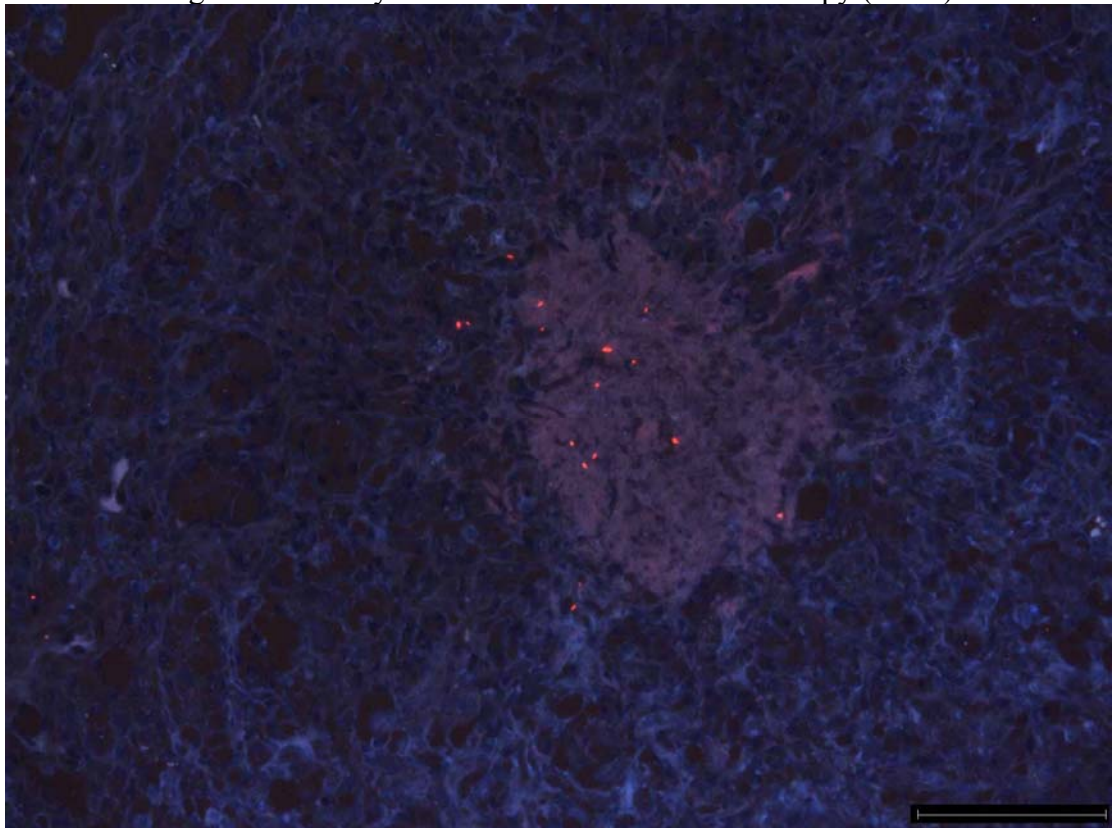


Fig. 2.6F Primary lesion 6 wks after TMC207 therapy (200X)



2.4 DISCUSSION

A sequence of *in vitro* assays and animal models are used in TB drug discovery and development to identify and select early experimental compounds. Mouse models provide important information regarding pharmacokinetics and efficacy of novel compounds (63, 64, 70, 97) but fail to reproduce pathological aspects of human disease. Recently, other animal models that reflect the progression in TB lung pathology seen in humans are being included in later stages of drug development such as the rat, guinea pig, rabbit, and non-human primate models (50, 88, 90). The efficacy of an experimental compound is generally measured by the reduction in CFU with little investigation into the effect of drug treatment on TB pathogenesis or in different locations within the lung that harbor distinct *in vivo* environments. In the studies presented here, we investigated these aspects in three different animal models used in-house for TB drug evaluations: a short term murine model using immunocompromised (GKO) mice (76), the immunocompetent C57BL/6 mouse model (70), and the guinea pig model (117). All *M. tuberculosis* infections were performed by LDA infection (administering 30-100 CFU in lungs of the animals). The ultimate goals of these studies were: i) to characterize the *in vivo* location of tubercle bacilli during infection in different animal models, ii) to assess the effect of drug treatment on lung pathology and bacillary clearance in these models, and iii) to determine the location of bacilli persisting after drug treatment histologically in a cross-species microscopic analysis. Comparing and contrasting the heterogeneous *in vivo* environments of *M. tuberculosis* before and after drug treatment in different animals used for preclinical drug testing will provide a clearer understanding of the specific aspects of

TB infection experimental compounds are tested against in one animal versus another. Furthermore, knowing the location of bacilli persisting after treatment in different animal models will undoubtedly unlock clues into the mechanisms that allow this pathogen to survive a variety of harsh *in vivo* environments.

In past studies, the ZN acid-fast staining method has been traditionally employed to visualize tubercle bacilli in tissue samples. Identification of mycobacteria using this stain requires high magnification contributing to user fatigue when microscopic analysis requires the evaluation of a large number of whole tissue sections. A novel staining combination consisting of the acid-fast fluorochromes AR, hematoxylin, and the fluorescent nuclear stain DAPI used in the present study enabled visualization of tubercle bacilli across entire pulmonary tissue sections from TB-infected animal models. Both drug-treated and untreated lung tissues from animals from each model were analyzed for histopathological comparison as well as the location of bacilli revealed by the novel AR-staining combination. Although the fluorescent acid-fast stains auramine and rhodamine facilitated the evaluation of tubercle bacilli location across different animal species, there are several important caveats that must be taken into consideration when interpreting these results. Firstly, acid-fast stains do not differentiate between live and intact, dead (and not yet cleared) tubercle bacilli. Therefore, bacilli that may have been killed by chemotherapy may remain in tissues if immune cells are unable to reach and subsequently clear the pathogen (such as in necrotic cores of lesions) and rate of clearance will also depend on the activated immune state. Secondly, since the AR staining method relies on staining acid-fast *M. tuberculosis*, the possibility remains that not all viable tubercle bacilli are being visualized by this detection method. This line of

reasoning is supported by the fact that cell-wall alterations can and do occur in tubercle bacilli chronically infecting mice that confer a loss of acid-fastness (17, 112). Lastly, the results reported here are only relevant under the infection conditions observed within each of the animal models evaluated including the length of treatment and duration of infection. Regardless, the use of the novel acid-fast staining combination described here proved insightful as a tool to gain information on the locations of tubercle bacilli persisting after chemotherapy in different animal models used for preclinical TB drug testing and increases our understanding of the specific conditions drugs are evaluated under in these models.

The first animal model analyzed was the WT C57BL/6 mouse. The effect of chemotherapy over time on lung pathology and clearance of AR+ bacilli in this model was gradual and perhaps the most homogeneous of all animal models evaluated in this study. Significant resolution of pulmonary inflammation and a clear reduction in the number of AR+ bacilli number compared to the pre-treatment controls only become apparent after 6 weeks of treatment. The AR acid-fast stain showed bacilli to inhabit a heterogeneous set of environments during infection. Under the conditions observed in this model, bacilli are intracellular for the initial 10 weeks after LDA. Macrophages located in the center of inflammatory lesions surrounded by lymphocytes as well as foamy macrophages composing the outer edges of these lesions were the predominant cell types harboring AR+ bacilli for both drug-treated and untreated mice. Interestingly, FMs appear to play a more prominent role during TB infection in the WT C57BL/6 mouse than during infection in either of the other two animal models studied here. Cardona *et al.* has speculated that FMs may harbor persistent bacilli which he has

observed both *in vitro* in a human granuloma model (107) and *in vivo* in WT C57BL/6 mice and guinea pigs (27). These studies have shown that FMs are an abundant nutrient source due to their high lipid content, arise from *M. tuberculosis*-infected mΦs, and contain bacilli in a non-replicating, persistent state. Taken together, the results of the histopathological analysis presented here and the work of Cardona *et al.* suggest FMs may be a long-term reservoir for persisting bacilli. However, the specific role of FMs in *M. tuberculosis* persistence during infection of WT C57BL/6 mice would need to be further elucidated under conditions in which bacterial numbers have been driven to below detectable levels with chemotherapy and in which reactivation has been allowed to occur.

AR-staining of lung tissue samples from untreated IFN-gamma GKO mice infected with *M. tuberculosis* revealed a rapidly dividing population of AR+ bacilli that reached very high numbers by the end of the trial period 29 days post-LDA. Bacilli were intracellular early during infection (18 to 20 days post-LDA) but steadily transitioned into an increasingly extracellular state as the infection progressed and necrosis became more extensive (22 to 29 days post-LDA). Interestingly, *M. tuberculosis* bacilli revealed by AR in the lungs of drug-treated GKO mice remained intracellular throughout the course of infection and declined in numbers dramatically after the initial days of treatment. A distinct lack of necrosis was also observed for drug-treated GKO mice. The distinct pathological differences between drug-treated and treated mice observed in this study can most likely be attributed to the fact that effective drug therapy (i.e., either with INH or RIF monotherapy) was initiated prior the onset of necrosis in those mice receiving treatment.

Many important differences in the progression of TB disease and the effects of chemotherapy were observed between WT C57BL/6 mice and IFN-gamma GKO mice. Observing the growth kinetics in untreated mice, we found that the growth of TB bacilli is very similar between both groups of mice during the first 18 to 20 days post-LDA. However, bacterial growth is effectively contained in WT mice at a time that is concurrent with onset of adaptive immunity. IFN-gamma GKO mice fail to contain the mycobacterial infection resulting in a constantly dividing bacterial population that leads to death of the mice about 1 month post-LDA. Untreated IFN-gamma GKO mice developed extensive necrotic lesions in their lungs which was preceded by accumulations of PMN cells within areas of inflammation. In contrast, early infiltrates of PMN cells were not observed in WT mice nor did they develop pulmonary necrosis suggesting that IFN-gamma, in part, may play a role in early lesion formation by preventing specific innate immune cells from aggregating early during infection. Environmental conditions such as decreased O₂ tension are known to induce *M. tuberculosis* into a drug-refractory state of non-replicating persistence (140), and have long been considered attributes of TB infection in humans. A central criticism of using WT C57BL/6 mice for studying TB and/or evaluating experimental treatment modalities has been the lack of reproducible *in vivo* conditions seen during human disease including the presence of hypoxia (132). Using the hypoxia marker piminidazole, we show here that GKO mice develop extensive areas of hypoxia in regions of necrosis in pulmonary lesions and in foamy cells aggregating outside areas of granulomatous inflammation. Further dissecting the specific differences in growth kinetics of bacilli and the progression of TB pathogenesis between WT and GKO mice will undoubtedly facilitate our understanding of how *M. tuberculosis*

responds to different immune responses and how these differences should be interpreted for preclinical drug testing.

Guinea pigs present a more relevant animal model for the evaluation of experimental compounds due to their similarities in TB pathogenesis to humans. The results of AR staining of infected guinea pig lung tissues with the modified AR staining method revealed that *M. tuberculosis* mainly presents itself as an extracellular pathogen, predominantly found in the necrotic cores of primary granulomas. This finding goes against classical dogma that *M. tuberculosis* is an intracellular pathogen (69) as very few intracellular bacilli were found throughout the time points studied (time points were 4, 6, 8, and 10 weeks post-LDA). The intracellular bacilli found were predominantly located in secondary lesions with a small proportion found in the outer cell layer of primary granulomas, however most secondary lesion types harbored no detectable bacilli at all. Why secondary lesions were found to contain few, if any, bacilli remains to be determined. However, two hypotheses could possibly explain this finding. In the first hypothesis, bacilli in the initial, primary infection disseminate from the lungs to lymph nodes, replicate and then re-seed the lung at a time when the adaptive immune response has been established. This acquired immune response may be effective at eliminating bacteria upon arrival to the lungs. A recent publication by Ly *et al.* demonstrated vastly different mRNA cytokine expression profiles between primary granulomas and secondary lesions in unimmunized guinea pigs (81). Primary granulomas contained a higher bacterial burden and were dominated by the pro-inflammatory cytokine tumor necrosis factor-alpha (TNF- α) while secondary lesions were found to have fewer bacilli and were dominated by the immunosuppressive cytokine transforming growth factor-

beta. Ly *et al.* (2008) speculated that primary granulomas may serve to “vaccinate” portions of the lung not exposed to the primary infection. The onset of cell-mediated immunity in conjunction with the lack of TNF- α (which functions to recruit new inflammatory cells to sites of infection) in secondary lesions may improve the ability of anti-TB drugs to effectively target and kill *M. tuberculosis* bacilli (78, 81). This scenario is supported by the findings presented in this study in which it was observed that secondary lesions and bacilli within them were preferentially targeted and cleared first by both INH and TMC207 monotherapy while primary granulomas and bacilli within them exhibited a delay in resolution and clearance. A second hypothesis may be that bacilli that disseminate and re-infect the lung are not cleared upon re-infection but are merely transported by phagocytic cells to already-established primary granulomas. Studies involving super-infection of mycobacteria into fish, frogs, and mice have shown that *M. marinum*, *M. tuberculosis*, and *M. bovis* BCG migrate to pre-established granulomas that were formed upon the initial infection (36, 37). These studies provide evidence that granulomatous lesions may be more dynamic structures than previously thought during TB infection. At later time points, the greatest number of AR+ bacilli in each tissue section from untreated guinea pigs were consistently found within the largest primary granulomas displaying necrotic cores and surrounded by acellular rims. Occasionally, *M. tuberculosis*-macrophages were observed in the outer cell layers of primary granulomas. Some of these m Φ s appeared to have fused with the acellular rim (data not shown) suggesting that active migration to established primary granulomas may be occurring during TB infection of guinea pigs. And yet it is still possible that it is a combination of these described scenarios actually occurring which further underscores the importance of

fully elucidating the mechanisms of *M. tuberculosis* survival and disease progression in this animal.

In summary, the results of AR staining lung tissue samples from different preclinical animal models used to evaluate TB drugs revealed that *M. tuberculosis* inhabits a diverse range of *in vivo* environments. The significance of these findings lies in the interpretation of drug efficacy results obtained from one animal versus another as these different environments likely influence the metabolic state of bacilli. In the WT C57BL/6 mouse, drugs are being tested against a fairly homogeneous population of slowly replicating, intracellular bacilli as necrosis was neither observed in untreated or drug-treated WT mice. *M. tuberculosis* was also found to be intracellular in drug-treated IFN-gamma GKO mice throughout infection who also exhibited a lack of necrosis in their lungs. In contrast, untreated GKO IFN-gamma mice demonstrated extensive necrosis with large numbers of extracellular AR+ bacilli found within these areas suggesting that this spp. may provide the most heterogeneous population of *M. tuberculosis* with which to test the efficacy of experimental drugs offered by any of the animal models studied here. If drug-treatment of infected GKO mice is withheld until pulmonary necrosis has been established (i.e., around 22 days post-LDA), experimental drugs can be tested against near equal proportions of intracellular bacilli within a variety of cell types and extracellular bacilli in necrotic areas within lesions and airways. Furthermore, the finding that areas of necrosis and foamy mΦs found outside of granulomatous tissue are hypoxic provide evidence that IFN-gamma GKO mice reproduce key features of human TB disease and thus provide a very relevant animal model to test experimental compounds in preclinical trials. The guinea pig model offers

the most heterogeneous set of environmental conditions of all animal models studied using AR staining method described in this study. Experimental drugs are tested against intracellular bacilli found within secondary lesions and the outer cell layer of primary granulomas and extracellular bacilli found in necrotic cores and surrounding acellular rims of primary granulomas.

Taking a more comparative approach to studying the metabolic response of *M. tuberculosis* to chemotherapy under the varied *in vivo* conditions encountered in different animal models used to test preclinical drugs will undoubtedly improve our interpretation of drug efficacy data. The ability to accurately predict an experimental compounds efficacy in humans based off preclinical testing will greatly facilitate the selection of only those drugs with real potential of shortening standard TB treatment for further clinical trial testing.

CHAPTER THREE

METRONIDAZOLE LACKS ANTIBACTERIAL ACTIVITY IN GUINEA PIGS INFECTED WITH *MYCOBACTERIUM TUBERCULOSIS*

Note: The following chapter is adapted from of the article published in *Antimicrobial Agents and Chemotherapy*, Hoff DR, Caraway ML, Brooks EJ, Driver ER, Ryan GJ, Peloquin CA, Orme IM, Basaraba RJ, Lenaerts AJ. 2008, Vol. 52, No. 11, p. 4137–4140.

The following additions were made:

- 1) Paragraph 1 of the Introduction – p. 82
- 2) Table 3.1. Viable numbers of *M. tuberculosis* recovered from the lungs and spleens of infected guinea pigs – p. 89
- 3) Toxicity results reported for guinea pigs receiving metronidazole – p. 93
- 4) Discussion results from drug trials evaluating metronidazole in non-human primates and rabbits – p. 96-97

3.1 INTRODUCTION

The results of the study described in chapter 2 revealed the location of bacilli persisting after drug treatment in WT C57BL/6 mice, IFN-gamma GKO mice, and guinea pigs. The differences in TB pathogenesis observed in these animal models indicate that some models reproduce facets of human pulmonary disease better than others. These findings along with results from previous experiments done in our lab (**Location of Persisting Bacilli**) lead us to hypothesize that if the location of persistent *M. tuberculosis* remaining after drug treatment is known then the environmental conditions of this location may be exploited by drugs with specific mechanisms of action to target this sub-population of bacilli and ultimately shorten TB treatment. We therefore chose to investigate the effects of metronidazole on *M. tuberculosis* in a guinea pig model of TB disease.

The excellent distribution of metronidazole (MET) in all organs and its good bactericidal activity, including against quiescent bacteria, make it the compound of choice in infections in which anaerobes are implicated (such as digestive, genital, and pleuropulmonary infections, brain abscess, endocarditis and septicemia). *M. tuberculosis* also has the ability to adapt to microaerophilic conditions when grown under gradual O₂ depletion or when cultures change from exponential to stationary growth, a phenomenon studied extensively by Wayne and described as a sequential progression through two stages defined as NRP-1 (non-replicating phase) and NRP-2 (140). MET has no effect on exponentially growing cultures or on NRP-1 bacilli, but is bactericidal on bacilli in

stationary phase at higher concentrations (64 µg/ml) and on bacilli in the NRP-2 at 16 µg/ml (139).

Non-progressive *M. tuberculosis* lesions in the lungs often have limited vascularisation (due to necrosis and dystrophic mineralization), causing limited O₂ supply. Bacterial persistence in these hypoxic lesions is thought to be accompanied by susceptibility to MET. In mouse models of tuberculosis (TB), MET has failed to show activity consistently (25, 42, 103). This is not surprising as hypoxia was found completely absent in *M. tuberculosis* lesions of infected WT mice (8, 124), as the progression of disease rarely reaches the stages of extensive necrosis (15, 16, 78, 127). Lung lesions in guinea pigs infected with *M. tuberculosis*, on the other hand, show caseous necrosis, mineralization and hypoxia, which are also seen in natural infections in humans (129, 130). Guinea pigs develop necrotic primary granulomas that differ in their morphology compared to those of secondary lesions that result after the activation of adaptive immunity (78). In an earlier paper, we described that the persisting, acid-fast bacilli are primarily found extracellularly in a hypoxic microenvironment of primary granuloma necrosis and that only a few are found in secondary lesions (78). These findings were confirmed using the novel staining combination of auramine-rhodamine, DAPI, and hematoxylin on lung tissues of drug-treated guinea pigs reported in chapter 2. The same study also showed evidence of hypoxia in these primary granulomas of guinea pigs when pimonidazole was used (78), and therefore, we chose to explore the potential bactericidal activity of metronidazole in the guinea pig at its appropriate dose.

3.2 MATERIALS AND METHODS

Pharmacokinetic analysis. To determine an appropriate dose in guinea pigs, pharmacokinetic (pK) analysis was performed using a single dose of isoniazid (INH) at 30 mg/kg, rifampin (RIF) at 50 mg/kg, pyrazinamide (PZA) at 40 mg/kg, and metronidazole (MET) at 50 mg/kg. All drugs were obtained from Sigma Chemical Co. (St. Louis, MO) and administered by oral gavage via instillation in the back of the mouth. INH, PZA and MET were dissolved in distilled water while RIF was initially dissolved in 100% DMSO and diluted in H₂O to final 5% DMSO concentration. Pharmacokinetic data using validated HPLC assays (National Jewish Center, Denver, CO) yielded for INH an AUC₀₋₂₄ of 18.22 hr*mg/ml, 6.22 hr*mg/ml for RIF, 31.82 hr*mg/ml for PZA and 35 hr*mg/ml for MET. To reach equipotent doses in the animals versus clinical doses (based on AUC₀₋₂₄, C_{max}), doses were calculated, tested and adjusted to omit toxicity: INH at 30 mg/kg, RIF at 50 mg/kg, PZA at 100 mg/kg, MET at 100 mg/kg. In the combination trial, the dose of MET had to be reduced to 50 mg/kg after one week of treatment due to toxicity issues.

Infection and chemotherapy in guinea pigs. To assess the efficacy of the compounds in guinea pigs, the protocol followed was performed as described before (67, 78). Briefly, female outbred Hartley guinea pigs (Charles River Laboratories, North Wilmington, MA) were exposed to an aerosol of *M. tuberculosis* H37Rv (Trudeau Institute, Saranac Lake, NY) using a Madison chamber aerosol generation device calibrated to deliver approximately 20-30 bacilli into the lungs (22). *M. tuberculosis*

H37Rv was grown as described before and frozen in aliquots at -70°C until use (22). Thirty days after aerosol infection, 5 guinea pigs were sacrificed to determine the bacterial load at the start of treatment. Animals were treated by administering each dose in the back of the mouth, 5 days per week (5 animals per group). Drugs were prepared as described for the pharmacokinetic analysis and adjusted to concentrations achieving bioequivalent doses in humans. Every experiment contained an untreated sucrose control group, i.e. daily oral administration of 1 ml 40% w/v sucrose. Drug preparations in water were prepared weekly in final w/v 40% sucrose to increase palatability for the guinea pigs and stored at 4°C.

Bacterial enumeration. Animals were sacrificed at intermittent time points (after 2, 4 and 6 weeks for initial experiment, at 2 and 4 weeks for the drug combination trial) by sodium barbital injection (Sleepaway; Fort Dodge Laboratories), and the organs were aseptically removed. The right cranial lung lobe (22% of bacterial numbers versus whole lungs) was homogenized and plated as described before (67, 78). The detection limit of the plating procedure was ~25 CFU. The viable bacterial numbers were converted to logarithms. Statistical analysis of CFU data was performed by one-way analysis of variance (ANOVA) followed by an all pairwise multiple comparison procedure utilizing the Tukey test for the analysis of lung data (SigmaStat® v.2.03, SPSS Inc.).

Histology. Following euthanasia, the left cranial lung lobe was infused *in situ* with 5 ml of 10% neutral-buffered formalin and preserved until processed for histopathological assessment. At the time of processing, all tissues were embedded in

paraffin, sectioned at 5 μm , and stained with hematoxylin and eosin (H&E) or stained with acid fast stain for histologic evaluation and photography. A veterinary pathologist reviewed in a blinded study two serial sections from each guinea pig obtained from equivalent areas of the left cranial lung lobe (section made to obtain largest surface area). H&E stained sections were ranked in order of severity on lesion burden by sub-gross and microscopic examination and the individual lesions were scored as described earlier (98).

3.3 RESULTS

Metronidazole efficacy in guinea pigs administered as a single drug. The efficacy of INH at 30 mg/kg and MET at 100 mg/kg were evaluated in guinea pigs infected with *M. tuberculosis* via a low dose aerosol (LDA) infection. At the start of treatment (30 days post LDA), the bacterial load in the lungs reached approximately 6 log₁₀ CFU in the guinea pig lungs (Figure 3.1 A). At the completion of the study (after 6 weeks of treatment), the bacterial load in the sucrose control group was around 5 log₁₀ CFU (Table 3.1). In this study, INH at 30 mg/kg and metronidazole at 100 mg/kg were tested after 6 weeks of treatment with sacrifices every two weeks. INH reduced the bacterial load significantly after 6 weeks of chemotherapy in the lungs (2.35 log₁₀ CFU decrease); its activity versus untreated controls was more pronounced in spleens (no bacteria could be cultured from any guinea pigs in this group) ($P < 0.05$) (Fig. 3.1 B). MET did not show any significant activity in the lungs and spleens compared to the sucrose-treated group for all the time points tested (Fig. 3.1 and Table 3.1).

Figure 3.1: Viable bacterial numbers in **A** whole lungs and **B** spleens of *M. tuberculosis* infected guinea pigs treated with sucrose, isoniazid (INH) or metronidazole (MET) for 2-4-6 weeks.

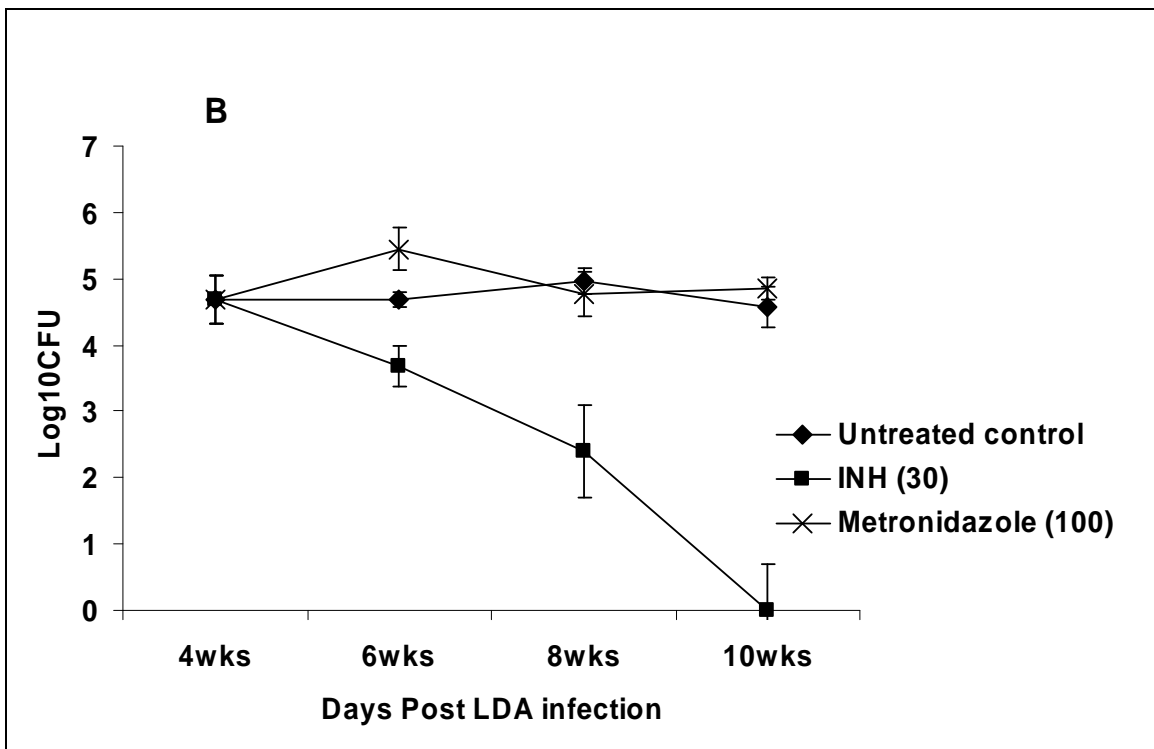
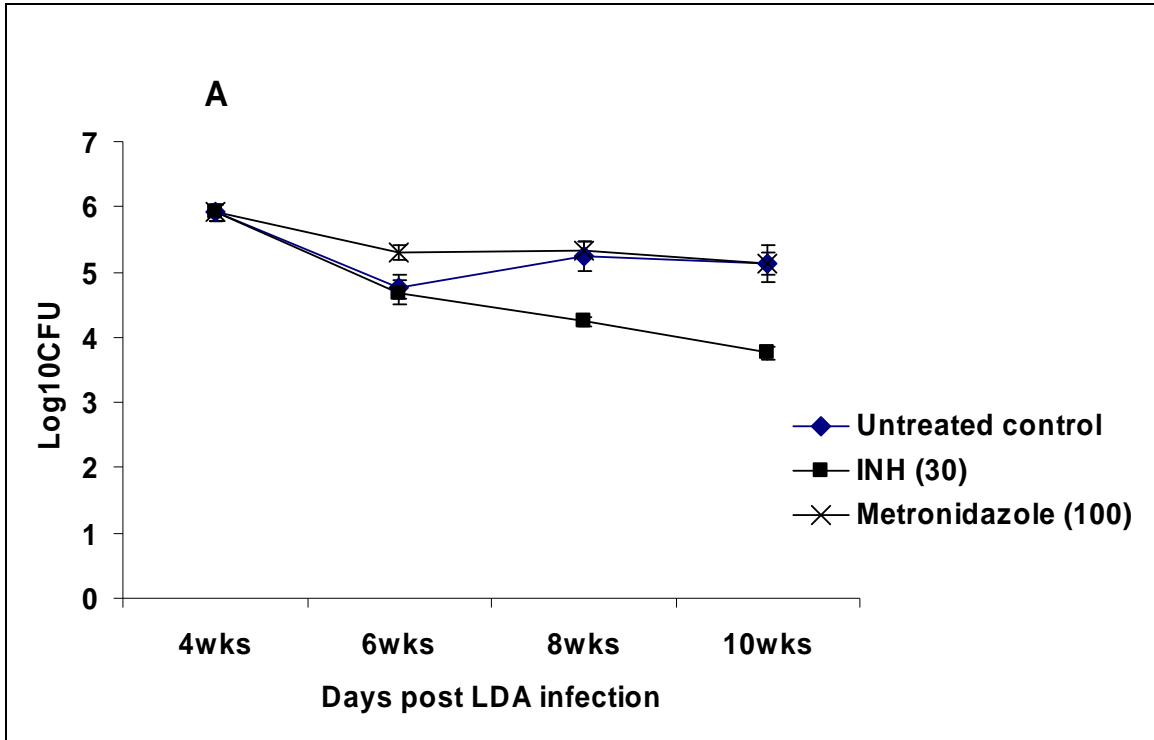


Table 3.1. Bacterial numbers in right cranial lung lobes and spleens of guinea pigs infected with *M. tuberculosis* after 2, 4, & 6 weeks of drug treatment.

Treatment Regimen [in mg/kg]	Log ₁₀ CFU ± SEM			
	Lung	<i>n/N</i> ^a	Spleen	<i>n/N</i> ^a
*Day 1, Start of Treatment (Untreated Controls)	5.91±0.12	5/5	4.68±0.37	5/5
2wk, Untreated Controls	4.76±0.18	5/5	4.69±0.10	5/5
2wk, INH [30]	4.69±0.19	5/5	3.66±0.31	5/5
2wk, Metronidazole [100]	5.30±0.12	5/5	5.45±0.31	5/5
4wk, Untreated Controls	4.65±0.38	5/5	4.83±0.31	5/5
4wk, INH [30]	4.24±0.06	5/5	2.40±0.70	3/5
4wk, Metronidazole [100]	5.36±0.12	4/4	4.76±0.35	4/4
6wk, Untreated Controls	5.19±0.29	5/5	4.54±0.31	5/5
6wk, INH [30]	3.56±0.23	5/5	0.00 ^b	0/5
6wk, Metronidazole [100]	5.14±0.16	5/5	5.09±0.16	5/5

* Day 1 = 30 days post-LDA

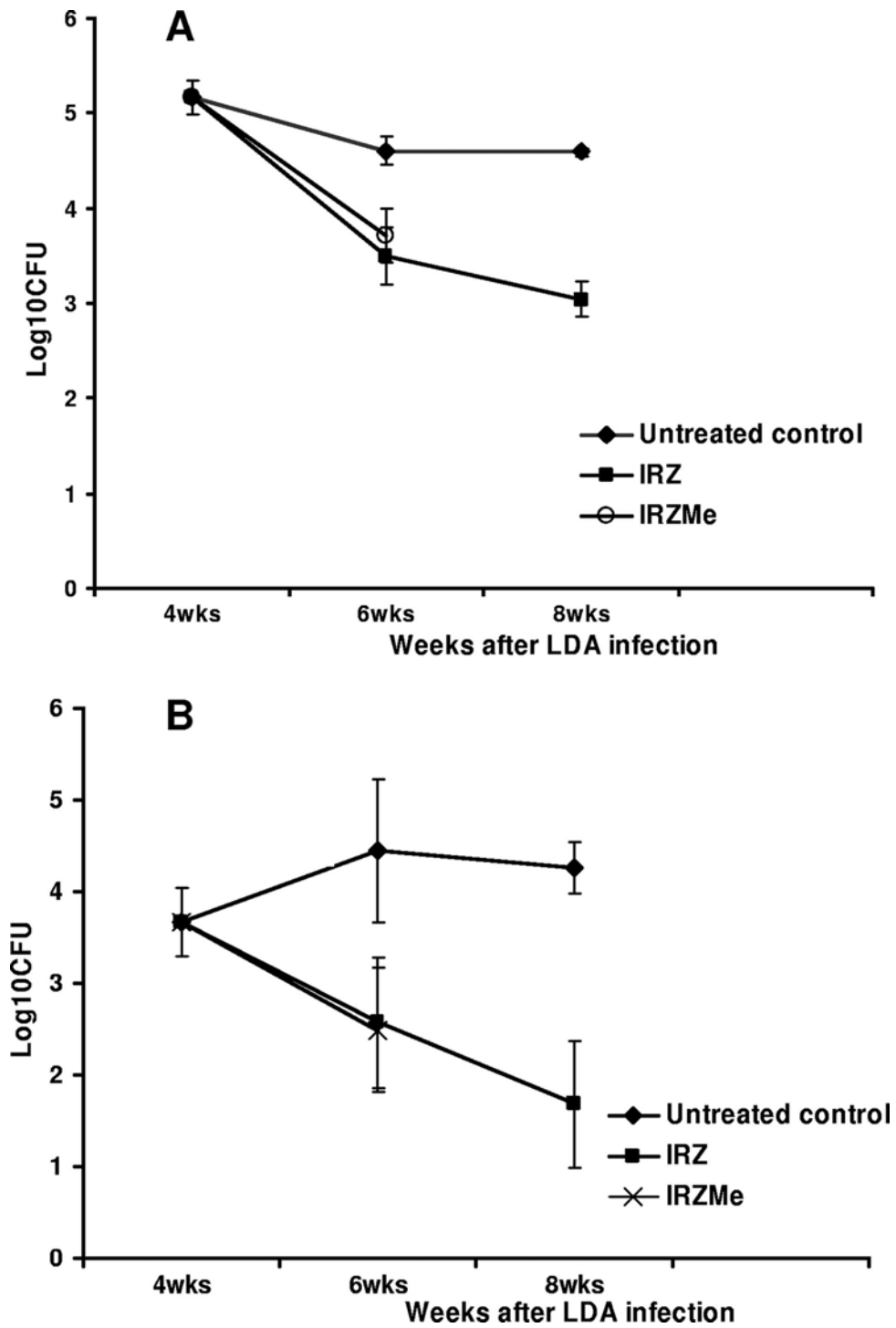
^a *n/N*, number of guinea pigs that yielded viable CFU data (*n*) over the total number of guinea pigs in that group (*N*)

^b zero CFUs were yielded by all guinea pigs within their respective group

Metronidazole efficacy in guinea pigs in combination treatment regimens.

MET (at 50 mg/kg) was tested in combination with INH (30 mg/kg), RIF (50 mg/kg), and PZA (100 mg/kg) (IRZMe), and its activity was compared to that of the standard regimen of INH, RIF, and PZA (IRZ). At the start of treatment, the bacterial load in the guinea pig lungs reached approximately $5.2 \log_{10}$ CFU. After 4 weeks of treatment, the bacterial load in the sucrose-treated control group was approximately $4.8 \log_{10}$ CFU (Fig. 3.2). The animals were scheduled to be killed after 2 and 4 weeks of treatment. After 2 weeks of treatment, the bacterial numbers in the lungs of guinea pigs receiving IRZMe treatment were significantly reduced compared with those in the untreated controls ($0.89 \log_{10}$ CFU decrease) ($P < 0.05$) but was found to be similar to that in the IRZ control group ($1.33 \log_{10}$ CFU decrease compared to untreated controls) ($P > 0.05$) (Fig. 3.2 A). The bacterial burden in the spleens of guinea pigs receiving IRZ or IRZMe treatment were also similar and significantly reduced compared to the untreated controls after 2 weeks of treatment (1.78 and $2.14 \log_{10}$ CFU decrease compared to untreated controls, respectively) ($P < 0.05$) (Fig. 3.2 B). In conclusion, no additional activity was observed for MET when it was combined with the standard regimen. In addition, MET caused severe toxicity starting the second week of the combination treatment. The animals in the IRZMe group started to lose weight (more than 20% of their body weight), and four animals had to be euthanized. The remaining animals were killed at the 2-week treatment time point, and therefore, no data for the IRZMe group are available beyond this time point due to the severe toxicity (Fig. 3.2).

Figure 3.2: Viable bacterial numbers in *A* whole lungs and *B* spleens of *M. tuberculosis* infected guinea pigs treated with sucrose, the combination of INH, RIF and PZA (IRZ) or INH, RIF, PZA and MET (IRZMe) for 2 to 4 weeks.



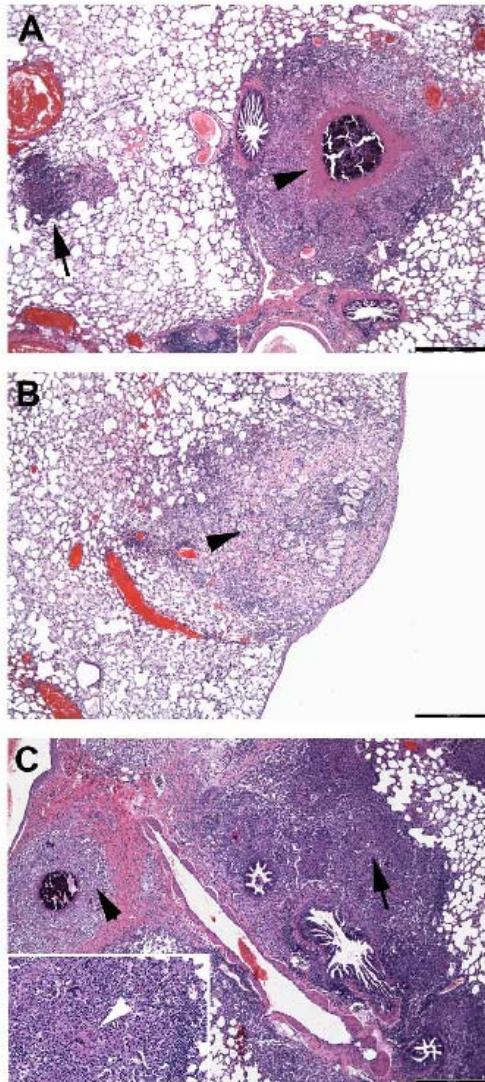
Lung histopathology analysis. Histologic analysis showed both primary granulomas and secondary lesions at the start of treatment in the lungs of infected guinea pigs. Treatment with INH or MET did not show any significant effect on the morphology of primary granulomas as expected (Fig. 3.3 A), but treatment significantly affected the development and progression of secondary inflammatory lesions. Untreated guinea pigs showed an increase in secondary lesion inflammation over time. While INH appeared to stop the progression of inflammation and prevented the development of new secondary lesions (Fig. 3.3 B), MET exacerbated the inflammation and increased the secondary lesion involvement in the lung considerably versus the untreated controls (Fig. 3.3 C). Of importance, the increased inflammation in the metronidazole group is not due to an increased bacillary burden at the time points measured, and therefore the progression of the lesions appears to be drug-induced. Acid fast staining of lung sections of untreated guinea pigs show the presence of few intracellular bacilli in the secondary lesions, while most acid fast bacilli (AFB) were found extracellular in the primary granulomas predominantly within necrotic debris and the outer inflammatory zone (data not shown). Guinea pigs treated with INH or MET both had morphologically intact acid-fast bacilli remaining within primary lung granulomas. In both groups, individual and micro-colonies of bacilli were found extracellular within the necrotic center of lesions and within the acidophilic acellular rim of residual necrosis delineating the central mineralized core as was described before (78).

The reasons for the increase in inflammation in the MET-treated group are unclear. Although the bacillary burden in the MET-treated group was not statistically different from that in the sucrose-treated control group for the time points tested, one can

speculate that a slight difference in the early dissemination of the bacteria (suggested by a slightly increased bacterial load 2 weeks after MET treatment; Fig. 3.1) may have effects later on. Alternatively, the accelerated formation of TB lesions may be induced by the drug itself by influencing the host immune response.

Additional information. Among the commonly reported side effects encountered with MET therapy, peripheral neuropathy, leukopenia, and thrombocytopenia have been reported (96). Guinea pigs receiving MET exhibited flaccid paralysis of the hind legs suggesting that peripheral neuropathy may have been induced by drug treatment, however no post-mortem necropsy was done in order to confirm or disregard the presence of nerve damage. Future experiments could include blood work to assess levels of leukocytes and red blood cells in order to confirm leukopenia and/or thrombocytopenia in guinea pigs as possible reasons for increased inflammation.

Figure 3.3: Secondary lesions in lungs of *M. tuberculosis* infected guinea pigs after drug treatment. The extent and morphology of the lesions in *M. tuberculosis* infected guinea pigs either untreated or treated for 4 wks with INH or MET. Images show lesions of one representative animal for each group (average animal). **A**, Untreated guinea pig treated with 40% (wt/vol) sucrose for 4 wks. A single primary granuloma (arrowhead) has central calcification and residual central lesion necrosis. A single secondary lesion is characterized by increased numbers of LCs (basophilia) and is devoid of central necrosis (arrow). **B**, An INH-treated guinea pig has a single primary granuloma that lacks necrosis and calcification but has fibrosis (arrowhead). No secondary lesions are evident in the field. **C**, A MET-treated guinea pig has extensive inflammation represented primarily by secondary lesions (arrow) that coalesce in the perivascular and peribronchial pulmonary parenchyma. Among the LCs and mononuclear phagocytes are occasional multinucleated giant cells (inset, white arrowhead). A single primary granuloma is evident by the central calcification (black arrowhead). H&E staining was used. Bar, 460 μ m.



3.4 DISCUSSION

Metronidazole is a drug compound that is efficacious against anaerobic bacteria. *M. tuberculosis* is known to adapt to anaerobic conditions when grown under conditions of gradual O₂ depletion, and this O₂-dependent adaptive state renders bacilli susceptible to MET (42, 139, 140). In chapter 2, it was observed that bacilli persisting after drug treatment in guinea pigs were predominantly found in the necrotic cores and surrounding acellular rims of primary granulomas. We have previously shown these primary granulomas from the lungs of *M. tuberculosis*-infected guinea pigs to be hypoxic (78), and this formed the premise to investigate the antimicrobial efficacy of MET in a guinea pig model of TB by: i) assessing the bacterial burdens in the organs of guinea pigs after treatment compared to untreated controls, and ii) by comparing the histopathology of guinea pigs receiving INH or MET therapy to untreated guinea pigs. We found that MET treatment elicited no antibacterial effect and caused a more severe histopathology of TB disease in guinea pigs when compared to both the INH-treated and untreated guinea pigs.

The reason for MET not showing any reduction in culturable bacterial numbers in *M. tuberculosis* infected guinea pigs can be multifold. We know that guinea pigs infected with *M. tuberculosis* develop hypoxic lesions that show caseous necrosis, fibrosis and mineralization. It seems, however, improbable that the inner core of this caseous necrosis is totally anoxic. The dynamic structure of the granuloma lacking a physical barrier will likely show an oxygen gradient across the acellular rim and the caseous necrosis with some oxygen diffusing through air pockets and tissue fluid. MET has been shown to be mostly effective against *M. tuberculosis* under completely anaerobic conditions (at 16 µg/ml) *in vitro* whereas higher drug concentrations are required at microaerophilic

conditions (64 µg/ml) (42, 139). To reach drug levels required for activity against *M. tuberculosis* under these microaerophilic conditions, high drug doses would have to be administered, which would likely result in significant toxicity. In humans for instance, a dose of 500 mg of MET is recommended, which results only in a blood level of 13 µg/ml at 3 hours after oral administration. This is similar to the dose we used here where in guinea pigs a dose of 50 mg/kg of MET reached a C_{max} of 17 µg/ml.

In TB patients, it is possible that certain lesion types which are not present in the guinea pig (such as solid caseous necrosis or liquefactive necrosis as well as closed calcified lesions) could be entirely anoxic. Therefore, the issue of the antituberculosis activity of MET *in vivo* cannot be completely closed without further trials involving animal models with these pathological features.

Additional information. To illustrate this point, MET was found to have efficacy in rabbits infected with *Mycobacterium bovis* Ravenel (132). Rabbits receiving MET at 20 mg/kg twice per day for 28 consecutive days exhibited a 1.09 log₁₀ decrease in CFU compared to untreated controls. This same group also evaluated MET in mice infected with the same strain of *M. bovis* but found MET to have no beneficial effects. Rabbits are known to be exquisitely susceptible to infection with *M. bovis* and can form cavitory lesions composed of liquefactive necrosis (38), a type of lesion not present in the guinea pig. Another study found MET to be efficacious in treating non-human primates infected with *M. tuberculosis* (49). In this study, cynomolgus macaque monkeys developing a latent TB infection were initiated on INH or MET as single drugs or INH and RIF in combination for 2 months. NHPs were administered anti-TNF-alpha to induce reactivation of persisting bacilli, however no monkeys from any of the treatment groups

reactivated. NHPs are known to develop the full range of heterogeneous pulmonary lesions seen in man after infection with *M. tuberculosis* (29). The significance of these studies and the one presented here highlights the importance of testing experimental compounds in relevant animal models that accurately mimic *in vivo* conditions encountered in human infection. However, differences in drug activity between animal models can also be utilized to increase our understanding of the *M. tuberculosis* response to chemotherapy under different *in vivo* environments as some drugs require specific conditions to be active (i.e., PZA – acidic pH, MET - anaerobiosis).

Nevertheless, the lack of reproducible MET activity in mice and guinea pigs may limit the use of this drug for TB treatment. Clinical trials are currently underway to explore the efficacy and tolerability of MET in combination with the second-line drug regimen for TB treatment. will provide definite answers to these questions. Patients will receive either 8 weeks of standard second-line drugs plus placebo or 8 weeks of standard second-line agents plus MET. The investigators in charge of this clinical trial hope that MET therapy will more effectively treat patients with MDR-TB. These trials will serve to validate the use of specific animal models in the testing of experimental compounds (96).

CHAPTER FOUR

INVESTIGATING THE KILLING KINETICS OF ANTI-TUBERCULOSIS DRUGS IN A MURINE MODEL OF BACTERICIDAL ACTIVITY

4.1 INTRODUCTION

Considering the current global TB crisis, there has never been a more urgent need for new, highly effective chemotherapeutic regimens. Although a number of promising candidates are in the clinical trial pipe-line, the overwhelming odds of a compound making it to registry still leaves a significant chance that none of these drugs will be introduced into standard therapy. Few pharmaceutical companies are willing to take the risk of investing large sums of money to develop a compound that will probably fail some aspect of preclinical or clinical trials. Thus, if a compound should ultimately be determined unfit for human use, better it to be found out sooner rather than later. Drugs that satisfactorily complete preclinical *in vitro* and *in vivo* criteria may be selected for further investigation in clinical TB trials. Clinical trials are long, labor-intensive, and require a large number of participants to generate significant data making their funding one of the most expensive aspects of drug development (5). This underscores the importance of designing and implementing relevant animal models that yield predictive information on an experimental compound's potential efficacy in humans during preclinical trials.

Some drugs in phase II clinical trials undergo an early bactericidal activity (EBA) test. Although not required by the FDA, these tests can give pharmaceutical companies developing the experimental compound the confidence to proceed with larger phase IIb drug combination trials. EBA tests also allow for the selection of an active drug dose to pursue in subsequent trials (45). EBA in clinical trials is measured as the \log_{10} fall in sputum CFU obtained from patients with an active TB infection over the initial days of therapy. The EBA of a compound under investigation is as follows:

$$\text{EBA}_{0-x} = (\log_{10} \text{CFU } S_0 - \log_{10} \text{CFU } S_x) / x,$$

where S_0 = baseline sputum CFU at day₀, S_x is the sputum CFU after x days of treatment.

The first large-scale clinical EBA trial was performed in 1980 by Jindani *et al.* (65). This landmark study evaluated the antimicrobial activity of drugs against *M. tuberculosis* administered alone or in combination over the initial 14 days of treatment. Among the findings obtained from this study, the EBA of the drugs tested was found to be greatest during the first 2 days of therapy (EBA_{0-2}) and markedly reduced in the following 12 days (EBA_{2-14}). This observation has yielded much information and generated much speculation on the killing kinetics of TB drugs. The EBA_{0-2} of INH is greater than any known drug clinically approved to treat TB. However, INH efficacy reduces drastically after the first 2 days of treatment. In contrast, the EBA_{0-2} of RIF is less than that of INH, but RIF maintains activity greater than INH in the subsequent 12 days of treatment. These killing kinetic variations are believed to reflect different populations of *M. tuberculosis* bacilli being selectively targeted by drugs depending on their mechanisms of action. INH inhibits cell wall synthesis of mycobacteria and as such is only effective against dividing bacilli. The activity of INH is greatest during the first 2

days of treatment and dramatically loses efficacy afterwards. This trend in INH killing kinetics is believed to reflect the elimination of actively replicating bacilli leaving only the persistent, non-replicating population of bacilli (115) and is why INH is said to have good early bactericidal activity. The mechanism of action of RIF involves the disruption of protein synthesis, a metabolic process performed by dividing and non-dividing bacteria alike. RIF is bactericidal during the initial 2 and following 12 days of therapy because it is efficacious against both replicating and persisting bacilli (115). As such, RIF is said to have sterilizing activity as it maintains a bactericidal effect against *M. tuberculosis* after the actively replicating population has died off.

The sterilizing activity of a drug or drug regimen is the single most important parameter to consider when evaluating novel compounds as this factor ultimately determines how long treatment must be administered in order to effectively sterilize patients. Since Jindani *et al.*, studies have investigated the bactericidal activity of drugs over various time periods in order to determine whether sterilizing activity can be measured in the initial days of therapy. Treatment periods examined in these EBA and extended EBA (eEBA) studies have included EBA over 2 days (EBA₀₋₂) (31), measured over 5 days (EBA₀₋₅) (114), over 7 days (EBA₀₋₇) (111), over 14 days (EBA₀₋₁₄) (44), and/or measured between days 2 and 5 of treatment (EBA₂₋₅) (115), between days 2 and 7 of treatment (EBA₂₋₇) (43), between days 2 and 14 of treatment (EBA₂₋₁₄) (66). Furthermore, attempts to measure sterilizing activity have also included modifications such as augmenting clinical EBA methodology and statistical calculations (115). Yet conclusive results that sterilizing activity can be accurately assessed are still lacking and therefore the utility of clinical EBA trials is a controversial topic.

The need for multidrug therapy for TB treatment makes separating one drug activity versus another difficult. To date, relapse studies or assessing sputum conversion rates in patients 2 months after culture negativity is achieved with chemotherapy are the only methods for measuring sterilizing activity (26, 92). These phase III clinical trials require up to 1,000 patients to be followed for at least 18 months to follow-up on treatment efficacy and necessitate an enormous financial investment in order to complete. Clearly, a preclinical test that could identify sterilizing activity of a compound prior to going into these clinical trials would be invaluable for TB drug discovery. Furthermore, biomarkers that could differentiate patients responding poorly to treatment from those responding positively would allow for individualized TB chemotherapeutic regimens to be employed (136).

There is a need for preclinical models to generate as much information on a drug as possible to adequately predict the potential efficacy of a lead compound against tuberculosis in the clinic. A preclinical *in vivo* model which would assess potential sterilizing activity elicited by an experimental compound in a relatively short amount of time would be invaluable for TB drug development. The purpose of the experiments described in this chapter was to: i) establish a short term mouse model which can yield predictive info. on a compounds antimycobacterial efficacy in clinical EBA trials, and ii) determine if a compounds potential sterilizing activity can be measured in the initial days of treatment.

To this end, a murine model of TB disease was established using the same time points of TB treatment that are used in clinical EBA trials. We show here that this murine model provides significant information on drug killing kinetics including potential

sterilizing activity and preliminary data shows it provides predictive information on the outcome of experimental compounds under investigation for TB treatment in clinical EBA trials. These findings should have significant implications for preclinical TB drug development as the use of this model should facilitate the selection of only those compounds that have real potential to shorten current TB therapy for further testing in clinical trials.

4.2 MATERIALS AND METHODS

Bacterial isolate. The standard strain used for drug testing in mice in our laboratory, *M. tuberculosis* strain Erdman (TMCC 107), was prepared as previously described (70). Briefly, *M. tuberculosis* was grown to mid-log phase in Proskauer-Beck Medium containing 0.01% Tween 80 (Sigma Chemical Co., St. Louis, MO) and stored in vials frozen at -70°C until use.

Chemicals and drugs. Isoniazid (INH) and pyrazinamide (PZA) (Sigma Chemical Co.) were dissolved in distilled water. PA-824 obtained from the Global Alliance for TB Drug Development was formulated in cyclodextrin/lecithin (CM2) as described before (77). Briefly, PA-824 was added to 10% hydroxypropyl- β -cyclodextrin solution (Sigma Chemical Co.), and the mixture was stirred gently for 24 h at room temperature (RT). After mixing, suspension was sonicated with a Vibra Cell probe sonicator (model VC-130; Sonics and Materials, Inc., Newton, CT) for 10 min. at 20% amplitude while keeping the solution less than 50°C. Frozen lecithin (Sigma Chemical Co.) was subsequently added to a final concentration of 10% and stirred for 10 min. at RT. The solution was then sonicated at 30% amplitude on ice for 15 min. TMC207 was provided by Johnson and Johnson (Beerse, Belgium) and formulated according to their protocol as described previously (9). In short, compound was dissolved in 20% hydroxypropyl- β -cyclodextrin (Acros Organics, New jersey, USA) and then stirred for 24 h at RT shielded from light. After mixing, 1N HCl was added to a final concentration of 1% to facilitate dissolution and filter sterilized using 0.2 μ M syringe filter. LIN (21CEC

Pharmaceuticals, Bradenton, FL) was first weighed out in individual tubes and ground up using a sterile glass stir rod to break up any remaining clumps. Each tube then received 0.5% methyl cellulose to suspend compound. All drugs except LIN were prepared in a single batch and dispensed into individual tubes for each treatment day. All drugs were stored in the dark at 4°C until use.

Mice. Eight- to ten-week-old female specific-pathogen-free, C57BL/6-Ifngtm1ts gamma interferon gene-knockout (GKO) mice were purchased (Jackson Laboratories, Bar Harbor, Maine) and held under barrier conditions in a biosafety level III animal laboratory.

Experimental infection and chemotherapy. Mice were exposed to *M. tuberculosis* Erdman via a LDA in a Glas-Col inhalation exposure system (Glas-Col Inc., Terre Haute, IN) as described before (70). The absence of interferon-gamma renders these mice unable to prevent or control bacterial replication without antibiotic treatment. As a result, animals develop a rapidly progressive disease and succumb to effects 28-30 days post-LDA without treatment. Two mice were sacrificed one day post-aerosol challenge to verify bacterial inoculation of 50 to 100 CFU per mouse. Treatment was initiated 15 days post-LDA and continued for 14 consecutive days. Mice were euthanized on day 29 post-aerosol infection. One group of untreated mice was sacrificed at the onset of treatment and for each subsequent time point to establish a baseline CFU and track disease progression, respectively.

The present study is a continuation of two prior *in vivo* experiments using this murine model and follows a similar protocol with a few improvements and modifications. The variations between the two previous studies and the one presented here were the times of treatment initiation and the time points chosen to perform viable counts. For the 2 previous trials, treatment was started 18 days post-LDA. One experiment evaluated the bactericidal activity of drugs over days 0-2, 2-4, and 4-7 of treatment and the second experiment was extended to include treatment days 7-10.

For the murine trial described here, all drugs were administered via oral gavage once a day for 7 days/week to simulate dosing regimens used in clinical trials at the following doses: INH and TMC207 at 25 mg/kg each, PA-824 at 100 mg/kg, and PZA and LIN at 150 mg/kg each. Treatment groups consisted of 4 mice each for every time point. Untreated and drug-treated mice were sacrificed by CO₂ inhalation 24 hr after receiving the last dose of drug on days 2, 5, 7, 10, and 14 of treatment. Left cranial lung lobes were aseptically removed and disrupted using a tissue homogenizer. Organs from all treatment groups (except those receiving TMC207) were homogenized and serially dilute in sterile saline. Organs from mice treated with TMC207 were homogenized in sterile saline supplemented with 5% bovine serum albumin (BSA) (Sigma Aldrich St. Louis, MO) and serially diluted in saline supplemented with 20% BSA. TMC207-treated organs were processed in this fashion in order to address any potential drug carryover associated with protein binding as has been noted previously with this compound (80). The number of viable organisms was determined by plating serial dilutions of the homogenates on nutrient Middlebrook 7H11 agar plates (GIBCO BRL, Gaithersburg, Md.) for all groups except those receiving TMC207, which were plated on Lowenstein-

Jensen (LJ) (Sigma Aldrich St. Louis, MO) agar plates prepared as described by the manufacturer. LJ agar plates were used to address any drug carryover that may occur when processing TMC207-treated tissues at the time of necropsy as this compound is known to have an exceptionally long half-life with serum level concentrations easily exceeding the minimum inhibitory concentration (MIC) (80). Plates were incubated at 37°C in ambient air for 4 weeks before counting viable colonies of *M. tuberculosis* (CFU). Viable counts were converted to logarithms and expressed as the average log₁₀ CFU in lungs of mice per treatment group.

Statistical analysis. Prior to this study, a power analysis was performed in order to establish the number of mice per group necessary to have a statistical power of 0.8, with a type I error of 0.05. Statistical analysis was performed by Dr. Chapman from the Statistics Department at Colorado State University using SAS (SAS Institute Inc., Cary, NC, USA). Due to the degree of activity exhibited by efficacious drugs and the narrow standard deviations associated with this inbred strain of mouse (76), power analysis using a two-sample t test calculating for a mean difference of 1.0 between control and drug-treated groups revealed a sample size of 4 mice per group required for data to be considered statistically significant (data not shown).

CFU data was analyzed by one-way analysis of variance and was not normally distributed. A Kruskal-Wallis test was then performed comparing the median values from each treatment group for lung CFU data. CFU data from drug-treated groups was compared to the pre-treatment controls (base CFU number prior to the onset of treatment) and compared between different drug groups at the same time points. Statistical analysis

on CFU data generated at each time point was performed using GraphPad Prism (version 4.02, La Jolla, CA). Differences between median values generated by each treatment group were considered significant at the 95% level of confidence ($P < 0.05$).

Bactericidal Activity Calculations. The bactericidal activity of drug compounds administered in mice was calculated as the average \log_{10} fall in lung CFU per day of treatment. This is similar to the method used in clinical trials to assess drug activity in sputum. The following formula was used:

$$\text{EBA} = (\log_{10} \text{ lung CFU } d_x - \log_{10} \text{ lung CFU } d_y)/(y-x),$$

where d_x equals the \log_{10} CFU concentration in the lungs of drug-treated mice established at an early time point, d_y equals the \log_{10} CFU in the lungs of mice receiving chemotherapy for y days of treatment, and $y-x$ equals the number of treatment days between the two time points being compared.

Histology. At the time of sacrifice, the right caudal lung lobe from each mouse was infused with 10% paraformaldehyde (Electron Microscopy Sciences, Hatfield, PA) and preserved until processed for histopathological assessment. Lung lobes were embedded in paraffin at the time of processing and 5 μm sections were prepared and stained with hematoxylin and eosin (H&E) or acid-fast stain.

TMC207 protein binding assessment. TMC207 has a long half-life and is known to be extensively protein bound (80). Since only free, unbound drug is bactericidal, initial studies were undertaken to assess the potential for drug carryover

when processing tissues from mice receiving TMC207. Various media preparations differing in the amount of protein supplement were compared to sterile saline to determine if protein-enriched media influences the bactericidal activity of TMC207 on *M. tuberculosis* while under simulated conditions of tissue processing. The concentration of TMC207 at 20 µg/ml used in this *in vitro* study was based on available pharmacokinetic data from drug plasma concentrations in mice after administering a dose of 15 mg/kg (9). Each media preparation tested was plated on both 7H11 and LJ agar plates to determine if protein binding *ex vivo* influences the recovery of bacterial CFU while agar plates are incubating for mycobacterial growth. The following conditions were compared for protein binding capacity of TMC207: saline, saline supplemented with 10% BSA, or saline supplemented with 20% BSA. Every 3 ml aliquot was spiked with 1 ml of *M. tuberculosis* Erdman at 1×10^6 CFU/ml and with 1 ml of TMC207 at a final concentration of 20 µg/ml. Tubes were then slowly stirred for 1 h at 37°C. One milliliter from each culture tube was serially diluted in sterile saline or in saline supplemented with 20% BSA. Samples from each dilution were plated on nutrient Middlebrook 7H11 agar plates (GIBCO BRL, Gaithersburg, Md.), 7H11 agar plates supplemented with 10% BSA, or nutrient LJ agar plates (Sigma Aldrich St. Louis, MO). Plates were incubated for 3 weeks at 37°C in ambient air before counting viable colonies.

4.3 RESULTS

Assessment of TMC207 protein binding capacity. TMC207 is known to be extensively protein-bound and to have a long half-life in patients leading to serum concentration levels exceeding the MIC for *M. tuberculosis* (80). As this might pose a problem for the *in vivo* study using TMC207 in GKO mice, different conditions of media used for tissue processing and plating were tested to assess the presence of free drug and its influence on spiked cultures of *M. tuberculosis*. The results show that for all of the conditions tested, plating samples on LJ plates serially diluted in either saline or saline supplemented with 20% BSA gave the most consistent, accurate colony counts of all agar plate preparations (Table 4.1). A substantial difference (more than 1 log₁₀ increase in CFU) was observed between the samples plated on LJ agar when serially diluted in saline supplemented with 20% BSA versus saline alone regardless of the media used to incubate TMC207 with *M. tuberculosis* (saline, saline + 10% BSA, or saline + 20% BSA). CFUs from 7H11 agar plates were not detected until samples had been diluted 125- to 625-fold. The first dilutions generating countable CFUs on 7H11 plates yielded fewer colonies than subsequent dilutions indicating that drug carryover was impeding mycobacterial growth. Drug carryover was not observed only after the inoculum containing TMC207 and *M. tuberculosis* was diluted 625- to 3,125-fold, at which point reliable bacterial numbers were generated. A similar observation was seen in samples containing *M. tuberculosis* diluted in saline supplemented with 20% BSA. No CFUs whatsoever were detected on 7H11 agar plates supplemented with 10% BSA regardless of the media preparation used

to incubate *M. tuberculosis* with TMC207 indicating that the presence of free drug was exerting a bactericidal effect *ex vivo* (Table 4.1).

The results of these experiments suggest that drug carryover of TMC207 has a bactericidal effect on *M. tuberculosis ex vivo* and may influence the results of the *in vivo* study using TMC207 in mice. The most reliable CFU data was obtained when samples were serially diluted in saline + 20% BSA and plated on LJ agar plates. When the *M. tuberculosis* CFU concentration from all colony counts generated in this study were calculated to give a final bacterial concentration, serial dilution in saline + 20% BSA and plating on LJ agar plates was found to consistently yield the highest CFU concentration. From these results, it was decided that for the *in vivo* studies, organs from mice treated with TMC207 would be homogenized in saline supplemented with 5% BSA, serially diluted in saline supplemented with 20% BSA and plated on LJ plates in order to ensure that the most reliable CFU data possible would be generated for TMC207-treated mice.

Table 4.1 Growth of *M. tuberculosis* incubated with 20 µg/ml of TMC207 for 1 h in **A** saline or **B** saline supplemented with 20% BSA and subsequently plated on 7H11, 7H11 + 10% BSA, or LJ agar plates.

Table 4.1A					Table 4.1B				
Incubation Media	Fold-Dilution	7H11 Agar	7H11 Agar + 10% BSA	LJ Agar	Incubation Media	Fold-Dilution	7H11 Agar	7H11 Agar + 10% BSA	LJ Agar
Saline Only	0	0	0	TNTC	Saline Only	0	0	0	TNTC
	5-	0	0	TNTC		5-	0	0	TNTC
	25-	0	0	50		25-	0	0	TNTC
	125-	3	0	10		125-	0	0	10
	625-	19	0	1		625-	5	0	1
	3,125-	1	0	0		3,125-	5	0	0
	15,625-	1	0	0		15,625-	1	0	0
	78,125-	0	0	0		78,125-	0	0	0
Saline + 10% BSA	0	0	0	TNTC	Saline + 10% BSA	0	0	0	TNTC
	5-	0	0	TNTC		5-	0	0	TNTC
	25-	0	0	52		25-	0	0	TNTC
	125-	4	0	3		125-	0	0	63
	625-	8	0	0		625-	9	0	15
	3,125-	3	0	0		3,125-	4	0	1
	15,625-	1	0	0		15,625-	0	0	0
	78,125-	0	0	0		78,125-	0	0	0
Saline + 20% BSA	0	0	0	TNTC	Saline + 20% BSA	0	0	0	TNTC
	5-	0	0	TNTC		5-	0	0	TNTC
	25-	0	0	48		25-	0	0	TNTC
	125-	0	0	10		125-	0	0	73
	625-	4	0	0		625-	1	0	11
	3,125-	4	0	0		3,125-	3	0	2
	15,625-	1	0	0		15,625-	2	0	0
	78,125-	0	0	0		78,125-	0	0	0

BSA, bovine serum albumin, *TNTC*, Too Numerous To Count

Chemotherapy of *M. tuberculosis*-infected IFN-gamma GKO mice. The efficacy of the first line drugs INH and PZA as well as the experimental compounds PA-824, TMC207, and LIN were evaluated in IFN-gamma GKO mice infected with *M. tuberculosis* via LDA. The results are presented in Figure 4.1 and Table 4.2. At the start of treatment 15 days post-LDA, the bacterial load in the lungs of mice reached approximately 6.19 log₁₀ CFU. By the end of the study 14 days later, the lungs of untreated mice had a bacterial burden of approximately 8.55 log₁₀ CFU.

After 14 days of treatment with INH at 25 mg/kg, there was a significant reduction of 1.66 logs in the lungs of treated mice compared to the baseline CFU at the start of treatment ($P < 0.001$). In contrast, PZA at 150 mg/kg did not exhibit significant activity on the bacterial burden in the lungs over the same treatment period with an approximate 0.63 log₁₀ increase in lung CFU from baseline ($P > 0.05$) (Fig. 4.1). All mice receiving therapy with experimental compounds exhibited statistically significant reductions in lung CFU versus the untreated control mice after 14 days of treatment. Treatment with either PA-824 at 100 mg/kg or LIN at 150 mg/kg reduced the CFU in the lungs of mice by approximately 1.03 ($P < 0.01$) and 0.9 logs ($P < 0.05$), respectively. TMC207 dosed at 25 mg/kg resulted in a 1.51 log reduction in lung CFU of treated mice after 2 weeks of therapy ($P < 0.001$). TMC207 activity at this time approached that of INH (1.66 log₁₀ CFU reduction), and the difference in activity between these two drugs was statistically significant by the end of treatment ($P > 0.05$) (Fig. 4.1).

Figure 4.1. Viable *M. tuberculosis* in the lungs of IFN-gamma GKO mice infected *M. tuberculosis* (\log_{10} CFU \pm SEM) and treated or not for 14d starting 15d post-LDA. Drug-treated mice received monotherapy with INH, pyrazinamide (PZA), PA-824, TMC207, or linezolid and were administered drug once a day for 7 d/wk (4 animals per group). [], concentration in mg/kg

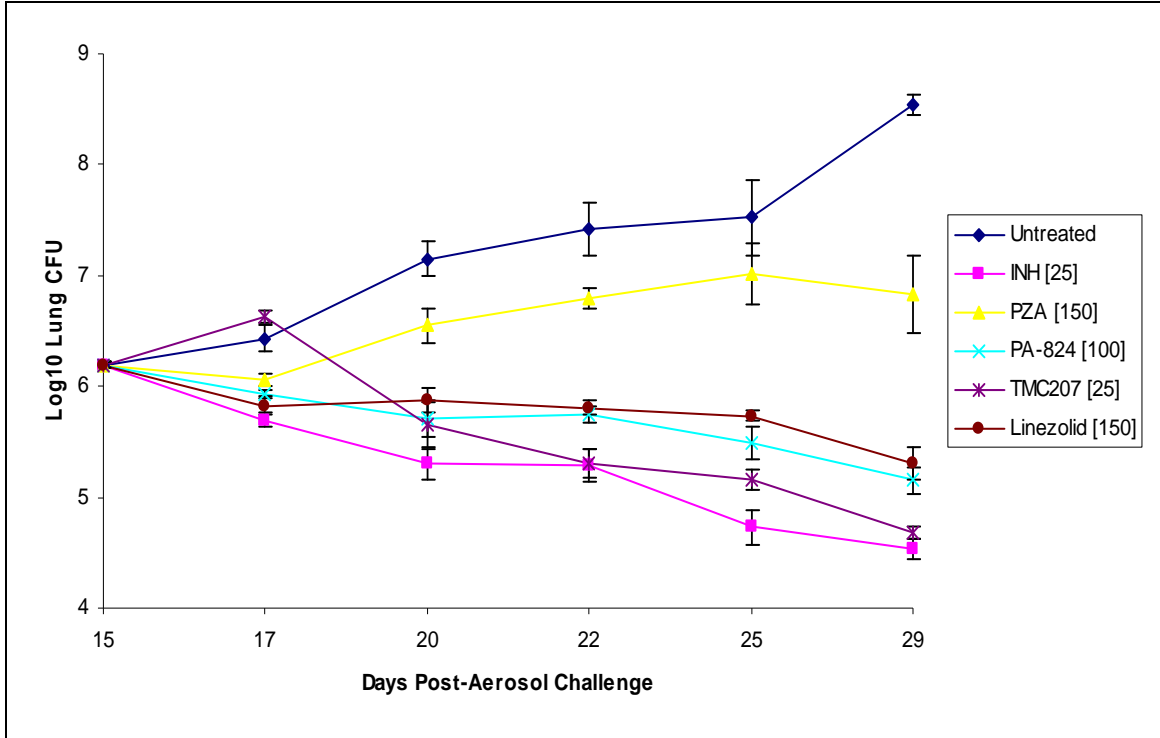


Table 4.2. Viable *M. tuberculosis* in the lungs of IFN-gamma GKO mice infected *M. tuberculosis* (\log_{10} CFU \pm SEM) and treated or not for 14d starting 15d post-LDA. Drug-treated mice received monotherapy with INH, pyrazinamide (PZA), PA-824, TMC207, or linezolid (LIN) and were administered drug once a day for 7 d/wk (4 animals per group). [], concentration in mg/kg

Treatment [mg/kg]	Log10 CFU \pm SEM					
	d15	d17	d20	d22	d25	d29
Pre-Treatment	6.19 \pm 0.03					
Untr Ctls		6.44 \pm 0.12	7.15 \pm 0.16	7.41 \pm 0.24	7.52 \pm 0.35	8.55 \pm 0.10
INH [25]		5.69 \pm 0.06	5.30 \pm 0.14	5.28 \pm 0.15	4.73 \pm 0.16	4.53 \pm 0.09
PZA [150]		6.06 \pm 0.05	6.55 \pm 0.16	6.80 \pm 0.09	7.02 \pm 0.28	6.82 \pm 0.35
PA-824 [100]		5.94 \pm 0.03	5.71 \pm 0.16	5.74 \pm 0.08	5.49 \pm 0.14	5.16 \pm 0.12
TMC207 [25]		6.63 \pm 0.03	5.66 \pm 0.20	5.31 \pm 0.13	5.16 \pm 0.10	4.68 \pm 0.06
LIN [150]		5.83 \pm 0.06	5.88 \pm 0.11	5.81 \pm 0.06	5.73 \pm 0.04	5.30 \pm 0.15

Multi-comparison analysis of data acquired from mouse models on TB drugs versus clinical data. The results obtained in IFN-gamma GKO mice described in the previous section were used to determine how the bactericidal activity of drugs in IFN-gamma mice (Table 4.3) compared to clinical EBA data available in literature (Table 4.4). The goal of this experiment was to assess if the IFN-gamma GKO mouse can be a predictive model for clinical EBA trials.

The bactericidal activity of standard and experimental TB drugs was evaluated in IFN-gamma GKO mice during the initial 14 days of therapy: at days 2, 5, 7, 10, and 14 of treatment (Table 4.3). These particular time points were chosen to enable comparison of murine and clinical EBA data based on typical time points used in clinical trials. The choice of compounds evaluated in this study was based on past clinical EBA trials assessing the same drugs. The first line drugs INH and PZA were chosen because of their well-documented early bactericidal and sterilizing activities, respectively. The experimental TB compounds PA-824, TMC207, and LIN were chosen for this study because they have recently undergone clinical EBA trials and thus, would serve as good indicators of the predictive value of this animal model.

Untreated IFN-gamma GKO mice were unable to control bacterial replication for the duration of the study exhibiting a steady increase in \log_{10} CFU in the lungs of mice throughout the study (Table 4.3). Data from untreated TB patients enrolled in clinical EBA trials is not available as it is obviously not ethical to withhold treatment from people suffering from an active infection.

The bactericidal activity of INH from days 0 to 2 of therapy exceeded that of all other compounds tested, showing an average of 0.25 \log_{10} fall in lung CFU per day of

treatment. INH efficacy markedly decreased after these initial 2 days of treatment. A second burst of activity was observed between days 7 and 10 of treatment ($0.183 \log_{10}$ CFU fall/day), however the INH bactericidal activity declined again after 10 days of treatment ($0.05 \log_{10}$ CFU fall/day) (Table. 4.3). The bactericidal activity of INH in TB patients exhibits a similar trend in killing kinetics (43, 56, 65, 111). In three separate clinical EBA trials, the efficacy of INH in TB patients was greatest in the initial 2 days of treatment (ranging from 0.285 to $0.722 \log_{10}$ CFU fall/day) and decreased from days 2 to 7 of treatment (ranging from 0.16 to $0.262 \log_{10}$ CFU fall/day) (Table 4.4).

PZA exhibited a $0.065 \log_{10}$ CFU fall/day in the lungs of mice over the first 2 days of treatment but exerted no bactericidal activity in the following 8 days of therapy ($0.083 \log_{10}$ CFU increase/day). Between treatment days 10 and 14, PZA again elicits modest activity showing a $0.05 \log_{10}$ CFU fall/day of treatment. The bactericidal activity of PZA in TB patients exhibits a low level of antimicrobial efficacy that increases marginally as treatment is prolonged (65). Over the initial 2 days of treatment in patients, PZA shows a $0.044 \log_{10}$ CFU fall/day, and the bactericidal activity of this drug between days 2 and 14 of treatment continues to increase (ranging from 0.069 to $0.113 \log_{10}$ CFU fall/day) (Table 4.4). In mice, the level of PZA activity was somewhat lower when compared to the clinical trial data. However, both the murine data as well as the human clinical EBA data reveals that PZA exerts most of its activity sometime after the initial days of treatment (Table 4.3 and 4.4).

PA-824 exhibited similar bactericidal activity during the first 2 days as it did after 10 consecutive days of treatment ($0.065 \log_{10}$ and $0.07 \log_{10}$ CFU fall/day, respectively) exhibiting a steady, continuous bactericidal effect over time. Efficacy was slightly

increased following 10 days of treatment (0.083 log₁₀ CFU fall/day) demonstrating antimicrobial efficacy throughout the 14 day treatment period (Table 4.3). In humans, PA-824 exhibits a low level of activity against *M. tuberculosis* over the initial 14 days of therapy similar to that of PZA (56) (Table 4.4). PA-824 shows a 0.047 log₁₀ CFU fall/day during the initial 2 days of treatment and increases to an average of 0.107 log₁₀ CFU fall/day from treatment days 2 to 14. The same trend of continuous bactericidal activity throughout treatment was shown for PA-824 in the murine trial presented here indicating that the killing kinetics of this drug are similar in IFN-gamma GKO mice and humans.

For TMC207, a delay in bactericidal activity was seen with an observed 0.22 log₁₀ CFU increase/day in the lungs of treated mice after the initial 2 days of treatment. TMC207 was the only compound tested not demonstrating bactericidal activity during this timeframe (Table 4.3). However, the bactericidal activity of this compound changed dramatically between treatment days 2 to 5 showing a 0.323 log₁₀ CFU fall/day in the lungs of mice. TMC207 maintains remarkable bactericidal activity from treatment days 10 to 14 showing a continued reduction of 0.12 log₁₀ CFU fall/day in mice. The killing kinetics of TMC207 in both humans (111) and mice show a distinctly similar trend. In both cases, TMC207 exhibits a delay in the onset of bactericidal activity that does not manifest until after 2 days of therapy (0.22 and 0.02 log₁₀ CFU increase/day for mice and humans, respectively). Thereafter, TMC207 displays a consistent level of antimicrobial activity in both this murine model and clinical EBA trials (0.264 and 0.162 log₁₀ CFU increase/day between days 2 and 7 of treatment for mice and humans, respectively) (Table 4.4).

The bactericidal activity of LIN in GKO mice over the first 2 days of treatment (0.18 log₁₀ CFU fall/day) was second only to INH but was reduced thereafter (Table 4.3). Significant activity was seen again by LIN between days 10 to 14 demonstrating a 0.108 log₁₀ CFU fall/day (Table 4.3). Similar to GKO mice, LIN in humans is most bactericidal in the initial 2 days of therapy (0.26 log₁₀ CFU fall/day) and reduced in the following 2 to 7 days of treatment (0.04 log₁₀ CFU fall/day) (Table 4.4) (43). In summary, the bactericidal activity of the drugs evaluated in the murine trial presented here (and the 2 previous GKO trials) closely parallel the killing kinetics generated from the same compounds tested in human clinical trials.

Table 4.3. Bactericidal activity (log₁₀ fall in lung CFU/day of treatment) of drugs in IFN-gamma GKO mice infected with *M. tuberculosis* and initiated on treatment 15d later (d0). Results presented from consecutive time points during the initial 14d of treatment.

Treatment [mg/kg]	Log10 Reduction CFU/Day					
	d0	d2	d5	d7	d10	d14
Baseline	0.000					
Untr Ctls		-0.125	-0.237	-0.130	-0.037	0.258
INH [25]		0.250	0.130	0.010	0.183	0.050
PZA [150]		0.065	-0.163	-0.125	-0.073	0.050
PA-824 [100]		0.125	0.077	-0.015	0.083	0.083
TMC207 [25]		-0.220	0.323	0.175	0.050	0.120
Linezolid [150]		0.180	-0.017	0.035	0.027	0.108

Table 4.4. Comparison of the bactericidal activities of drugs in mice (log₁₀ CFU fall/day treatment) and humans.

	Log10 Reduction CFU/Day				
	d0-2	d2-7	d0-7	d0-14	d2-14
	Murine ¹ /Human	Murine ¹ /Human	Murine ¹ /Human	Murine/Human	Murine/Human
INH	<i>0.250/0.285^a</i> <i>0.800/0.670^b</i> <i>0.365/0.722^c</i>	<i>0.082/0.262^a</i> <i>-0.054/0.160^b</i> <i>0.110</i>	<i>0.130/0.269^a</i> <i>0.190</i>	<i>0.119/0.192^c</i>	<i>0.097/0.113^c</i>
PZA	<i>0.065/0.044^c</i> <i>-0.015/0.044^c</i>			<i>-0.045/0.110^c</i>	<i>-0.063/0.113^c</i> <i>0.069^c</i>
PA-824	<i>0.125/0.047^d</i> <i>0.107^d</i>			<i>0.074/0.098^d</i>	<i>0.065</i>
TMC 207	<i>-0.220/-0.020^a</i>	<i>0.264/0.162^a</i>	<i>0.126/0.110^a</i>		
LIN	<i>0.180/0.260^b</i>	<i>0.004/0.040^b</i>			

Reference Data:

¹ Data from 3 separate murine trials following similar protocol, values in *italics* from murine trial described in this chapter

a (111), *b* (43), *c* (65), *d* (56)

Alternative analysis of bactericidal activity data to predict sterilizing activity of drugs in IFN-gamma GKO mice infected with *M. tuberculosis*. Clinical EBA trials generally measure bactericidal activity in the initial days of therapy by examining two time points, i.e., one early (EBA₀₋₂) and one late (EBA₂₋₁₄) which may provide a limited view of a drug's killing kinetics. Therefore, efforts were undertaken to evaluate the sterilizing activity of drugs by investigating changes in bactericidal activity occurring early during treatment (replicating bacilli) and at later stages (drug tolerant and slowly-replicating bacilli). Bactericidal activity data from the GKO murine trial described in the previous section was analyzed in a different way to gain further insight into the killing kinetics of anti-TB drugs *in vivo*. To this end, the average log₁₀ CFU fall/day of each drug tested in GKO mice was compared between all time points described in the previous section. The bactericidal activity of each drug from days 0 to 2 and 2 to 14 of treatment (Fig. 4.2 A) and from days 0 to 10 and 10 to 14 of treatment (Fig. 4.2 B) are presented in Figure 4.2 to demonstrate how different treatment time periods can give very different perspectives on the killing kinetics of anti-TB drugs *in vivo*.

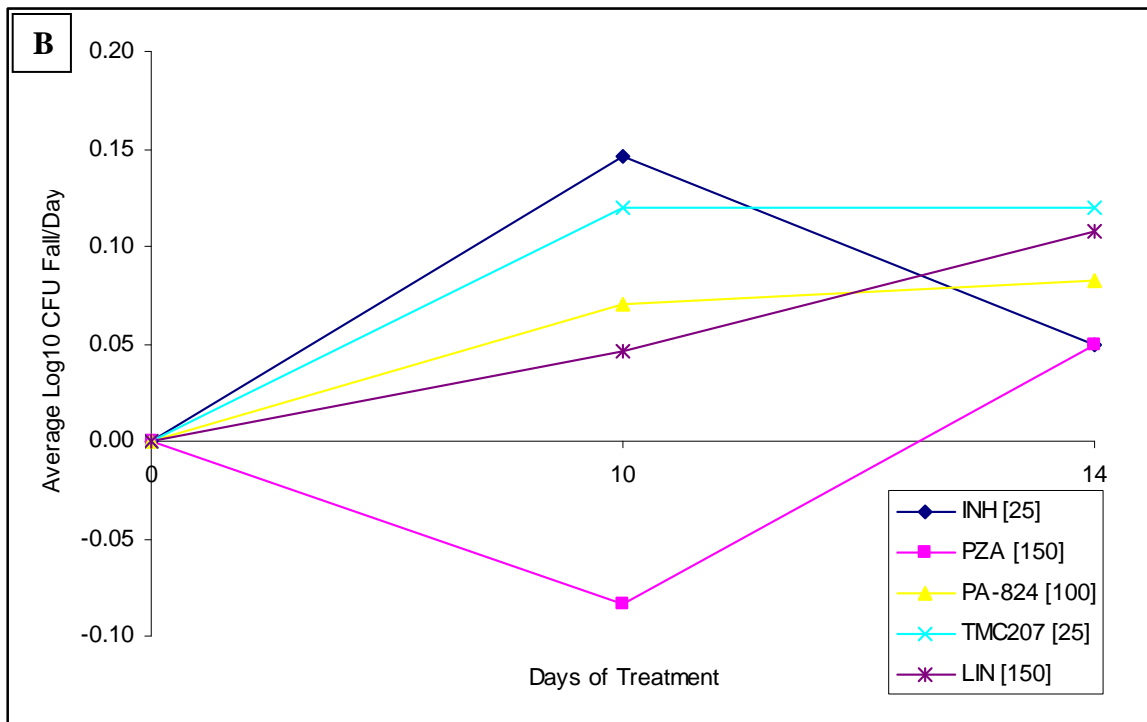
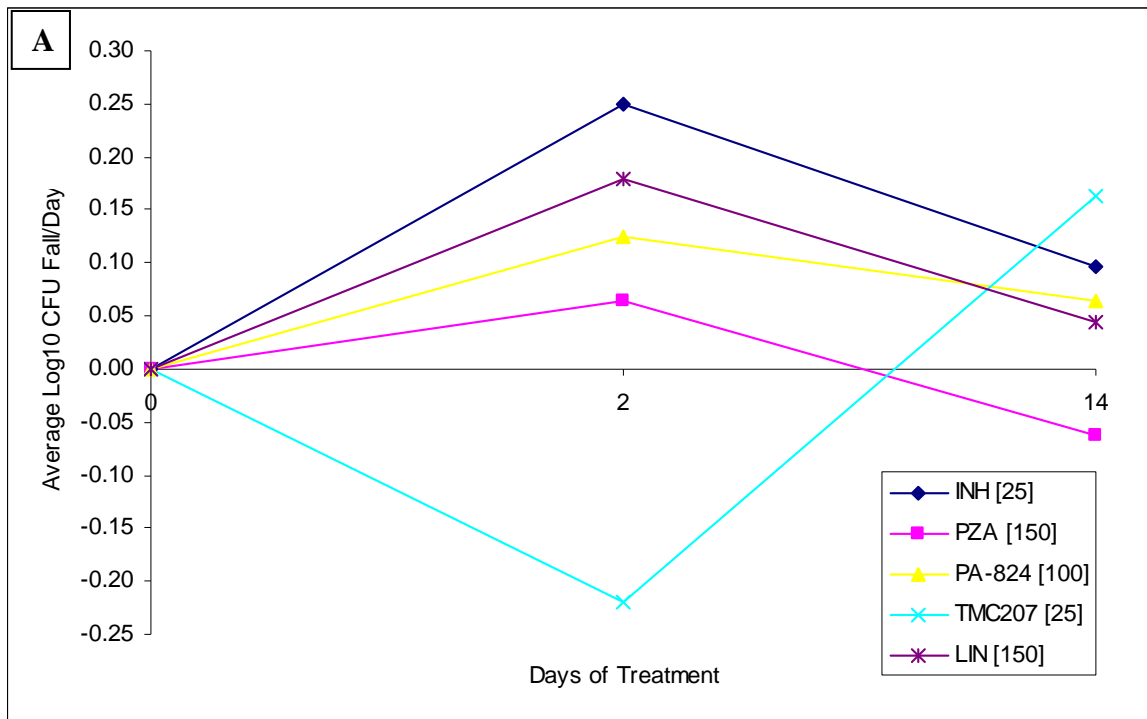
The results of this analysis show that INH exhibits a similar killing kinetic profile whether measured from days 0 to 2 and 2 to 14 of treatment (0.25 and 0.097 log₁₀ CFU fall/day, respectively) or days 0 to 10 and 10 to 14 of treatment (0.146 and 0.05 log₁₀ CFU fall/day, respectively) (Fig. 4.2). For both treatment periods, INH exerts most of its bactericidal activity in the initial days of treatment, which is markedly reduced thereafter. These results are in agreement with the fact that INH is efficacious against actively replicating bacilli early during treatment and less effective against persisting bacilli as treatment is prolonged (65). In contrast to INH, the killing kinetics of PZA are quite

different if measured from 0 to 2 and 2 to 14 days of treatment compared to 0 to 10 and 10 to 14 days of treatment. For the former, PZA demonstrates a 0.065 log₁₀ CFU fall/day over the initial 2 days of treatment followed by a 0.063 log₁₀ CFU increase/day of treatment from days 2 to 14 (Fig. 4.2 A). Examining the treatment period from 0 to 10 days reveals that PZA-treated mice exhibited a 0.083 log₁₀ CFU increase/day of treatment. However, from days 10 to 14 of treatment these mice demonstrate a 0.05 log₁₀ CFU fall/day (Fig. 4.2 B). Interestingly, PZA shows the single greatest change in bactericidal activity exhibited by any compound tested in the GKO mouse model presented here at this time (0.133 log₁₀ increase in bactericidal activity from days 10-14 of treatment compared to days 0-10 of treatment). This agrees with previously published controversial data that this drug might be an excellent sterilizing agent (142). Observing the bactericidal activity of PA-824 over the different treatment periods reveals opposite trends in killing kinetics for this compound. From days 0 to 2 and 2 to 14 of treatment, PA-824 exhibits a steady decline in bactericidal activity (0.125 and 0.065 log₁₀ CFU fall/day, respectively) (Fig. 4.2 A). However, examining days 0 to 10 and 10 to 14 of treatment reveals a steady increase in the bactericidal activity of PA-824 (0.07 and 0.083 log₁₀ CFU fall/day, respectively) (Fig. 4.2 B). These results are in agreement with previous reports that PA-824 exhibits sterilizing activity (77). No bactericidal activity was exerted by TMC207 against *M. tuberculosis* over the first 2 days of treatment (0.22 log₁₀ CFU increase/day). In the following days (days 2 to 14 of treatment), TMC207 demonstrated a 0.163 log₁₀ CFU fall/day of treatment (Fig. 4.2 A). The delayed onset of bactericidal activity by TMC207 observed in this murine trial agrees with previously published clinical EBA data evaluating this compound in humans (111). Shifting our

focus to days 0 to 10 and 10 to 14 of treatment, we observed that TMC207 maintains a steady level of bactericidal activity (0.12 log₁₀ CFU fall/day of treatment for both time periods) (Fig. 4.2 B). These results suggest that TMC207 is efficacious against actively replicating and drug tolerant tubercle bacilli, which is in agreement with previously published reports (71). Bactericidal activity results for LIN over the described time points compared in Fig. 4.2 reveal similar killing kinetic trends to PA-824. Like PA-824, LIN demonstrates a steady decrease in bactericidal activity when examined from days 0 to 2 and 2 to 14 of treatment (0.18 and 0.044 log₁₀ CFU fall/day, respectively) (Fig. 4.2 A). The killing kinetics of LIN from days 0 to 10 and 10 to 14 of treatment exhibit a different profile, showing a steady increase in bactericidal activity over these time periods (0.046 and 0.108 log₁₀ CFU fall/day, respectively) (Fig. 4.2 B). As for the other experimental compounds tested in this trial, these results suggest that LIN may be an effective sterilizing agent and support its continued use in clinical trials.

The purpose of the results presented here is to illustrate the point that a different perspective on a compounds killing kinetics can be gained simply by modifying the time points chosen to examine them. For this experiment, the bactericidal activity of compounds was examined over multiple time periods throughout the first 14 days of treatment. We used the time periods presented in figure 4.2 as an example to show that efficacy data can be skewed to generate dynamic trends in the killing kinetics of anti-TB drugs.

Figure 4.2. Bactericidal activity of drugs in GKO mice infected with *M. tuberculosis* and initiated on treatment 15 days later (d0). Results presented are from **A**, d0 to 2 and d2 to 14, and **B**, d0 to 10 and d10 to 14 of the initial 2 wks of treatment. [], conc. in mg/kg.



4.4 DISCUSSION

There is an urgent need for new, more effective treatment strategies for tuberculosis treatment. Novel anti-TB chemotherapeutic regimens must be composed of drugs that are effective against *M. tuberculosis* in all of its metabolic forms. Some of these drugs must target actively replicating bacilli such as those present during an active pulmonary infection. These drugs tend to be effective early after the onset of chemotherapy under such conditions and thus are sometimes said to have early bactericidal activity. However, the real key to shortening the length of TB therapy hinges on the ability of those drugs that target and eradicate *M. tuberculosis* persisting after drug treatment in a metabolically inactive state. These kinds of drugs are said to have sterilizing activity as they either continue to maintain or begin to exert a bactericidal effect against *M. tuberculosis* at a time when drugs effective against actively replicating bacilli exhibit a reduction in antimicrobial efficacy. Having a validated preclinical animal model to test experimental drugs for anti-TB efficacy that can yield predictive information on a compounds killing kinetics would be invaluable for TB drug development. The results of the experiments presented in this chapter describe such an animal model in which IFN-gamma mice were used to model clinical EBA trials.

Clinical EBA tests are generally performed early in phase II clinical trials and are designed to assess the bactericidal activity of drug compounds against *M. tuberculosis*. EBA trials have been controversial since their inception because they only measure the bactericidal activity of a compound in the initial days of therapy and generally have only 1 or 2 time points when sputum CFU of patients receiving therapy are determined. The

small number of time points coupled with the short duration of treatment (usually one week) employed in EBA trials may be limiting our interpretation of drug efficacy results. This has led some to question the utility of these trials as they have been criticized for their inability to measure sterilizing activity.

The first obstacle to overcome when designing an *in vivo* preclinical model for TB drug testing that could potentially yield predictive information on a compound's efficacy in humans was choosing the appropriate species. To this end, initial drug trials were carried out in WT C57BL/6 mice and IFN-gamma GKO mice in order to compare killing kinetic curves generated by the same compounds and to evaluate how the drug efficacy results in the mice compared to human data. In chapter 2 of this thesis, the drugs isoniazid and moxifloxacin were tested in both WT C57BL/6 mice and IFN-gamma GKO mice for 7 days starting 18 days post-LDA with *M. tuberculosis* in order to make drug efficacy comparisons with data obtained from human clinical EBA trials. INH and MXF exhibited only minor activity after 7 days of treatment in WT C57BL/6 mice (0.25 and 0.85 log₁₀ reduction in CFU, respectively). Calculating the EBA of these drugs generated in WT mice results in an EBA₀₋₇ of 0.036 for INH and 0.12 for MXF. On the other hand, INH elicited a 0.85 log₁₀ reduction in CFU after only 5 days of treatment while MXF therapy for 7 days led to a 3.5 log₁₀ reduction in lung CFU of IFN-gamma GKO mice. The EBAs of these compounds tested in GKO mice are as follows: EBA₀₋₅ for INH = 0.17 and EBA₀₋₇ for MXF = 0.5. In human clinical EBA trials, INH was calculated to have an EBA₀₋₂ of 0.67 and an EBA₂₋₇ of 0.08 while MXF had an EBA₀₋₂ of 0.33 and an EBA₂₋₇ of 0.17 (68). The EBAs of INH calculated over the same treatment periods as described for the human trial reveals that drug efficacy is remarkably similar in IFN-

gamma GKO mice with INH eliciting an EBA₀₋₂ of 0.365 and an EBA₂₋₇ of 0.11. MXF was also found to have similar effects in humans and GKO mice with an EBA₀₋₂ of 0.58 and an EBA₂₋₇ of 0.278. The level of drug activity in WT C57BL/6 mice was far less pronounced for both drugs over these time periods. The significance of these results is that the metabolic state of *M. tuberculosis* and not necessarily the location determines the outcome of drug treatment. If bacilli from the lungs of IFN-gamma GKO mice are metabolically similar to bacilli in human sputa, one would expect to see similar killing kinetics in the drugs tested in both, which was indeed the case in the trial presented here. Human patients recruited for EBA clinical trials must have an active TB infection (as opposed to a latent infection). Bacilli in an active TB infection are continually dividing much like they do in IFN-gamma GKO mice due to the absence of the pro-inflammatory cytokine INF-gamma (76). In contrast, bacilli in WT C57BL/6 mice are held at a steady-state level during chronic infection indicating that these bacilli may not be actively replicating and hence are not as susceptible to drugs as bacilli in the other two situations. The results of these drug efficacy comparisons validate the use of IFN-gamma GKO mice to test experimental compounds for anti-TB efficacy. Therefore, this species was chosen to: i) establish a preclinical *in vivo* model able to generate predictive information on an experimental drugs efficacy based on clinical EBA trial data, and ii) determine if the sterilizing activity of drugs can be assessed during the initial days of treatment. Using the frontline drugs INH and PZA and the experimental compounds PA-824, TMC207, and LIN currently in clinical trials, we show here that IFN-gamma GKO mice accurately reproduce the killing kinetics of drugs previously generated in published clinical EBA trials. Furthermore, by examining a greater number of time points within the initial two-

weeks of treatment, we obtained a more detailed profile of each drug's bactericidal activity including the measurement of potential sterilizing activity.

The bactericidal activity of drugs tested in humans was found to be consistently reproduced in IFN-gamma GKO mice based on the results of 3 separate experiments evaluating the same drugs over the same time points used in clinical EBA trials. The bactericidal activity of INH was found to be greatest during the first 2 days of treatment in mice (ranging from 0.25 to 0.8 log₁₀ CFU fall/day) and humans (ranging from 0.285 to 0.722 log₁₀ CFU fall/day treatment) (43, 65, 111) and markedly reduced thereafter. In both humans (65) and GKO mice, the bactericidal activity of PZA was minor over the first 7 days of treatment but exhibited a late onset beginning 1 week after starting treatment suggesting that the sterilizing activity of PZA, a compound long known for its excellent sterilizing activity against *M. tuberculosis in vivo*, can possibly be measured in the first 2 weeks of treatment. The rate of mycobacterial killing for PA-824 in GKO mice measured over the first 2 days and from days 2 to 14 of treatment (0.125 and 0.065 log₁₀ CFU fall/day treatment, respectively) were similar to the results of a recently completed clinical EBA trial evaluating PA-824 over the same treatment periods (0.047 and 0.107 log₁₀ CFU fall/day treatment, respectively) (56). TMC207 exhibited the most distinct killing kinetic profile of all the drugs evaluated in this study and in clinical EBA trials. TMC207 was the only drug tested not exerting a bactericidal effect against *M. tuberculosis* during the first 2 days of treatment. However, from days 2 to 5 of treatment, TMC207 exhibited a burst in bactericidal activity in GKO mice that was very similar to the burst of activity exerted by this drug in human clinical EBA trials (111). Furthermore, TMC207 was found to maintain a greater level of bactericidal activity from treatment

days 10 to 14 than any other drug tested in GKO mice. Interestingly, INH was found to have the lowest bactericidal activity during this time frame of all the drugs tested agreeing with the fact that this drug has good EBA but poor extended EBA (65, 66). The bactericidal activity of LIN was found to be greatest during the first 2 days of treatment in both mice (0.18 log₁₀ CFU fall/day treatment) and humans (0.26 log₁₀ CFU fall/day treatment) but was reduced from days 2 to 7 of treatment in each case as well (0.004 and 0.04 log₁₀ CFU fall/day treatment, respectively) (43). Examining the bactericidal activity of LIN in GKO mice over the first 2 days of treatment and from days 2 to 14 of therapy (2 time points commonly used in past clinical EBA settings) shows an EBA₀₋₂ that is second only to INH while the EBA₂₋₁₄ for this drug is greatly reduced falling behind the EBA₂₋₁₄ of both INH and TMC207. Interestingly, examining the same EBA data for LIN over the first 10 days of treatment and from days 10 to 14 of treatment shows an almost linear increase in bactericidal activity beginning at the start of treatment and increasing to the end of the trial. Of all the drugs examined at these latter time points, LIN was the only compound exhibiting a continuous increase in bactericidal activity against *M. tuberculosis* in this murine trial.

Taken together, the bactericidal activities of both standard and experimental drugs demonstrated similar killing kinetic trends during the initial weeks of chemotherapy in humans and in IFN-gamma GKO mice. Although additional trials evaluating a broader range of drugs from different drug classes needs to be done to confirm the ability of these mice to reproduce drug efficacy results generated in humans, the preliminary results of 3 separate GKO trials performed in our lab are promising. The similarities in drug killing kinetics also indicate that *M. tuberculosis* bacilli in IFN-gamma GKO mice and bacilli in

human patients recruited from clinical EBA trials are in a similar metabolic state. The choice of drugs evaluated for their bactericidal activity in GKO mice was based on the different mechanisms of drug action each one presented. Collectively, these mechanisms target a variety of metabolic pathways utilized by *M. tuberculosis* during times of active replication (i.e., INH), slow replication (PZA), and various other metabolic processes that required by this pathogen to survive (i.e., ATP – TMC207 and protein/lipid synthesis – LIN/PA-824). Therefore, the fact that *M. tuberculosis* demonstrated the same drug susceptibilities to the same compounds tested in either GKO mice or humans suggests that the same multiple metabolic forms of bacilli are encountered in each.

In addition to mimicking clinical EBA drug data in mice, the present study was also undertaken to see if sterilizing activity could be measured in the initial weeks of treatment by examining a larger number of time points within this timeframe than has been used in past EBA trials. Typical clinical EBA trials evaluate compounds for anti-TB efficacy by only measuring drug activity over 2 time points. In the GKO-EBA trial described here, the EBA of compounds was evaluated from days 0-2, 2-5, 5-7, 7-10, and 10-14 of treatment and calculated for all possible combinations of treatment periods within (i.e., days 0-5, 5-10, 10-14, etc.). The results of this multi-time point EBA comparison revealed that starkly contrasting killing kinetic profiles can be generated for the same drug if evaluated with one set of time points versus another within the initial 2 weeks of treatment. The alternative perspectives on a drug's bactericidal activity against *M. tuberculosis* obtained in this study underscore the importance of examining a greater number of time points in clinical EBA trials. The more time points an experimental drug is tested evaluated under, the better the drug profile generated will be which can

significantly alter inferences about a compounds ability to successfully shorten standard TB chemotherapy. By gleaning as much information as possible about the effects of experimental drugs against *M. tuberculosis* in preclinical trials, the chances of successfully choosing only those compounds with real potential to shorten TB chemotherapy for further clinical trial testing will be greatly increased. The selection of these compounds, compounds with sterilizing activity, will facilitate the development of a truly novel short course drug regimen for TB treatment.

CHAPTER FIVE

CONCLUSION

Few pathogens have been as successful as *Mycobacterium tuberculosis* at infecting humans throughout history. Today, *M. tuberculosis* latently infects approximately 2 billion people worldwide (99). Deficiencies in the available chemotherapeutics as well as waning interest in combating an “Old World” disease have allowed this pathogen to remain a significant cause of death globally. The main drawback associated with the frontline regimen for TB treatment is the lengthy 6-9 months of daily multidrug therapy required for sterilization. The long duration of this therapy leads to patient noncompliance resulting in incomplete sterilization, and ultimately, the propagation of *M. tuberculosis*. HIV/AIDS-TB co-infection is also contributing to the continued prevalence of TB. In fact, the number one killer of people infected with HIV is TB (99), mandating that new TB drugs be co-administratable with antiretroviral therapy. Patient noncompliance can also occasionally contribute to drug resistant strains of *M. tuberculosis*. The rise of multidrug- and extensively drug-resistant strains draws attention to the dire need for new, more effective drugs that can facilitate a short-course cure for TB patients.

The most significant obstacle in the way of shortening TB chemotherapy is perhaps the ability of some bacilli to persist in host tissues despite a vigorous host immune response and effective drug treatment. Indeed, the 6-9 months of daily therapy is thought to be required to eradicate this small sub-population of persisting *M. tuberculosis*. The ability to specifically target and eliminate this sub-population of bacilli

is the key to unlocking a truly short-course drug regimen. However, there are still large gaps in our understanding of TB persistence. The location, metabolic state, and environmental conditions associated with mycobacterial persistence are all such aspects of *M. tuberculosis* that still remain a mystery. We do know that *M. tuberculosis* is able to adapt to changes in its environment *in vitro* such as gradual O₂ depletion, and this change is accompanied by a shift in the pathogen's metabolic profile which renders bacilli drug-refractory (140). In addition, studies analyzing gene transcripts in human pulmonary tissues have shown differential gene expression patterns by *M. tuberculosis* found in different areas of the lung and in response to INH treatment (48). A better understanding of how *M. tuberculosis* responds to distinct *in vivo* environments as well as the effect of chemotherapy on *M. tuberculosis* under these specific conditions needs to be obtained in order to facilitate the design of new, highly effective TB drugs.

There is an urgent need to rapidly identify drugs that can eradicate persisting bacilli. Drugs like isoniazid and ethambutol are efficacious against actively replicating *M. tuberculosis* and elicit little antimicrobial effect against persisting, non-replicating bacilli. Rifampin and pyrazinamide on the other hand exhibit a bactericidal effect against persisting bacilli, and thus are said to have sterilizing activity. The combined actions of these 4 drugs kill approximately 99% of bacilli in the first few weeks of treatment and are used to drive bacterial burdens in patients to very low numbers in the first 4 months of treatment. Following this initial 'intensive' phase, INH and RIF are administered in a 2-5 month 'continuation' phase in order to eliminate the remaining ~1% of persisting bacilli. New drugs specifically targeting the persistent population of bacilli must be found to shorten anti-TB chemotherapy.

Preclinical drug testing is an important part in the drug development process. The use of animals to model TB in preclinical drug development has proven indispensable for the testing of experimental compounds for TB treatment. The mouse model has been widely used as an initial *in vivo* screen for drug efficacy of experimental compounds due to their ease in handling and low cost. Mice are relatively resistant to TB disease and develop a chronic infection that can last for more than a year in some mice. The central deficiency associated with mice lies in their limited pathology that develops in human pulmonary disease. Lung lesions in mice maintain a cellular composition throughout infection and lack caseous necrosis (109). Guinea pigs which are more susceptible than mice to disease also develop a chronic TB infection after inoculation with a low dose aerosol of *M. tuberculosis*, but will succumb to disease several months after infection. In drug development, guinea pigs animals are starting to be used as a secondary *in vivo* model to confirm the activity of lead compounds performing well in mice. Guinea pigs form primary granulomas and secondary lesions after infection with *M. tuberculosis* (127). These pathological manifestations bear great resemblance to pulmonary lesions seen in human disease making this model particularly attractive for testing experimental compounds at a late stage of preclinical development. In addition to mice and guinea pigs, other animal models have been used to evaluate drug efficacy including the rabbit and non-human primate, each with their own benefits and limitations (29, 33). It is clear that each animal model can provide useful information on different aspects of TB disease, which highlights the importance of fully understanding the differences in TB disease that manifests in different animal species used to study it.

Following preclinical trial testing, experimental compounds that show promise may enter clinical trials. One such clinical trial test is called an early bactericidal activity test. In clinical EBA trials, compounds are evaluated for their efficacy against *M. tuberculosis* over the initial days of treatment in sputum smear-positive, HIV-negative patients newly diagnosed with TB. The length (takes approximately 2 years to enroll patients), cost and effort to conduct these clinical trials makes the selection of compounds to be evaluated in EBA experiments of utmost importance. EBA tests can determine the efficacy of a compound in the initial days of therapy, which will indicate whether or not this drug is suitable for further testing, as well as assist in determining the optimal dose for subsequent, elaborate phase IIb and III efficacy clinical trials. However, EBA tests have also been criticized for their inability to measure sterilizing activity of experimental compounds. The ability to identify compounds that have sterilizing activity as early as possible in preclinical drug testing will ensure that only those compounds with real potential to shorten TB chemotherapy will be selected for evaluation in clinical trials.

The ultimate goal for this thesis project was to improve our understanding of the differences that exist in TB pathogenesis between different animal models used in preclinical drug testing and what these differences mean for testing experimental TB compounds. In order to do this, a multi-faceted approach was undertaken to: i) determine the location of bacilli persisting after drug treatment in different animal models used in preclinical drug testing, ii) determine if metronidazole therapy can specifically target persisting bacilli in a guinea pig model of disease, and iii) design a preclinical animal model able to generate predictive information on a compounds killing kinetics in humans and allows for potential sterilizing activity to be measured.

TB disease manifests very differently from one animal species to the next. WT mice develop a chronic infection after LDA with *M. tuberculosis* (109), form non-necrotic pulmonary lesions (128), and do not develop hypoxic conditions within the lung (8). Guinea pigs also develop a chronic infection after LDA with *M. tuberculosis* (117) but are much more susceptible to disease than WT mice. In addition, guinea pigs develop both necrotic and non-necrotic granulomas in their lungs and a number of studies have shown that necrotic, primary granulomas are hypoxic (78, 89, 127, 132). Both mice and guinea pigs are commonly used to test experimental TB drugs, however little attention has been paid to how these fundamental differences in TB disease between these two species may affect drug efficacy testing. Information on the location of *M. tuberculosis* bacilli in both untreated and drug-treated animals as well as the effects of chemotherapy on pathogenesis and bacillary clearance is lacking.

In chapter two, a novel acid-fast staining combination involving auramine-rhodamine was used on treated and untreated lung tissues from 3 animal models used in preclinical drug testing to compare the locations of bacilli and the effects of drug treatment. All animals were infected via LDA with *M. tuberculosis*. Bacilli in untreated and drug-treated C57BL/6 mice were intracellular throughout infection within epithelioid and foamy macrophages located in and around inflammatory lesions. No necrosis was found in any of the lung sections evaluated from these mice. Drug treatment with either INH or RIF had a gradual, uniform effect on bacillary clearance and reduction in lung pathology over the 6-week treatment period. Untreated IFN-gamma GKO mice infected developed extensive necrosis in pulmonary lesions and airways. Lesions contained exceptionally large numbers of both intracellular bacilli within macrophages and

multinucleated giant cells and extracellular bacilli found within necrotic tissue and among necrotic cellular debris filling airways. In contrast, bacilli were intracellular in GKO mice receiving either INH or RIF monotherapy as no necrosis was observed in their lungs most likely because therapy began before the onset of necrosis. Drug treatment had a dramatic effect on both the rate of bacillary clearance and pulmonary inflammation after only 7 days of treatment. The majority of bacilli in both treated and untreated guinea pigs were extracellular in the necrotic cores and acellular rims of primary granulomas while secondary lesions contained few, if any, intracellular bacilli. Drug treatment with either the standard drug INH or the experimental compound TMC207 resulted in a gradual reduction in the number of bacilli over time and preferentially cleared secondary lesions first with a delayed effect on primary granulomas.

Differences in the effects of drug treatment across the animal models evaluated here indicate that experimental compounds are tested against different populations of *M. tuberculosis* in different animals. Drug treatment was most pronounced in IFN-gamma GKO mice compared to either WT mice or guinea pigs most likely because bacilli grow uninhibited in the absence of IFN-gamma and therefore, drugs are being tested against a metabolically active population of *M. tuberculosis*. The slowly replicating populations of *M. tuberculosis* chronically infecting WT mice and guinea pigs are not as susceptible to drugs targeting metabolically active bacilli so a much more gradual effect in drug treatment was observed.

A key observation made in chapter two was that bacilli persisting after effective drug treatment in infected guinea pigs were consistently found in the necrotic cores and acellular rims of primary granulomas. These results confirmed the results of a previous

study performed by our lab in which hypoxia was also found to be present in these granulomas (78). Metronidazole is a compound known to be effective against anaerobic bacteria. Although not completely understood, the action of MET is thought to involve DNA strand breakage after reduction of this drug to its active metabolite by a pathogen under low redox potential (46). Studies by Wayne *et al.* have shown that bacilli grown under conditions of gradual O₂ depletion shift into 2 stages of non-replicating persistence (140). The shift into stages of non-replicating persistence is accompanied by increased susceptibility to MET and reduced susceptibility to the frontline drugs INH and RIF (139). We therefore hypothesized that MET therapy may preferentially target persisting bacilli located in the hypoxic environment of primary granulomas. MET was found not to be effective at reducing the bacterial load in the lungs and spleens of guinea pigs compared to the untreated controls and, in fact, exacerbated disease as revealed by increased secondary lesion inflammation. *M. tuberculosis* has a variety of adaptive mechanisms to respond to both drug treatment and environmental conditions. Although the results of this experiment were not positive, they highlight the importance of testing specific drugs and drug combinations that target the multiple mechanisms that allow *M. tuberculosis* to survive.

The results of chapter 3 also emphasize the importance of developing new TB drugs with potent sterilizing activity. The sterilizing activity of a drug or drug regimen is what ultimately determines the length of TB treatment required for sterilization as this type of activity targets persisting bacilli. Clinical EBA trials have been performed in the past to assess a compound's anti-TB activity during the first few days of treatment prior to testing the drug in more expensive, large-scale clinical trials. Attempts have been made to

measure potential sterilizing activity of experimental compounds in these trials (45) but none have generated conclusive results throwing into question the usefulness of these kinds of studies. Chapter four of this thesis describes a murine model of TB disease designed to generate drug efficacy data predictive of known clinical EBA data. The bactericidal activity of drugs was measured by calculating the EBA of compounds over treatment periods coinciding with ones traditionally used in clinical EBA trials (i.e., EBA₀₋₂, EBA₂₋₇, etc.). The killing kinetics generated by both standard and experimental TB drugs in human clinical EBA trials were found to be consistently reproduced in IFN- γ GKO mice based on the results presented here as well as those of two other GKO murine trials done previously in our lab. In addition, a detailed examination of drug killing kinetics was performed in order to determine if additional information on a drugs bactericidal activity can be gained by examining a greater number of treatment periods within the first 14 days of treatment. The results of the drug killing kinetic analysis revealed that interpretation of a drugs efficacy within the settings of a simulated clinical EBA trial can be dramatically altered depending on the number and distribution of treatment periods analyzed. Perhaps the argument that clinical EBA trials fail to measure sterilizing activity warrants further investigation. Examining drug killing kinetics of novel TB compounds in greater detail may reveal novel treatment strategies such as administering drugs with distinct mechanisms of action at different times during chemotherapy. This strategy may exploit metabolic pathways induced at specific times in *M. tuberculosis* to ultimately exert the maximal effect of antibiotic treatment on bacilli. More attention needs to be focused on studying how and why specific anti-TB drugs and drug combinations, including the frontline regimen, effect *M. tuberculosis* the way the do

in order to maximize the bactericidal effect of a novel, highly effective chemotherapeutic regimen.

Modeling TB in animals for the benefit of humans has one fundamental drawback: no one animal fully recapitulates all aspects of pulmonary TB disease in humans. This setback, however, does not mean that animals do not have their place in TB research, it just means that we need to fully understand how *M. tuberculosis* manifests in each one so we can more accurately interpret results obtained from them. The experiments presented here were carried out in order to gain a better understanding of 3 animal models commonly used to test experimental TB compounds. The results clearly demonstrate that experimental drugs are being evaluated for their anti-TB efficacy under very different *in vivo* conditions depending on which animal model is used. These results have significant implications for preclinical TB drug testing as the different *in vivo* conditions between animal models most likely influences the metabolic state of *M. tuberculosis*. Previous experiments have shown that the metabolic state of *M. tuberculosis* directly effects the pathogens susceptibility to known bactericidal drugs (138-140) so how an experimental compound behaves in one animal may not necessarily indicate that this drug would not be beneficial for human patients. Evaluating experimental drugs in multiple animal models and pooling that information will maximize our ability to predict which preclinical compounds may one day make it to registry.

The design of a new, highly effective chemotherapeutic regimen for TB treatment that can achieve a cure in less than 2 months will hinge on the ability of this combination of drugs to target persisting bacilli. As we learn more and more about how and where *M.*

tuberculosis persists in different animal models after drug treatment, drugs targeting the metabolic pathways that allow this pathogen to survive and that are effective under the condition in which it survives should be developed. These drugs will shorten current TB treatments making full patient compliance easier to achieve, all of which will ultimately aid in silencing the 'White Plague' forever.

REFERENCES

1. 2000. Diagnostic Standards and Classification of Tuberculosis in Adults and Children. This official statement of the American Thoracic Society and the Centers for Disease Control and Prevention was adopted by the ATS Board of Directors, July 1999. This statement was endorsed by the Council of the Infectious Disease Society of America, September 1999. *Am J Respir Crit Care Med* **161**:1376-95.
2. 1995. Global tuberculosis programme and global programme on vaccines. Statement on BCG revaccination for the prevention of tuberculosis. *Wkly Epidemiol Rec* **70**:229-31.
3. Merriam-Webster Online Dictionary. <http://www.merriam-webster.com/dictionary/persist/>.
4. 1996. The role of BCG vaccine in the prevention and control of tuberculosis in the United States. A joint statement by the Advisory Council for the Elimination of Tuberculosis and the Advisory Committee on Immunization Practices. *MMWR Recomm Rep* **45**:1-18.
5. 2006, posting date. Strategic Plan: Stop TB Partnership Working Group on New TB Drugs. Global TB Alliance. [Online.]
6. **Al-Moamary, M. S., W. Black, E. Bessuille, R. K. Elwood, and S. Vedal.** 1999. The significance of the persistent presence of acid-fast bacilli in sputum smears in pulmonary tuberculosis. *Chest* **116**:726-31.
7. **Alderwick, L. J., H. L. Birch, A. K. Mishra, L. Eggeling, and G. S. Besra.** 2007. Structure, function and biosynthesis of the Mycobacterium tuberculosis cell wall: arabinogalactan and lipoarabinomannan assembly with a view to discovering new drug targets. *Biochem Soc Trans* **35**:1325-8.
8. **Aly, S., K. Wagner, C. Keller, S. Malm, A. Malzan, S. Brandau, F. C. Bange, and S. Ehlers.** 2006. Oxygen status of lung granulomas in Mycobacterium tuberculosis-infected mice. *J Pathol* **210**:298-305.
9. **Andries, K., P. Verhasselt, J. Guillemont, W. Hinrich, H. Gohlmann, J. M. Neefs, H. Winkler, J.V. Gestel, P. Timmerman, M. Zhu, E. Lee, P. Williams, D. Chaffoy, E. Huitric, S. Hoffner, E. Cambau, C. Truffont-Pernot, N. Lounis, V. Jarlier.** 2005. A diarylquinolone drug active on the ATP synthase of Mycobacterium tuberculosis. *Science* **37**:223-227.
10. **Arriaga, A. K., E. H. Orozco, L. D. Aguilar, G. A. Rook, and R. Hernandez Pando.** 2002. Immunological and pathological comparative analysis between experimental latent tuberculous infection and progressive pulmonary tuberculosis. *Clin Exp Immunol* **128**:229-37.
11. **Arteel, G. E., R. G. Thurman, and J. A. Raleigh.** 1998. Reductive metabolism of the hypoxia marker pimonidazole is regulated by oxygen tension independent of the pyridine nucleotide redox state. *Eur J Biochem* **253**:743-50.
12. **Balaban, N. Q., J. Merrin, R. Chait, L. Kowalik, and S. Leibler.** 2004. Bacterial persistence as a phenotypic switch. *Science* **305**:1622-1625.
13. **Barreto, M. L., S. M. Pereira, and A. A. Ferreira.** 2006. BCG vaccine: efficacy and indications for vaccination and revaccination. *J Pediatr (Rio J)* **82**:S45-54.

14. **Basaraba, R. J.** 2008. Experimental tuberculosis: the role of comparative pathology in the discovery of improved tuberculosis treatment strategies. *Tuberculosis (Edinb)* **88 Suppl 1**:S35-47.
15. **Basaraba, R. J., D.D. Dailey, C.T. McFarland, C.A. Shanley, E.E. Smith, D.N. McMurray, and I.M. Orme.** 2006. Lymphadenitis as a major element of disease in the guinea pig model of tuberculosis. *Tuberculosis*. **86**:386-394.
16. **Basaraba, R. J., E. E. Smith, C. A. Shanley, and I. M. Orme.** 2006. Pulmonary lymphatics are primary sites of *Mycobacterium tuberculosis* infection in guinea pigs infected by aerosol. *Infect Immun* **74**:5397-401.
17. **Bhatt, A., N. Fujiwara, K. Bhatt, S. S. Gurcha, L. Kremer, B. Chen, J. Chan, S. A. Porcelli, K. Kobayashi, G. S. Besra, and W. R. Jacobs, Jr.** 2007. Deletion of *kasB* in *Mycobacterium tuberculosis* causes loss of acid-fastness and subclinical latent tuberculosis in immunocompetent mice. *Proc Natl Acad Sci U S A* **104**:5157-62.
18. **Bishai, W. R.** 2000. Rekindling old controversy on elusive lair of latent tuberculosis. *Lancet* **356**:2113-4.
19. **Bloom, B. R.** 1994. *Tuberculosis: Pathogenesis, Protection, and Control*. ASM Press, Washington, DC.
20. **Boshoff, H. I., V. Mizrahi, and C. E. Barry, 3rd.** 2002. Effects of pyrazinamide on fatty acid synthesis by whole mycobacterial cells and purified fatty acid synthase I. *J Bacteriol* **184**:2167-72.
21. **Bozdogan, B., and P. C. Appelbaum.** 2004. Oxazolidinones: activity, mode of action, and mechanism of resistance. *Int J Antimicrob Agents* **23**:113-9.
22. **Brandt, L., Y. A. Skeiky, M. R. Alderson, Y. Lobet, W. Dalemans, O. C. Turner, R. J. Basaraba, A. A. Izzo, T. M. Lasco, P. L. Chapman, S. G. Reed, and I. M. Orme.** 2004. The protective effect of the *Mycobacterium bovis* BCG vaccine is increased by coadministration with the *Mycobacterium tuberculosis* 72-kilodalton fusion polyprotein Mtb72F in *M. tuberculosis*-infected guinea pigs. *Infect Immun* **72**:6622-32.
23. **Brennan, P. J., D.B. Young, and B.D. Robertson (editors).** 2008. Handbook of anti-tuberculosis agents. *Tuberculosis (Edinb)* **88**:85-86.
24. **Brock, T. D.** 1999. *Robert Koch: A Life in Medicine and Bacteriology*. ASM Press, Washington, DC.
25. **Brooks, J. V., S. K. Furney, and I. M. Orme.** 1999. Metronidazole therapy in mice infected with tuberculosis. *Antimicrob Agents Chemother* **43**:1285-8.
26. **Burman, W. J.** 2003. The hunt for the elusive surrogate marker of sterilizing activity in tuberculosis treatment. *Am J Respir Crit Care Med* **167**:1299-301.
27. **Caceres, N., G. Tapia, I. Ojanguren, F. Altare, O. Gil, S. Pinto, C. Vilaplana, and P. J. Cardona.** 2009. Evolution of foamy macrophages in the pulmonary granulomas of experimental tuberculosis models. *Tuberculosis (Edinb)* **89**:175-82.
28. **Canetti, G.** 1955. *The Tubercle Bacillus in the Pulmonary Lesion of Man: Histobacteriology and Its Bearing on the Therapy of Pulmonary Tuberculosis*. Springer Publishing Co., New York, N.Y.
29. **Capuano, S. V., 3rd, D. A. Croix, S. Pawar, A. Zinovik, A. Myers, P. L. Lin, S. Bissel, C. Fuhrman, E. Klein, and J. L. Flynn.** 2003. Experimental

- Mycobacterium tuberculosis infection of cynomolgus macaques closely resembles the various manifestations of human M. tuberculosis infection. *Infect Immun* **71**:5831-44.
30. **Cegielski, J. P., B. H. Devlin, A. J. Morris, J. N. Kitinya, U. P. Pulipaka, L. E. Lema, J. Lwakatare, and L. B. Reller.** 1997. Comparison of PCR, culture, and histopathology for diagnosis of tuberculous pericarditis. *J Clin Microbiol* **35**:3254-7.
 31. **Chan, S. L., W. W. Yew, W. K. Ma, D. J. Girling, V. R. Aber, D. Felmingham, B. W. Allen, and D. A. Mitchison.** 1992. The early bactericidal activity of rifabutin measured by sputum viable counts in Hong Kong patients with pulmonary tuberculosis. *Tuber Lung Dis* **73**:33-8.
 32. **Cho, S. H., D. Goodlett, and S. Franzblau.** 2006. ICAT-based comparative proteomic analysis of non-replicating persistent Mycobacterium tuberculosis. *Tuberculosis (Edinb)* **86**:445-60.
 33. **Converse, P. J., A. M. Dannenberg, Jr., J. E. Estep, K. Sugisaki, Y. Abe, B. H. Schofield, and M. L. Pitt.** 1996. Cavitory tuberculosis produced in rabbits by aerosolized virulent tubercle bacilli. *Infect Immun* **64**:4776-87.
 34. **Cooper, A. M., D. K. Dalton, T. A. Stewart, J. P. Griffin, D. G. Russell, and I. M. Orme.** 1993. Disseminated tuberculosis in interferon gamma gene-disrupted mice. *J Exp Med* **178**:2243-7.
 35. **Cooper, A. M., A. Kipnis, J. Turner, J. Magram, J. Ferrante, and I. M. Orme.** 2002. Mice lacking bioactive IL-12 can generate protective, antigen-specific cellular responses to mycobacterial infection only if the IL-12 p40 subunit is present. *J Immunol* **168**:1322-7.
 36. **Cosma, C. L., O. Humbert, and L. Ramakrishnan.** 2004. Superinfecting mycobacteria home to established tuberculous granulomas. *Nat Immunol* **5**:828-35.
 37. **Cosma, C. L., O. Humbert, D. R. Sherman, and L. Ramakrishnan.** 2008. Trafficking of superinfecting Mycobacterium organisms into established granulomas occurs in mammals and is independent of the Erp and ESX-1 mycobacterial virulence loci. *J Infect Dis* **198**:1851-5.
 38. **Dannenberg, A. M.** 2006. Pathogenesis of Human Pulmonary Tuberculosis: Insights from the Rabbit Model. ASM Press, Washington, DC.
 39. **Davies, G. R., A. S. Pym, D. A. Mitchison, E. L. Nuermberger, and J. H. Grosset.** 2007. Evaluation of new antituberculosis drugs in mouse models. *Antimicrob Agents Chemother* **51**:403; author reply 403-4.
 40. **Davies, P., P. Barnes, & S.B. Gordon (editors).** 2008. Clinical Tuberculosis, 4th ed. Hodder Arnold, London.
 41. **Davis, E. O., E. M. Dullaghan, and L. Rand.** 2002. Definition of the mycobacterial SOS box and use to identify LexA-regulated genes in Mycobacterium tuberculosis. *J Bacteriol* **184**:3287-95.
 42. **Dhillon, J., B. W. Allen, Y. M. Hu, A. R. Coates, and D. A. Mitchison.** 1998. Metronidazole has no antibacterial effect in Cornell model murine tuberculosis. *Int. J. Tuberc. Lung Dis.* **2**:736-742.
 43. **Dietze, R., D. J. Hadad, B. McGee, L. P. Molino, E. L. Maciel, C. A. Peloquin, D. F. Johnson, S. M. Debanne, K. Eisenach, W. H. Boom, M. Palaci, and J. L.**

- Johnson.** 2008. Early and extended early bactericidal activity of linezolid in pulmonary tuberculosis. *Am J Respir Crit Care Med* **178**:1180-5.
44. **Dietze, R., L. Teixeira, L. M. Rocha, M. Palaci, J. L. Johnson, C. Wells, L. Rose, K. Eisenach, and J. J. Ellner.** 2001. Safety and bactericidal activity of rifalazil in patients with pulmonary tuberculosis. *Antimicrob Agents Chemother* **45**:1972-6.
45. **Donald, P. R., and A. H. Diacon.** 2008. The early bactericidal activity of anti-tuberculosis drugs: a literature review. *Tuberculosis (Edinb)* **88 Suppl 1**:S75-83.
46. **Edwards, D. I.** 1979. Mechanism of antimicrobial action of metronidazole. *J Antimicrob Chemother* **5**:499-502.
47. **Elowitz, M. B., A. J. Levine, E. D. Siggia, and P. S. Swain.** 2002. Stochastic gene expression in a single cell. *Science* **297**:1183-6.
48. **Fenhalls, G., L. Stevens, L. Moses, J. Bezuidenhout, J. C. Betts, P. Helden Pv, P. T. Lukey, and K. Duncan.** 2002. In situ detection of *Mycobacterium tuberculosis* transcripts in human lung granulomas reveals differential gene expression in necrotic lesions. *Infect Immun* **70**:6330-8.
49. **Flynn, J.** 2009. Keynote address 109th General ASM meeting, Philadelphia, PA.
50. **Flynn, J. L.** 2006. Lessons from experimental *Mycobacterium tuberculosis* infections. *Microbes Infect* **8**:1179-88.
51. **Flynn, J. L., S. V. Capuano, D. Croix, S. Pawar, A. Myers, A. Zinovik, and E. Klein.** 2003. Non-human primates: a model for tuberculosis research. *Tuberculosis (Edinb)* **83**:116-8.
52. **Flynn, J. L., J. Chan, K. J. Triebold, D. K. Dalton, T. A. Stewart, and B. R. Bloom.** 1993. An essential role for interferon gamma in resistance to *Mycobacterium tuberculosis* infection. *J Exp Med* **178**:2249-54.
53. **Flynn, J. L., Goldstein, M.M., Chan, J., Triebold, K.J., Pfeffer, K., Lowenstein, C.J., Schreiber, R., Mak, T.W., Bloom, B.R.** 1995. Tumor necrosis factor- α is required in the protective immune response against *M. tuberculosis* in mice. *Immunity* **2**:561-572.
54. **Friedman, L. N.** 1994. *Tuberculosis: Current Concepts And Treatments*, 2nd ed. CRC Press, United Kingdom.
55. **Gill, W. P., N. S. Harik, M. R. Whiddon, R. P. Liao, J. E. Mittler, and D. R. Sherman.** 2009. A replication clock for *Mycobacterium tuberculosis*. *Nat Med* **15**:211-4.
56. **Ginsberg, A., A. Diacon, R. Dawson, K. Whitney, A. Venter, P. Donald, and M. Spigelman.** 2008. Presented at the 48th Annual ICAAC/IDSA 46th Annual Meeting, Washington, DC.
57. **Goel, M. M., and P. Budhwar.** 2007. Immunohistochemical localization of mycobacterium tuberculosis complex antigen with antibody to 38 kDa antigen versus Ziehl Neelsen staining in tissue granulomas of extrapulmonary tuberculosis. *Indian J Tuberc* **54**:24-9.
58. **Gumbo, T., C. S. Dona, C. Meek, and R. Leff.** 2009. Pharmacokinetics-pharmacodynamics of pyrazinamide in a novel in vitro model of tuberculosis for sterilizing effect: a paradigm for faster assessment of new antituberculosis drugs. *Antimicrob Agents Chemother* **53**:3197-204.

59. **Gutierrez Cancela, M. M., and J. F. Garcia Marin.** 1993. Comparison of Ziehl-Neelsen staining and immunohistochemistry for the detection of *Mycobacterium bovis* in bovine and caprine tuberculous lesions. *J Comp Pathol* **109**:361-70.
60. **Hampshire, T., S. Soneji, J. Bacon, B. W. James, J. Hinds, K. Laing, R. A. Stabler, P. D. Marsh, and P. D. Butcher.** 2004. Stationary phase gene expression of *Mycobacterium tuberculosis* following a progressive nutrient depletion: a model for persistent organisms? *Tuberculosis (Edinb)* **84**:228-38.
61. **Hoff, D. R., M. L. Caraway, E. J. Brooks, E. R. Driver, G. J. Ryan, C. A. Peloquin, I. M. Orme, R. J. Basaraba, and A. J. Lenaerts.** 2008. Metronidazole lacks antibacterial activity in guinea pigs infected with *Mycobacterium tuberculosis*. *Antimicrob Agents Chemother* **52**:4137-40.
62. **Jassal, M., and W. R. Bishai.** 2009. Extensively drug-resistant tuberculosis. *Lancet Infect Dis* **9**:19-30.
63. **Jayaram, R., S. Gaonkar, P. Kaur, B. L. Suresh, B. N. Mahesh, R. Jayashree, V. Nandi, S. Bharat, R. K. Shandil, E. Kantharaj, and V. Balasubramanian.** 2003. Pharmacokinetics-pharmacodynamics of rifampin in an aerosol infection model of tuberculosis. *Antimicrob Agents Chemother* **47**:2118-24.
64. **Jayaram, R., R. K. Shandil, S. Gaonkar, P. Kaur, B. L. Suresh, B. N. Mahesh, R. Jayashree, V. Nandi, S. Bharath, E. Kantharaj, and V. Balasubramanian.** 2004. Isoniazid pharmacokinetics-pharmacodynamics in an aerosol infection model of tuberculosis. *Antimicrob Agents Chemother* **48**:2951-7.
65. **Jindani, A., V. R. Aber, E. A. Edwards, and D. A. Mitchison.** 1980. The early bactericidal activity of drugs in patients with pulmonary tuberculosis. *Am Rev Respir Dis* **121**:939-49.
66. **Jindani, A., C. J. Dore, and D. A. Mitchison.** 2003. Bactericidal and sterilizing activities of antituberculosis drugs during the first 14 days. *Am J Respir Crit Care Med* **167**:1348-54.
67. **Johnson, C. M., R. Pandey, S. Sharma, G.K. Khuller, R.J. Basaraba, I.M. Orme, and A.J. Lenaerts.** 2005. Oral therapy using nanoparticle-encapsulated antituberculosis drugs in guinea pigs infected with *Mycobacterium tuberculosis*. *Antimicrob Agents Chemother* **49**:4335-4338.
68. **Johnson, J. L., D. J. Hadad, W. H. Boom, C. L. Daley, C. A. Peloquin, K. D. Eisenach, D. D. Jankus, S. M. Debanne, E. D. Charlebois, E. Maciel, M. Palaci, and R. Dietze.** 2006. Early and extended early bactericidal activity of levofloxacin, gatifloxacin and moxifloxacin in pulmonary tuberculosis. *Int J Tuberc Lung Dis* **10**:605-12.
69. **Kaufmann, S. H., S. T. Cole, V. Mizrahi, E. Rubin, and C. Nathan.** 2005. *Mycobacterium tuberculosis* and the host response. *J Exp Med* **201**:1693-7.
70. **Kelly, B. P., S. K. Furney, M. T. Jessen, and I. M. Orme.** 1996. Low-dose aerosol infection model for testing drugs for efficacy against *Mycobacterium tuberculosis*. *Antimicrob Agents Chemother* **40**:2809-12.
71. **Koul, A., L. Vranckx, N. Dendouga, W. Balemans, I. Van den Wyngaert, K. Vergauwen, H. W. Gohlmann, R. Willebrords, A. Poncelet, J. Guillemont, D. Bald, and K. Andries.** 2008. Diarylquinolines are bactericidal for dormant

- mycobacteria as a result of disturbed ATP homeostasis. *J Biol Chem* **283**:25273-80.
72. **Kruml, J., L. Trnka, R. Urbancik, and J. Kuska.** 1965. Histological differences between experimental cavernous tuberculosis in rabbits and human cavitory disease. *Am Rev Respir Dis.* **92**:299-302.
 73. **Kumar, N., M. C. Tiwari, and K. Verma.** 1998. AFB staining in cytodagnosis of tuberculosis without classical features: a comparison of Ziehl-Neelsen and fluorescent methods. *Cytopathology* **9**:208-14.
 74. **Kumar, V., A.K. Abbas, and N. Fausto.** 2004. *Robbins and Cotran Pathologic Basis of Disease*, 7th ed. Elsevier Science.
 75. **Lenaerts, A. J., M. A. Degroote, and I. M. Orme.** 2008. Preclinical testing of new drugs for tuberculosis: current challenges. *Trends Microbiol* **16**:48-54.
 76. **Lenaerts, A. J., V. Gruppo, J. V. Brooks, and I. M. Orme.** 2003. Rapid in vivo screening of experimental drugs for tuberculosis using gamma interferon gene-disrupted mice. *Antimicrob Agents Chemother* **47**:783-5.
 77. **Lenaerts, A. J., V. Gruppo, K. S. Marietta, C. M. Johnson, D. K. Driscoll, N. M. Tompkins, J. D. Rose, R. C. Reynolds, and I. M. Orme.** 2005. Preclinical testing of the nitroimidazopyran PA-824 for activity against *Mycobacterium tuberculosis* in a series of in vitro and in vivo models. *Antimicrob Agents Chemother* **49**:2294-301.
 78. **Lenaerts, A. J., D. Hoff, S. Aly, S. Ehlers, K. Andries, L. Cantarero, I. M. Orme, and R. J. Basaraba.** 2007. Location of persisting mycobacteria in a Guinea pig model of tuberculosis revealed by r207910. *Antimicrob Agents Chemother* **51**:3338-45.
 79. **Levin, B. R., and D. E. Rozen.** 2006. Non-inherited antibiotic resistance. *Nat Rev Microbiol* **4**:556-62.
 80. **Lounis, N., T. Gevers, J. Van Den Berg, T. Verhaeghe, R. van Heeswijk, and K. Andries.** 2008. Prevention of drug carryover effects in studies assessing antimycobacterial efficacy of TMC207. *J Clin Microbiol* **46**:2212-5.
 81. **Ly, L. H., M. I. Russell, and D. N. McMurray.** 2008. Cytokine profiles in primary and secondary pulmonary granulomas of Guinea pigs with tuberculosis. *Am J Respir Cell Mol Biol* **38**:455-62.
 82. **Manabe, Y. C., A. K. Kesavan, J. Lopez-Molina, C. L. Hatem, M. Brooks, R. Fujiwara, K. Hochstein, M. L. Pitt, J. Tufariello, J. Chan, D. N. McMurray, W. R. Bishai, A. M. Dannenberg, Jr., and S. Mendez.** 2008. The aerosol rabbit model of TB latency, reactivation and immune reconstitution inflammatory syndrome. *Tuberculosis (Edinb)* **88**:187-96.
 83. **McCune, R. M., F. M. Feldmann, H. P. Lambert, and W. McDermott.** 1966. Microbial persistence. I. The capacity of tubercle bacilli to survive sterilization in mouse tissues. *J Exp Med* **123**:445-68.
 84. **McCune, R. M., F. M. Feldmann, and W. McDermott.** 1966. Microbial persistence. II. Characteristics of the sterile state of tubercle bacilli. *J Exp Med* **123**:469-86.
 85. **McCune, R. M., Jr., W. McDermott, and R. Tompsett.** 1956. The fate of *Mycobacterium tuberculosis* in mouse tissues as determined by the microbial enumeration technique. II. The conversion of tuberculous infection to the latent

- state by the administration of pyrazinamide and a companion drug. *J Exp Med* **104**:763-802.
86. **McCune, R. M., Jr., and R. Tompsett.** 1956. Fate of Mycobacterium tuberculosis in mouse tissues as determined by the microbial enumeration technique. I. The persistence of drug-susceptible tubercle bacilli in the tissues despite prolonged antimicrobial therapy. *J Exp Med* **104**:737-62.
 87. **McIlleron, H., G. Meintjes, W. J. Burman, and G. Maartens.** 2007. Complications of antiretroviral therapy in patients with tuberculosis: drug interactions, toxicity, and immune reconstitution inflammatory syndrome. *J Infect Dis* **196 Suppl 1**:S63-75.
 88. **McMurray, D. N.** 2001. Disease model: pulmonary tuberculosis. *Trends Mol Med* **7**:135-7.
 89. **McMurray, D. N.** 2003. Hematogenous reseeding of the lung in low-dose, aerosol-infected guinea pigs: unique features of the host-pathogen interface in secondary tubercles. *Tuberculosis (Edinb)* **83**:131-4.
 90. **McMurray, D. N.** 2000. A nonhuman primate model for preclinical testing of new tuberculosis vaccines. *Clin Infect Dis* **30 Suppl 3**:S210-2.
 91. **Mdluli, K., R. A. Slayden, Y. Zhu, S. Ramaswamy, X. Pan, D. Mead, D. D. Crane, J. M. Musser, and C. E. Barry, 3rd.** 1998. Inhibition of a Mycobacterium tuberculosis beta-ketoacyl ACP synthase by isoniazid. *Science* **280**:1607-10.
 92. **Mitchison, D. A.** 1993. Assessment of new sterilizing drugs for treating pulmonary tuberculosis by culture at 2 months. *Am Rev Respir Dis* **147**:1062-3.
 93. **Munoz-Elias, E. J., J. Timm, T. Botha, W. T. Chan, J. E. Gomez, and J. D. McKinney.** 2005. Replication dynamics of Mycobacterium tuberculosis in chronically infected mice. *Infect Immun* **73**:546-51.
 94. **Munro, S. A., S. A. Lewin, H. J. Smith, M. E. Engel, A. Fretheim, and J. Volmink.** 2007. Patient adherence to tuberculosis treatment: a systematic review of qualitative research. *PLoS Med* **4**:e238.
 95. **Murphy, D. J., and J. R. Brown.** 2008. Novel drug target strategies against Mycobacterium tuberculosis. *Curr Opin Microbiol* **11**:422-7.
 96. **NIAID.** 2009. Metronidazole for pulmonary tuberculosis. <http://clinicaltrials.gov/show/NCT00425113>.
 97. **Nikonenko, B. V., K. A. Sacksteder, S. Hundert, L. Einck, and C. A. Nacy.** 2008. Preclinical study of new TB drugs and drug combinations in mouse models. *Recent Pat Antiinfect Drug Discov* **3**:102-16.
 98. **Ordway, D., G. Palanisamy, M. Henao-Tamayo, E. E. Smith, C. Shanley, I. M. Orme, and R. J. Basaraba.** 2007. The cellular immune response to Mycobacterium tuberculosis infection in the guinea pig. *J Immunol* **179**:2532-41.
 99. **Organization, W. H.** 2008, posting date. 2008 Tuberculosis Facts. www.who.int/tb. [Online.]
 100. **Organization, W. H.** 2009. Global tuberculosis control : epidemiology, strategy, financing : WHO report 2009. WHO Press, Geneva, Switzerland.
 101. **Organization, W. H.** 2004, posting date. The Top Ten Causes Of Death. <http://www.who.int/mediacentre/factsheets/fs310/en/index.html>. [Online.]

102. **Orme, I. M., D. N. McMurray, and J. T. Belisle.** 2001. Tuberculosis vaccine development: recent progress. *Trends Microbiol* **9**:115-8.
103. **Paramasivan, C. N., G. Kubendiran, and D. Herbert.** 1998. Action of metronidazole in combination with isoniazid & rifampicin on persisting organisms in experimental murine tuberculosis. *Indian J Med Res* **108**:115-9.
104. **Park, H. D., Guinn, K.M., Harrell, M.I., Liao, R., Voskuil, M.I., Tompa, M., Schoolnik, G.K., and Sherman, D.R.** 2003. Rv3133c/DosR is a transcription factor that mediates the hypoxic response of *Mycobacterium tuberculosis* *Mol Microbiol.* **48**:833-843.
105. **Parrish, N. M., J. D. Dick, and W. R. Bishai.** 1998. Mechanisms of latency in *Mycobacterium tuberculosis*. *Trends Microbiol* **6**:107-12.
106. **Pearl, J. E., B. Saunders, S. Ehlers, I. M. Orme, and A. M. Cooper.** 2001. Inflammation and lymphocyte activation during mycobacterial infection in the interferon-gamma-deficient mouse. *Cell Immunol* **211**:43-50.
107. **Peyron, P., J. Vaubourgeix, Y. Poquet, F. Levillain, C. Botanch, F. Bardou, M. Daffe, J. F. Emile, B. Marchou, P. J. Cardona, C. de Chastellier, and F. Altare.** 2008. Foamy macrophages from tuberculous patients' granulomas constitute a nutrient-rich reservoir for *M. tuberculosis* persistence. *PLoS Pathog* **4**:e1000204.
108. **Prammananan, T., A. Chaiprasert, and M. Leechawengwongs.** 2009. In vitro activity of linezolid against multidrug-resistant tuberculosis (MDR-TB) and extensively drug-resistant (XDR)-TB isolates. *Int J Antimicrob Agents* **33**:190-1.
109. **Rhoades, E. R., A. A. Frank, and I. M. Orme.** 1997. Progression of chronic pulmonary tuberculosis in mice aerogenically infected with virulent *Mycobacterium tuberculosis*. *Tuber Lung Dis* **78**:57-66.
110. **Rustad, T. R., M. I. Harrell, R. Liao, and D. R. Sherman.** 2008. The enduring hypoxic response of *Mycobacterium tuberculosis*. *PLoS One* **3**:e1502.
111. **Rustomjee, R., A. H. Diacon, J. Allen, A. Venter, C. Reddy, R. F. Patientia, T. C. Mthiyane, T. De Marez, R. van Heeswijk, R. Kerstens, A. Koul, K. De Beule, P. R. Donald, and D. F. McNeeley.** 2008. Early bactericidal activity and pharmacokinetics of the diarylquinoline TMC207 in treatment of pulmonary tuberculosis. *Antimicrob Agents Chemother* **52**:2831-5.
112. **Seiler, P., T. Ulrichs, S. Bandermann, L. Pradl, S. Jorg, V. Krenn, L. Morawietz, S. H. Kaufmann, and P. Aichele.** 2003. Cell-wall alterations as an attribute of *Mycobacterium tuberculosis* in latent infection. *J Infect Dis* **188**:1326-31.
113. **Sinsimer, D., G. Huet, C. Manca, L. Tsenova, M. S. Koo, N. Kurepina, B. Kana, B. Mathema, S. A. Marras, B. N. Kreiswirth, C. Guilhot, and G. Kaplan.** 2008. The phenolic glycolipid of *Mycobacterium tuberculosis* differentially modulates the early host cytokine response but does not in itself confer hypervirulence. *Infect Immun* **76**:3027-36.
114. **Sirgel, F. A., F. J. Botha, D. P. Parkin, B. W. Van De Wal, P. R. Donald, P. K. Clark, and D. A. Mitchison.** 1993. The early bactericidal activity of rifabutin in patients with pulmonary tuberculosis measured by sputum viable counts: a new method of drug assessment. *J Antimicrob Chemother* **32**:867-75.

115. **Sirgel, F. A., P. R. Donald, J. Odhiambo, W. Githui, K. C. Umapathy, C. N. Paramasivan, C. M. Tam, K. M. Kam, C. W. Lam, K. M. Sole, and D. A. Mitchison.** 2000. A multicentre study of the early bactericidal activity of anti-tuberculosis drugs. *J Antimicrob Chemother* **45**:859-70.
116. **Sissons, J., B. S. Yan, A. V. Pichugin, A. Kirby, M. J. Daly, and I. Kramnik.** 2009. Multigenic control of tuberculosis resistance: analysis of a QTL on mouse chromosome 7 and its synergism with *sst1*. *Genes Immun* **10**:37-46.
117. **Smith, D. W., V. Balasubramanian, and E. Wiegshauss.** 1991. A guinea pig model of experimental airborne tuberculosis for evaluation of the response to chemotherapy: the effect on bacilli in the initial phase of treatment. *Tubercle* **72**:223-31.
118. **Somoskovi, A., J. E. Hotaling, M. Fitzgerald, D. O'Donnell, L. M. Parsons, and M. Salfinger.** 2001. Lessons from a proficiency testing event for acid-fast microscopy. *Chest* **120**:250-7.
119. **Steingart, K. R., M. Henry, V. Ng, P. C. Hopewell, A. Ramsay, J. Cunningham, R. Urbanczik, M. Perkins, M. A. Aziz, and M. Pai.** 2006. Fluorescence versus conventional sputum smear microscopy for tuberculosis: a systematic review. *Lancet Infect Dis* **6**:570-81.
120. **Stover, C. K., P. Warrener, D. R. VanDevanter, D. R. Sherman, T. M. Arain, M. H. Langhorne, S. W. Anderson, J. A. Towell, Y. Yuan, D. N. McMurray, B. N. Kreiswirth, C. E. Barry, and W. R. Baker.** 2000. A small-molecule nitroimidazopyran drug candidate for the treatment of tuberculosis. *Nature* **405**:962-6.
121. **Styblo, K., and J. Meijer.** 1976. Impact of BCG vaccination programmes in children and young adults on the tuberculosis problem. *Tubercle* **57**:17-43.
122. **Sutton, M. D., B. T. Smith, V. G. Godoy, and G. C. Walker.** 2000. The SOS response: recent insights into umuDC-dependent mutagenesis and DNA damage tolerance. *Annu Rev Genet* **34**:479-497.
123. **Telenti, A., W. J. Philipp, S. Sreevatsan, C. Bernasconi, K. E. Stockbauer, B. Wiele, J. M. Musser, and W. R. Jacobs, Jr.** 1997. The emb operon, a gene cluster of *Mycobacterium tuberculosis* involved in resistance to ethambutol. *Nat Med* **3**:567-70.
124. **Tsai, M. C., S. Chakravarty, G. Zhu, J. Xu, K. Tanaka, C. Koch, J. Tufariello, J. Flynn, and J. Chan.** 2006. Characterization of the tuberculous granuloma in murine and human lungs: cellular composition and relative tissue oxygen tension. *Cell Microbiol* **8**:218-32.
125. **Tsenova, L., E. Ellison, R. Harbacheuski, A. L. Moreira, N. Kurepina, M. B. Reed, B. Mathema, C. E. Barry, 3rd, and G. Kaplan.** 2005. Virulence of selected *Mycobacterium tuberculosis* clinical isolates in the rabbit model of meningitis is dependent on phenolic glycolipid produced by the bacilli. *J Infect Dis* **192**:98-106.
126. **Tsenova, L., K. Sokol, V. H. Freedman, and G. Kaplan.** 1998. A combination of thalidomide plus antibiotics protects rabbits from mycobacterial meningitis-associated death. *J Infect Dis* **177**:1563-72.

127. **Turner, O. C., R. J. Basaraba, and I. M. Orme.** 2003. Immunopathogenesis of pulmonary granulomas in the guinea pig after infection with *Mycobacterium tuberculosis*. *Infect Immun* **71**:864-71.
128. **Turner, O. C., R.J. Basaraba, A.A. Frank, and I.M. Orme.** 2003. Granulomatous Infections and Inflammations: Cellular and Molecular Mechanisms. ASM Press, Washington, DC.
129. **Ulrichs, T., and S.H. Kaufmann.** 2006. New insights into the function of granulomas in human tuberculosis. *J Pathol.* **208**:261-269.
130. **Ulrichs, T., M. Lefmann, M. Reich, L. Morawietz, A. Roth, V. Brinkmann, G. A. Kosmiadi, P. Seiler, P. Aichele, H. Hahn, V. Krenn, U. B. Gobel, and S. H. Kaufmann.** 2005. Modified immunohistological staining allows detection of Ziehl-Neelsen-negative *Mycobacterium tuberculosis* organisms and their precise localization in human tissue. *J Pathol* **205**:633-40.
131. **van der Zanden, A. G., A. H. Hoentjen, F. G. Heilmann, E. F. Weltevreden, L. M. Schouls, and J. D. van Embden.** 1998. Simultaneous detection and strain differentiation of *Mycobacterium tuberculosis* complex in paraffin wax embedded tissues and in stained microscopic preparations. *Mol Pathol* **51**:209-14.
132. **Via, L. E., P. L. Lin, S. M. Ray, J. Carrillo, S. S. Allen, S. Y. Eum, K. Taylor, E. Klein, U. Manjunatha, J. Gonzales, E. G. Lee, S. K. Park, J. A. Raleigh, S. N. Cho, D. N. McMurray, J. L. Flynn, and C. E. Barry, 3rd.** 2008. Tuberculous granulomas are hypoxic in guinea pigs, rabbits, and nonhuman primates. *Infect Immun* **76**:2333-40.
133. **Vilcheze, C., and W. R. Jacobs, Jr.** 2007. The mechanism of isoniazid killing: clarity through the scope of genetics. *Annu Rev Microbiol* **61**:35-50.
134. **Voskuil, M. I.** 2004. *Mycobacterium tuberculosis* gene expression during environmental conditions associated with latency. *Tuberculosis (Edinb)* **84**:138-43.
135. **Voskuil, M. I., D. Schnappinger, K. C. Visconti, M. I. Harrell, G. M. Dolganov, D. R. Sherman, and G. K. Schoolnik.** 2003. Inhibition of respiration by nitric oxide induces a *Mycobacterium tuberculosis* dormancy program. *J Exp Med* **198**:705-13.
136. **Wallis, R. S., M. D. Perkins, M. Phillips, M. Joloba, A. Namale, J. L. Johnson, C. C. Whalen, L. Teixeira, B. Demchuk, R. Dietze, R. D. Mugerwa, K. Eisenach, and J. J. Ellner.** 2000. Predicting the outcome of therapy for pulmonary tuberculosis. *Am J Respir Crit Care Med* **161**:1076-80.
137. **WatreLOT-Virieux, D., E. Drevon-Gaillet, Y. Toussaint, and P. Belli.** 2006. Comparison of three diagnostic detection methods for tuberculosis in French cattle. *J Vet Med B Infect Dis Vet Public Health* **53**:321-5.
138. **Wayne, L. G.** 1994. Dormancy of *Mycobacterium tuberculosis* and latency of disease. *Eur J Clin Microbiol Infect Dis* **13**:908-14.
139. **Wayne, L. G., and H.A. Sramek.** 1994. Metronidazole is bactericidal to dormant cells of *Mycobacterium tuberculosis* *Antimicrob Agents Chemother* **38**:2054-2058.
140. **Wayne, L. G., and L. G. Hayes.** 1996. An in vitro model for sequential study of shutdown of *Mycobacterium tuberculosis* through two stages of nonreplicating persistence. *Infect Immun* **64**:2062-9.

141. **Yan, B. S., A. V. Pichugin, O. Jobe, L. Helming, E. B. Eruslanov, J. A. Gutierrez-Pabello, M. Rojas, Y. V. Shebzukhov, L. Kobzik, and I. Kramnik.** 2007. Progression of pulmonary tuberculosis and efficiency of bacillus Calmette-Guerin vaccination are genetically controlled via a common *sst1*-mediated mechanism of innate immunity. *J Immunol* **179**:6919-32.
142. **Zhang, Y., and D. Mitchison.** 2003. The curious characteristics of pyrazinamide: a review. *Int J Tuberc Lung Dis* **7**:6-21.
143. **Zhang, Y., M. M. Wade, A. Scorpio, H. Zhang, and Z. Sun.** 2003. Mode of action of pyrazinamide: disruption of *Mycobacterium tuberculosis* membrane transport and energetics by pyrazinoic acid. *J Antimicrob Chemother* **52**:790-5.